Revealing Neuroendocrine Cell Heterogeneity of Prostate Cancer in Tumours and Liquid Biopsies

Arynne Santos

Faculty of Medicine, Division of Experimental Surgery

McGill University, Montreal

April, 2021

A thesis submitted to McGill University in partial fulfillment of the requirements of the degree of Master of Science

Abstract

Prostate cancer is a lethal disease for both high risk patients who present with metastases at diagnosis, and for those experiencing biochemical recurrence (BCR) after curative therapies for a localized disease. Although most patients respond well to androgen deprivation therapy (ADT), they inevitably fail, become castration resistant, further progress, and die from a metastatic (m) castration resistant prostate cancer (CRPC). The clinical heterogeneity of the disease underscores the intra-tumoral cell heterogeneity, by which neuroendocrine differentiation (NED) mirrors hormone resistance and contributes to progression. Neuroeondocrine products and their receptors are current targets in ongoing clinical trials as therapies and/or targets for molecular imaging of metastases. The central hypothesis is that circulating markers reflect the increasing contribution of neuroendocrine (NE) cells during the progression of the disease and are traceable in liquid biopsies (whole blood), exemplifying extensive NE tumour heterogeneity. It was tested by investigating NE-products in primary tumour foci, followed by their transcripts in liquid biopsies of patients with advanced disease. Nuclear algorithms were used to analyze 5 different NE-markers in the prostate from patients who received neo-adjuvant ADT prior to radical prostatectomy (RP). Several patterns were observed, corroborating highly heterogenous subpopulation of NE cells in both benign glands and tumour foci. Mining of 35 NE-related genes in six transcriptomic datasets confirmed their significant association with disease progression and predominance expression in diverse types of metastases. The 17 most over-expressed transcripts in a series of 35 transcripts were assayed by RT-qPCR in the blood of 15 mCRPC patients and 8 healthy controls. 10 patients over-expressed at

least one NE-related gene, providing 9 unique NE signatures. A high overlap of commonly over-expressed genes was found in the datasets and liquid biopsies, suggesting a favorable signature to be studied further. Our findings highlight our ability to detect NED with new, non-invasive methods in the blood of mCRPC patients and support that disease progression correlates with signatures involving NED. Taken together, these NE signatures not only emphasize the importance of the NE cell subsets when combatting the most aggressive form of the disease but may also open the door to Precision Medicine.

Abrégé

Le cancer de la prostate (CaP) est une maladie mortelle pour les patients de haut risque, ceux qui ont des métastases au moment du diagnostic, et ceux qui récidivent biochimiquement (BCR) suite à des traitements curatifs pour un cancer localisé. Alors que la majorité de ces patients répondent favorablement aux thérapies éliminant et/ou bloquant l'action des androgènes (ADT), ils rechutent inévitablement tous, deviennent résistants à la castration (CRPC), puis progressent davantage et décèdent d'un cancer métastatique (mCRPC). L'hétérogénéité clinique du CaP souligne l'hétérogénéité cellulaire intra-tumorale, dont la différenciation neuroendocrine (NED) reflète la résistance aux androgènes et contribute à sa progression. Certains produits issus des cellules neuroendocrines (NE) et leurs récepteurs sont présentement des cibles thérapeutiques en cours d'essais cliniques, et/ou servent de base pour la détection des métastases par imagerie moléculaire à des fins pronostiques et thérapeutiques. L'hypothèse centrale veut que plusieurs marqueurs circulants reflètent la contribution croissante des cellules NE lors de la progression de la maladie et qu'ils soient traçables dans les biopsies liquides (sang entier) des patients, illustrant ainsi la grande hétérogénéité des cellules NE dans les tumeurs et métastases. Elle a été testée en étudiant divers produits NE dans les foyers tumoraux de la prostate, suivie de l'analyse de transcrits NE dans les biopsies liquides de patients au stade avancé du CaP. Des algorithmes ont été utilisés pour analyser cinq marqueurs-NE dans la prostate de dix patients ayant reçu de l'ADT néo-adjuvante avant leur prostatectomie radicale (RP). Plusieurs patrons d'expression ont été observés, appuyant ainsi la grande hétérogénéité de la population NE, dans les glandes bénignes et les foyers tumoraux. L'analyse bio-

informatique de 35 gènes-NE dans six bases de données de transcrits accessibles publiquement a confirmé une association significative avec la progression de la maladie et la prédominance de leur sur-expression dans diverses métastases. Les 17 gènes NE les plus sur-exprimés ont été testés par RT-qPCR dans le sang de 15 patients mCRPC et 8 contrôles en santé. Dix patients sur-expriment au moins un gène NE, générant 9 NE-signatures uniques. Un grand chevauchement des gènes NE communément sur-exprimés a été trouvé dans les bases de données et les biopsies liquides, suggérant une signature prometteuse à confirmer lors d'études à venir. Nos données soulignent notre capacité à détecter la NED dans le sang de patients mCRPC par des méthodes nouvelles et non-invasives et supportent que la progression de la maladie corrèle avec des signatures impliquant la NED. Pris dans leur ensemble, ces signatures NE ne mettent pas seulement l'emphase sur l'importance des sous-populations de cellules NE lorsque les patients combattent la forme la plus agressive de la maladie mais peuvent ouvrir la porte à la médecine de précision.

Acknowledgements

There are so many mentors, peers, and colleagues that I would like to thank from the bottom of my heart. First off, I would like to thank my supervisor, Dr. Simone Chevalier. Her constant curiosity and dedication to science motivates and constantly instills inspiration in me. She is truly an outstanding mentor, full of advice, and insight and above all else, always supportive while pushing students to achieve their goals.

I would also like to thank my committee members: Dr. Veena Sangwan, Dr. Julia Burnier, and Dr. Victor McPherson. Their questions and feedback helped to strengthen my knowledge and my project. I appreciate their guidance and unique views on my project. Each member brought a different perspective to my thesis plan, as a whole.

I wish to thank the Uro-Oncology Research group for their technical help, scientific advice and criticism. I would like to thank my lab members, notably, Ms. Seta Derderian, Dr Lucie Hamel and Dr. Mohan Amaravadi, for guiding me and teaching me all the technical details and analyses required. I would also like to express my gratitude for the financial support provided by the Urology Division through the two studentship awards received during my Master's here at McGill.

Lastly, the biggest thank you to my family. They were always there to support me, listen to my presentations, provide feedback, and encourage me after stressful days at the lab. They instilled an unshakeable confidence in me, that helped me push through to the very end.

Preface and Contribution of Authors

All the work presented was conducted at the Research Institute of the McGill University Heath Center (RI-MUHC). For studies on human tissue by immunohistochemistry (IHC), the protocol BMD-10-1160 was approved by the ethics board of the research institute and renewed yearly. For studies on human liquid biopsies, the protocol (number MP-37-2017-3189) was approved by the Ethics Review Board of the McGill University Health Center (MUHC).

Experimental planning, data collection and analysis, and preparation of the thesis were carried out by Arynne Santos, under the supervision of Dr. Simone Chevalier.

Statistical analysis for clinical characteristics were performed by Seta Derderian. Blood collection and processing from patients was carried out by nurse Nathalie Cote, processing and RNA extraction by Dr. Lucie Hamel, respectively and occasionally Ms. Derderian and myself. Dr. Amaravadi helped with the planning of RT-qPCR assays and analyses of raw data.

Table of Contents

List of Figures

List of Abbreviations

5-HT serotonin

ADT androgen deprivation therapy

AR androgen receptor

ARIs androgen receptor inhibitors

BCR biochemical recurrence

BPH benign prostatic hyperplasia

CALCA calcitonin

CALCR calcitonin receptor

cfDNA circulating free tumour DNA

CHGA chromogranin A

CRPC castration resistant prostate cancer

CSCs cancer stem cells

CTCs circulating tumour cells

DHT dihydrotestosterone

DRE digital rectal examination

ECM extracellular matrix

EMT epithelial to mesenchymal transition

ENO2 neuron-specific enolase 2

EpCAM epithelial cell adhesion molecule

EVs extracellular vesicles

FAK focal adhesion kinase

FDA Food and Drug Administration

FLT1 vascular endothelial growth factor receptor 1

FSH follicle-stimulating hormone

GRPR gastrin-releasing peptide receptor

GRP gastrin-releasing peptide

GS Gleason score

IF immunofluorescence

IHC immunohistochemistry

ISUP International Society of Urological Pathology

LBD ligand binding domain

LH luteinizing hormone

LHRH luteinizing hormone-releasing hormone

LN lymph node

NCAM1 neural cell adhesion molecule

NE neuroendocrine

NED neuroendocrine differentiation

NEPC neuroendocrine prostate cancer

NSE neuron-specific enolase

PBMCs peripheral blood mononuclear cells

PCa prostate cancer

PKCs protein kinase C

POU3F2 / BRN2 class III POU, family 2 transcription factor

PSA prostate specific antigen

PTKs protein tyrosine kinases

RP radical prostatectomy

RT-qPCR reverse transcriptase - quantitative polymerase chain reaction

SSTR2 somatostatin receptor 2

SST somatostatin

SYP synaptophysin

TF transcription factor

TNM tissue, node, metastasis

TURP transurethral resection of the prostate

VEGFA vascular endothelial growth factor A

VIP vasoactive intestinal protein

VIPR1 vasoactive intestinal protein receptor 1

VIPR2 vasoactive intestinal protein receptor 2

mCRPC metastatic CRPC

WBCs white blood cells

Chapter 1

Introduction

1.1 The Prostate

The human prostate is a walnut-sized organ at the base of the urinary bladder. It is the site of three major causes of morbidity: prostatitis, benign prostatic hyperplasia (BPH), and prostate cancer (PCa). The prostate gland is the largest accessory gland of the male urogenital or reproductive system. It functions to secrete a thin, alkaline fluid that forms a portion of the seminal fluid [1]. This prostatic fluid is rich in enzymes, proteins and minerals that help protect and nourish sperm cells. Hormones, including peptides and proteins produced by the hypothalamus eg., luteinizing hormone-releasing hormone (LHRH) and the pituitary gland eg., luteinizing hormone (LH) and follicle-stimulating hormone (FSH), along with androgens produced by the testis and adrenal glands control the function of the prostate.

The most commonly used nomenclature to describe the structure of the human prostate is that of McNeal [2], as seen in Figure 1.1. The prostate was divided into three major histologically distinct and anatomically separate areas. These areas are the non-glandular fibromuscular stroma that surrounds the organ and the two glandular regions, called peripheral and central zones. The central zone consists of the base of the prostate and

surrounds the ejaculatory ducts and has little contribution in the occurrence of the disease.

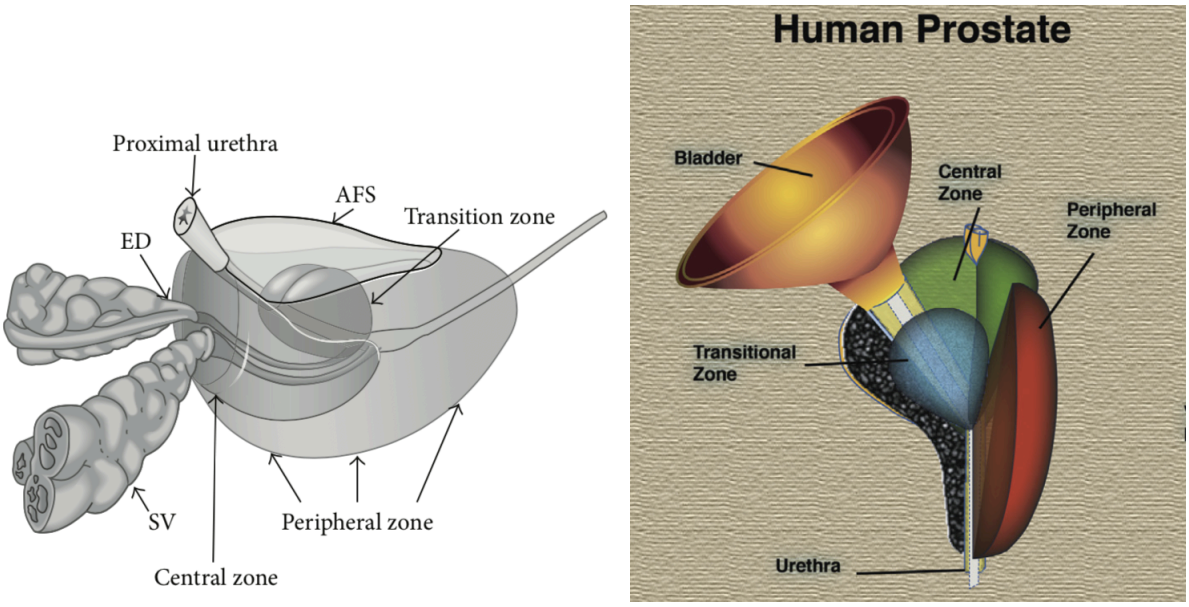

Figure 1.1: Anatomy of the Human Prostate
(Left): showing the ejaculatory ducts (ED), seminal vesicles (SV), and anterior fibromuscular stroma (AFS). (Right): showing the urethra and bladder in relation to the three major glandular regions [1,3].

The peripheral zone makes up the remainder of the gland, while surrounding most of the central zone and extending caudally to partially surround the distal portion of the urethra. The peripheral zone ducts consist of small, simple round to oval acinar structures that empty into long narrow ducts surrounded by a stroma of loosely arranged muscle bundles. Glandular acini in the peripheral zone are the main site for prostatitis and PCa [1].

McNeal also identified an additional, smaller, glandular region that surrounded the prostatic urethra, called the transition zone and extending between the bladder and the verumontanum. It is a small volume of the prostate, comprising of only 5% of the normal organ and is the principal site of BPH pathogenesis [2].

1.2 Prostate Cancer

PCa is the first most common non-cutaneous cancer in men in the Western World and the third leading cause of cancer-related deaths among Canadian men [4]. Since the mid 1900's, the prostate in ageing men has become a major site for medical problems. According to Prostate Cancer Canada statistics, an estimated 1 in every 9 Canadian men in 2019 will have been diagnosed with PCa in their lifetime. Further, for every 63 men diagnosed, 11 men will die from the disease. If detected early, the survival is close to 100 percent. If detected late, 3 out of 4 men will die.

In 1941, Huggins and Hodges initially proved that PCa growth was androgen-regulated and responsive to ADT achieved by surgical castration [5]. Hence due to tumour heterogeneity, certain androgen-independent tumour cells emerge under treatments, while some subsets become androgen-insensitive. Although a majority of patients treated by surgery or radiation therapy remain cancer-free over time, about 30% experience a biochemical recurrence (BCR) and require systemic treatments. At this point, PCa progression becomes inevitable and lethal, as patients fail successive lines of treatments, resulting in palliative care and death from the disease. Newer and more effective targeted therapies are a primary concern for researchers in the field of PCa.

1.2.1 Detection and Diagnosis

During the detection and diagnosis process, a doctor or specialist, primary urologist may perform a digital rectal examination (DRE), along with a prostate specific antigen (PSA) test in blood. PSA is a prostate specific serine protease normally released into the seminal fluid to keep the seminal plasma fluid from lysing the seminal fluid protein, seminogelin, during the process of semen liquefaction [6]. PSA is produced by the luminal cells of the prostatic epithelium and in well-differentiated cancer cells.

The introduction of PSA screening in the late 1980s and early 1990s has led to an earlier detection of PCa [6, 7]. It is now considered a validated serum PCa biomarker, with the

greatest limitation being that it is not specific for PCa alone. It is not used for diagnosis, but instead for progression and response to therapy. Values within the range of 4-10 ng/mL would be commonly observed in BPH cases. Pathological and histological biopsy tests coupled with a suspicious DRE would confirm the diagnosis. The challenge remains: still to define firm biomarkers that specifically signal cancer initiation and/or progression to metastasis.

With advanced genomic and proteomic technologies, there has been a growth in PCa biomarker research, showing promise in both improved sensitivity and specificity. Newer generations of biomarkers can be tested via liquid biopsies (serum, urine, blood) or with tissue-based assays that are Food and Drug Administration (FDA) approved. The identification and characterization of the disease have become increasingly precise through improved risk stratification and advances in magnetic resonance and functional imaging, as well as from the emergence of biomarkers. However, to this day PSA remains the standard biomarker, while some biomarkers included in circulating tumour cells (CTCs), microRNAs, and exosomes are in their infancy [8].

1.2.2 Grading and Staging

The standard approach for grading PCa relies on the Gleason score (GS), which was introduced about 50 years ago and has achieved worldwide acceptance. The Gleason system was specifically designed to take histological heterogeneity into account, making it an outstanding predictor of prognosis for patients. It was developed in 1966, by Donald F. Gleason and consists of five grades or patterns, as seen in Figure 1.2 [9]. This classification system looks at the differentiation of cancer cells and how they differ from normal cell types and glandular acini, with the lowest grades showing well-differentiated cells and representing the least aggressive prognosis. For analysis, the most commonly occurring grade is added to the second most common grade to give the GS. The scores are then grouped together, known as a Group Grade as seen in Figure 1.2 [9].

In 2014, the International Society of Urological Pathology (ISUP) made the most recent changes to this grading system. Some of which include classifying all cribiform cancer and glomeruloid patterns as Gleason Grade 4, the grading of mucinous adenocarcinoma based on underlying architecture rather than uniformly considering these tumors as pattern 4, and the introduction of a GS - based 5 grade system [10]. The designated ISUP grade consists of five grades: grade 1 (GS $\leq$ 3+3), grade 2 (GS 3+4), grade 3 (GS 4+3), grade 4 (GS 4+4, 3+5, 5+3), and grade 5 (GS 9-10 from 4+5, 5+4, and 5+5) [10].

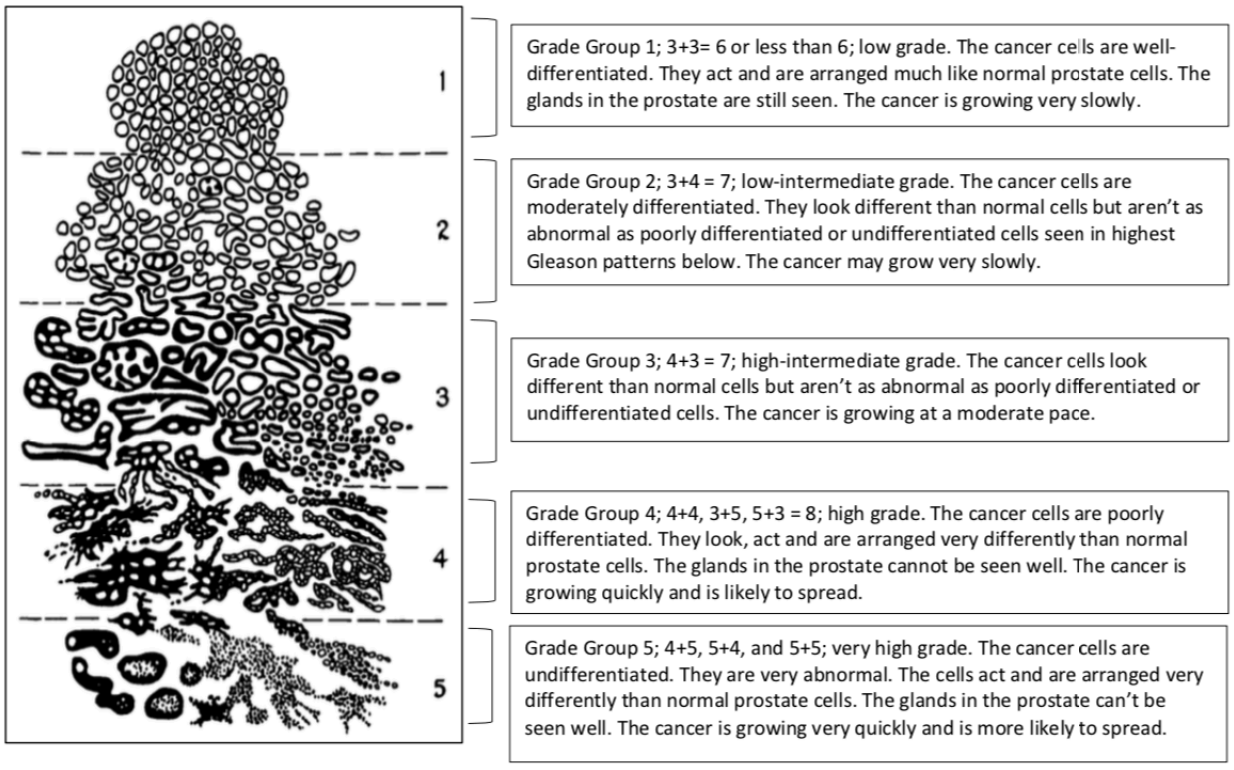

Figure 1.2: Gleason Grading System
Prostatic adenocarcinoma (histological patterns) according to Gleason Grading System inclusive of grading Group system for scoring, and respective descriptions [9].

The most common staging system for PCa is the tissue, node, metastasis (TNM) system. The TNM combinations are then grouped into 4 stages, with the highest stage number being the most spread cancer. (T) describes if the tumour has grown outside of the prostate to the surrounding tissue and is usually assigned a number from 1 to 4, with the higher number meaning that the tumour has grown outside the prostate. (N) describes

lymph node (LN) near the prostate where cancer cells have spread. N0 is negative for LN and N1 is positive for LN. (M) represents metastasis and describes whether or not the cancer has spread to other parts of the body. M0 is negative for metastasis, whereas M1 represents a positive metastasis.

Stage 1: (T1 or T2a, N0, M0)

- The cancer was found in the tissue upon prostate biopsy consisting of 12 cores in general, numbered according to their location within the organ. (T2a) is when the tumour is in one lobe of the prostate and takes up one-half or less of the lobe.

Stage 2: (T2b or T2c, N0, M0)

- The tumour is in more than half of one lobe (T2b) or in both lobes (T2c) or the prostate.

Stage 3: (T3 or T4, N0, M0)

- The tumour has grown through the capsule and either into the lower part of the bladder or into one or both seminal vesicles (T3).
- The tumour has attached to or grown into any of the following (T4): rectum, external sphincter of the anus, levator muscles of the pelvic floor, pelvic wall.

Stage 4: Any (T, N1, M0) or any (T, N0, M1)

1.2.3 Treatment

Patients diagnosed with PCa have a variety of options, depending on the stage of cancer, the grade or Gleason score, as well as the overall health status and life expectancy. Patients with low-risk cancer may be offered active surveillance and delayed treatments if there is evidence of progression upon re-biopsy and increase in blood PSA levels. During active surveillance, the doctor surveys for any signs and symptoms of cancer progression, while tests are administered every 3-6 months. Patients with a medium to high risk have

the option of undergoing curative therapies, such as a radical prostatectomy (RP) and/or radiation therapy. RP implies the removal of the prostate and some surrounding tissues, including the seminal vesicles and in some instances, the pelvic lymph nodes. Surgery and radiation continue to be effective treatments for men with more significant cancer, such as those with a PSA level greater than 10 ng/mL [11].

Systematic treatments are reserved for patients with locally advanced or non-organ confined disease at diagnosis and patients who fail curative therapies, as monitored by detectable blood PSA during follow-up. This is commonly referred to as BCR, and occurs in about 30% of patients. ADT then becomes standard of care for all patients. Further recurrence during ADT implies that patients become castration resistant, referred to as CRPC, with PSA blood levels rising when testosterone is at zero. Currently, these patients continue to receive ADT until they progress to metastatic CRPC (mCRPC). In this scenario, the PSA levels of a patient will continue to rise, even though no metastases are detected upon imaging. Agents targeting androgen synthesis like Abiraterone and blocking and competing for androgen binding to the androgen receptor (AR), such as Enzalutamide, both inhibit its signalling pathway. These are the most up to date lines of therapy introduced in mCRPC patients remaining on ADT [12].

Taxane-based therapy with docetaxel and more recently cabazitacel, along with immunotherapeutic agent sipuleucel-T^4, and the radiopharmaceutical radium-223 chloride (Ra-223) have proven survival benefits in CRPC patients [13]. Further, there are several ongoing clinical trials with new and innovative drugs for more complete inhibition of either androgen synthesis or blocking and competing for binding to the AR. As of 2017, the median survival has improved for men with metastatic disease and is now 5 years, due to the early administration of chemotherapy and the aforementioned therapeutic drugs [11].

1.3 Resistance to Therapy

As previously mentioned, about 30% of patients will experience a BCR after receiving the gold standard hormone treatment, being ADT. It is a constant battle between varying lines of therapy, and cells acquiring resistance and immune-tolerance to these drugs. There are endless ways that this might be accomplished. One such possibility is that the tumour cells might convert into a different histological subtype that is associated with a loss of dependency on the original oncogenic driver. Another possibility could be that the drug or therapy given to the patient, might not be specific or even targetable to the phenotype of the patient's cancer cells. For PCa specifically, there are several studies looking at the correlation between the effectiveness of hormone therapy (involving androgens) and plasticity or heterogeneity of the tumour cells. A subset of CRPC cases appear to be AR-independent, with minimal to no AR expression in some cancer cells of prostatic tissues. These tumours may be highly heterogeneous and display a specific NE phenotype [14–16].

1.3.1 Function and Effect of Androgens on Prostate Cancer

Prostate cancer cell growth and survival depends on androgens, the major ligands for the AR. Testosterone is the primary circulating androgen, with approximately 90% produced by the Leydig cells in the testes and 10% produced by the adrenal cortex. Testosterone is converted to dihydrotestosterone (DHT) by the $5a$-reductase enzyme present in prostatic luminal cells. DHT and to some extent testosterone can both bind to the AR in prostate cells, although DHT has greater affinity for AR, via the ligand binding domain (LBD) of the AR protein as seen in Figure 1.3. This binding causes a conformational change that leads to dissociation of the HSP90 (heat shock protein 90) complex, homo-dimerization of the receptor, translocation to the nucleus, and through its DNA binding domain, then binds to androgen-response elements (AREs) in the promoter region of androgen-regulated genes and activate their transcription [17, 18]. For instance,

nuclear AR binds to the promoter of the *KLK3* gene encoding PSA and whose transcription is primarily driven by androgens in androgen-sensitive and/or -dependent prostate cells.

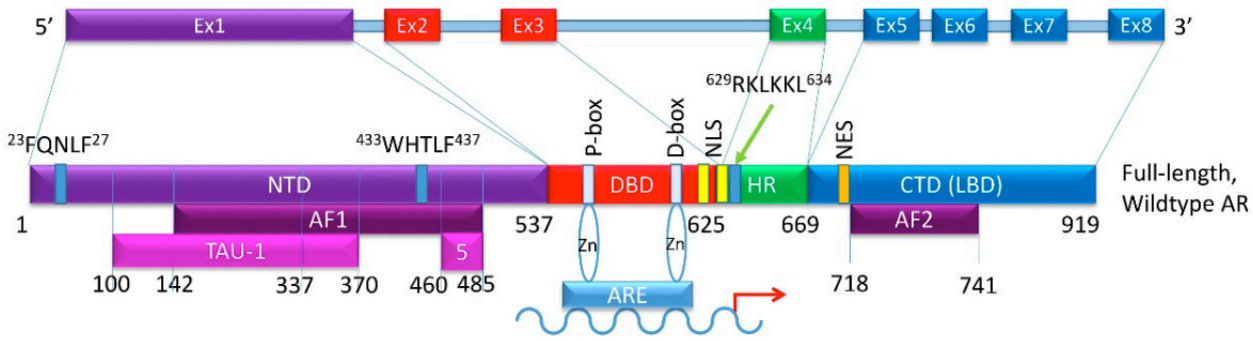

Figure 1.3: Canonical Full-Length Wild Type AR Exons and Domains in the Encoded Full-Length Protein [19]

Top: Exon structure of the AR gene. Bottom: Protein domains of the full-length wild-type AR showing which exon encodes for which domain. Additional minor domains are indicated [19].

Although most patients respond well to ADT, they inevitably fail, become CRPC, further progress, and die from mCRPC. The primary mechanism of resistance of prostate cancers involves the androgen/ AR axis. Tumour cells that survive ADT, grow and may differentiate despite inhibition of steroid synthesis and blockade of androgens/ AR binding which effectively prevents downstream signalling in the canonical pathway [18, 20, 21]. This pathway is central to the development and pathogenesis of CRPC. Some mechanisms that ultimately alter AR axis signalling, disease progression, and treatment resistance can be stratified into AR-dependent and AR-independent resistance mechanisms. AR-dependent resistance mechanisms include AR amplification, AR point mutations, expression of constitutively active AR splice variants, and altered intra-tumoral androgen biosynthesis [17, 18, 20]. Truncated mutants, as well as splice variants lacking the LBD are constitutively active and resistant to many AR-targeted therapies [22–25]. There have been an extensive amount of studies indicating that out of all the variants, the greatest effect of resistance against therapies come from AR-V7 [19,26,27]. At least 22 AR-Vs have been described (some of which are seen in Figure 1.4 with AR-V3, AR-V7/AR3, AR-V9,

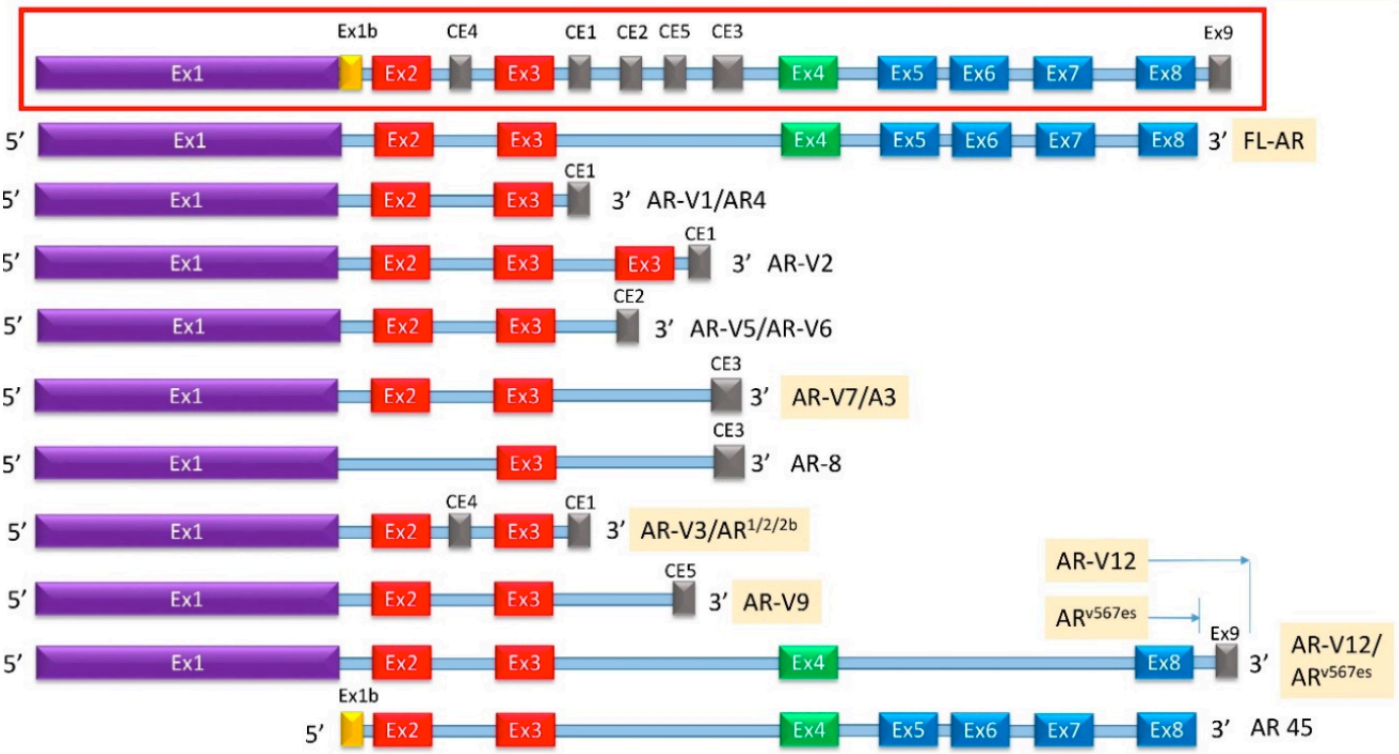

Figure 1.4: Known AR-Variants (V) Lacking Specific Domains [19]
Inset: A simplified schematic of the gene encoding for AR with designated cryptic and canonical exons as well as intronic sequences known to be integrated into alternatively spliced AR protein products. Main: The subset of AR-Vs known to lack the LBD are shown above with the translated sequences represented on the left and the name(s) of the corresponding variant on the right [19].

and AR^{v567es} currently clinically identifiable from prostate tumour tissues and CTCs in blood associated with CRPC [28–31]. All AR-Vs lacking the LBD do contain the full N-terminal domain and at least one exon of the canonical DNA-binding domain and may thus activate gene transcription. Of note, AR-V5 and AR-V6 are distinct variants that contain different translated 3′ sequences of cryptic exon 2 [19].

As a result of the mutations, no clinical therapy to date completely addresses AR-independent pro-tumoural activity. The AR-Vs production, activity, and enrichment during disease progression emphasize a clinical need for AR inhibitors that target non-LBD sites, as seen in Figure 1.5. There are already many treatments that target the LBD. Gonaotropin-releasing hormone (GnRH) agonists (leuprolide or goserelin), in addition to

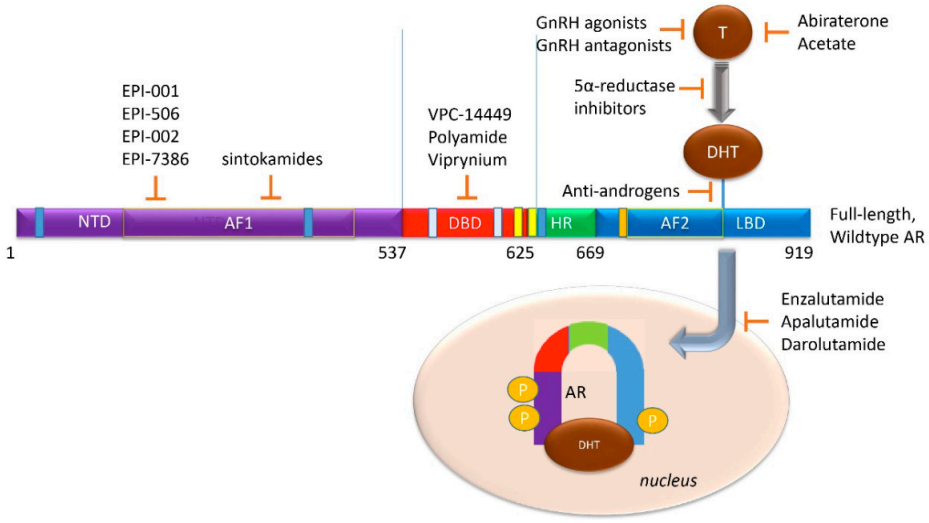

Figure 1.5: Current Androgen/AR-targeted Treatments in Clinical Use or in Development [19].

androgen biosynthesis inhibitors (like abiraterone acetate), block testosterone-mediated activation of the AR. 5-α reductase inhibitors (finasteride or dutasteride) may have a role in a combination therapy to prevent testosterone conversion to its higher affinity form, DHT. Anti-androgens (bicalutamide, nilutamide, and flutamide) are competitive inhibitors of AR ligand binding domain. Direct AR inhibitors such as enzalutamide, apalutamide, or darolutamide, block androgen binding to the AR LBD to prevent AR activation. Even though, N-terminal and DNA-binding domains are targets for AR inhibition, there are no clinically approved therapies specifically targeting these domains. However, several studies are looking at developing such a drug, for example the NTD-directed EPI-001 series or the DBD-targeted VPC-14449 [19].

1.3.2 Plasticity and Tumour Cell Heterogeneity

A tumour, or cluster of cancer cells consists of varying degrees of molecular phenotypes. Cancer cell plasticity can be defined as the ability of a cell to substantially modify its identity and acquire new phenotypic traits that more closely resemble a distinct developmental lineage. Such plasticity is increasingly recognized as having a key role in drug resis-

tance and metastasis, two major causes of cancer mortality [32–34]. Phenotypic and functional heterogeneity may arise among cancer cells as a consequence of genetic changes, environmental differences or stress, and reversible changes within cell properties, causing cancer cell plasticity. There are two main types of tumour heterogeneity: intra- and inter-tumoural heterogeneity, both of which play an equally important part in the therapeutic resistance of PCa treatments.

Lineage plasticity, the ability to transition from one committed developmental pathway to another, has been proposed as a source of intra-tumoural heterogeneity and of tumour adaptation to an adverse tumour microenvironment including exposure to targeted anticancer treatments [22, 32]. One such transition is epithelial to mesenchymal transition (EMT), which is a loss of epithelial phenotype and induction of mesenchymal characteristics. This is known to be associated with the increased capacity of tumour cells to migrate and invade other tissues [35]. Another well-known pathway of lineage plasticity in cancer is the histological transformation of adenocarcinomas, for example PCa, to aggressive NE derivatives. This was originally found in lung cancers harbouring an EGFR mutation, and was subsequently reported in PCa in the presence of anti-androgens [32]. In their study, Zou et al. provided evidence of plasticity in a *Tp53*-knockout and *Pten*-knockout mouse model of PCa in which tumours were less durably responsive to the anti-androgen abiraterone than their counterparts from a *Pten*-knockout mouse model [36]. Tumours deficient in p53 and PTEN displayed a variety of histological subtypes, including squamous, sarcomatoid, small-cell NE-like and other non-adenocarcinoma phenotypes, which were not found in the single *Pten*-knockout model [36].

Multiple mechanisms of resistance to anti-androgens have been described in patients, some but not all of which include loss of AR expression. Mechanisms in therapy-resistance PCa exhibiting the AR loss include the following: NE transformed prostate tumours, tumours with altered tyrosine kinase signalling (FGFR and MAPK) showing stemness characteristics and sensitivity to the inhibition of these kinases [37]; and tumours with up-regulation of KMD1A (or LSD1), a histone demethylase that regulates this gene expres-

sion in stem cells [38]. In tumours resistant to anti-androgen therapy while retaining AR expression, a subset of patients has been described to have an intermediate adenocarcinoma-NE phenotype, displaying transcriptomic hallmarks of NE tumours, all while having a high AR expression [39]. Some important transcripts or families that are known to be involved with the NED transition include the *MYC* family members, *RB1* and *TP53*, *AKT-mTOR* signalling pathway, *SOX* family members, and several other lineage plasticity drivers like *AURKA* and *FOXA1* [14, 40–44].

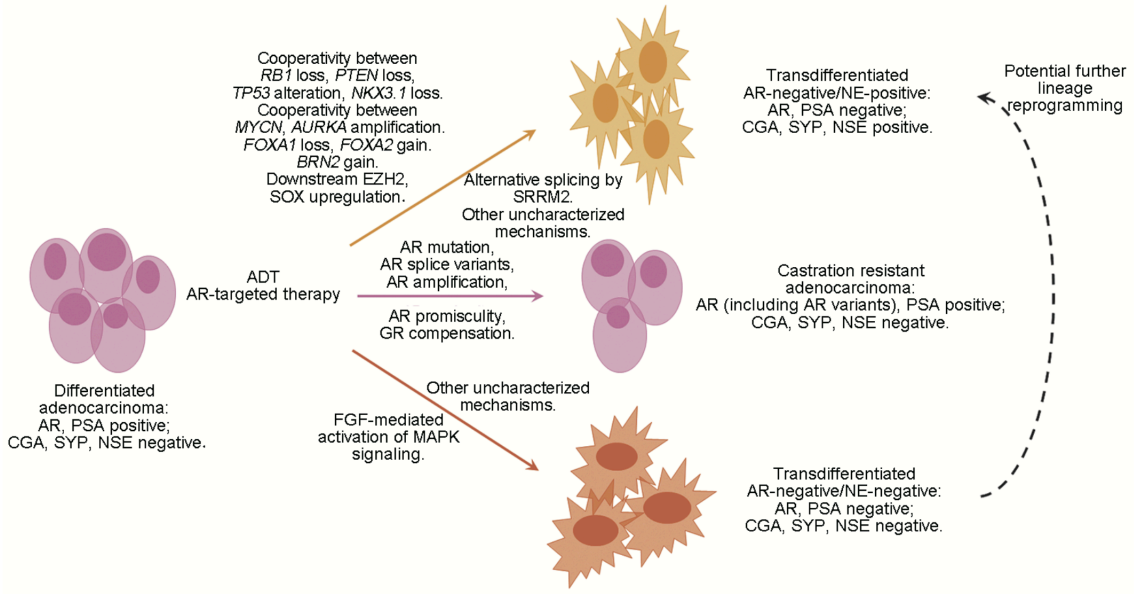

Figure 1.6: Model of Therapy-Induced Prostate Cancer Cell Lineage Plasticity [22]
Treatment of adenocarcinoma with ADT or AR-targeted therapy ultimately leads to therapy resistance through multiple mechanisms. ADT: androgen deprivation therapy; AR: androgen receptor; BRN2: POU Class 3 Homeobox 2; CGA: Chromogranin A; EZH2: Enhancer of zeste 2 polycomb repressive complex 2 subunit; GFG: Fibroblast growth factor; FOXA1: forkhead box protein A1; FOXA2: forkhead box protein A2; GR: glucocorticoid receptor; MAPKs: mitogen-activated protein kinases; MYCN: neuroblastoma-derived v-myc avian myelocytomatosis viral related oncogene; NE: neuroendocrine; NKX3.1: NK3 homeobox 1; NSE: neuron-specific enolase; PSA: prostate-specific antigen; PTEN: phosphatase and tensin homolog; RB1: retinoblastoma 1; SOX: sex-determining region Y-box; SRRM2: serine/arginine repetitive matrix 2; SYP: synaptophysin; TP53: tumour protein p53. Note: This figure was adapted from [22]. The acronym's used in my thesis for chromogranin A (CHGA) and neuron-specific enolase (NSE or ENO2) may differ from those in the figure.

There are several models explaining theories of how this phenomenon of plasticity ultimately leads to intra-tumoural heterogeneity. This was first noted based on tumour cell morphology by experimental pathologists in the 1800s. Aside from cellular morphology and tumour histology, improved technology uncovered additional molecular features including variation in cell surface markers, genetic abnormalities, growth rates, and responses to therapy [45, 46]. One of the popular models explaining cancer cell plasticity is the cancer stem-cell model. This model suggests that some cancers are organized into a hierarchy of subpopulations of tumourigenic cancer stem cells (CSCs) and their non-tumourigenic progeny [47]. Evidence from both experimental models and clinical studies indicate that CSCs survive against several commonly used cancer therapeutics. Moreover, the properties and transcriptional signatures specific to CSCs are highly predictive of overall patient survival pointing to their clinical relevance [48]. However, there are still many challenges to represent and prove the validity of this model. There is difficulty replicating solid-cancer stem-cell markers and inter-patient variability from xenograft models were unclear about what if the majority or minority of cancers follow this model [49]. New experimental approaches such as genetic mapping in the cancer cells of tumours growing in mice models, as well as transplantation assays to evaluate the potential of cancer cells to form tumours may help to address the uncertainty of this model. Further attempts to explain how tumour cells gain plasticity, and ultimately how this leads to resistance of therapies are underway.

1.4 The Neuroendocrine Phenotype

The normal prostate glandular acini consists of three main cell subtypes: luminal, basal, and stem cells, with very few NE cells. A mature prostate epithelium contains several distinct cell types that differ in their morphology, as seen in figure 1.7. The luminal cells are tall columnar epithelial cells that express cytokeratins 8 and 18, as well as secretory proteins such as PSA [50]. Below the luminal layer are the non-secretory basal cells that

line the basement membrane and express CK5 and CK14. The basal cells express low or undetectable levels of AR compared to the luminal cells, nearly all of which express high levels of AR. Stem cells are believed to be housed in this cell layer, although they are not detected per se, due to a lack of markers distinguishing them from their daughter cells. Finally, the rare NE cells correspond to basally localized cells that express secreted neuropeptides and other hormones. They are found to appear slightly more in the transitional and peripheral zone of the prostate, and are lacking in the central zone. There are two different morphological types of NE cells: the open-type cells and the closed-type cells as seen in Figure 1.7 [50].

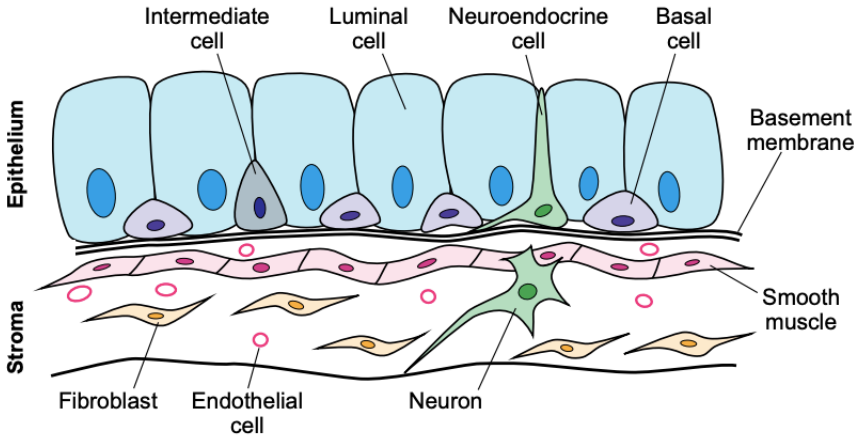

Figure 1.7: Epithelial Cell Types in the Normal Prostate [50]
Schematic representation of cell types in the adult prostate. The epithelial compartment is composed of basal cells that line the basement membrane, secretory luminal cells, and rare intermediate and NE cell subpopulations. These epithelial ducts are adjacent to a stromal compartment that includes smooth muscle cells, fibroblasts, and vascular and neural components and inflammatory cells [50].

The open-type possess long surface microvilli through which the cells reach the lumen and receive luminal stimuli (pH, chemicals). It was actually hypothesized that when these NE cells open to the lumen, their secretory products may be found in the seminal fluids. The closed-type NE cells have lateral processes through which the cells can contact the adjacent luminal and basal epithelial cells (luminal and basal) and receive stimuli from

nerve ending, neighboring blood vessels and underlying stromal cells. Usually these cells are not recognized under the light microscope or by hematoxylin and eosin staining, but can easily be seen by immunohistochemistry (IHC) staining with specific markers such as synaptophysin (SYP), chromogranin A (CHGA), and neuron-specific enolase (NSE). However, in general NE cells are sparse and sometimes found in clusters or 'nests'.

Neuroendocrine cells receive neuronal input (neurotransmitters released by nerve cells or neuro-secretory cells) and, as a consequence of this input, they release message molecules (hormones) into the blood. As part of a diversified NE system, the NE cells in the prostate secrete a variety of molecules, hormones, or peptides, such as serotonin (5-HT), histamine, CHGA, calcitonin (CALCA), and other members of the calcitonin family, neuropeptide Y, vasoactive intestinal protein (VIP), bombesin/ gastrin-releasing peptide (GRP), also best known as bombesin, its amphibian analog, parathyroid hormone-related protein, NSE, thyroid stimulating hormone-like peptide, somatostatin (SST), VEGF-A and others [51–54]. Although the physiological functions have not yet been fully understood, it is thought that prostatic NE cells are involved with regulation, secretion, differentiation, and proliferation of prostatic secretory and basal cells through exocrine, endocrine, paracrine and autocrine mechanisms [51,55]. A role in reproduction cannot be excluded due to the presence of NE-products in the seminal plasma.

1.4.1 Neuroendocrine Classification

In 2004, the World Health Organization (WHO) created a classification of tumours of the urinary system and male genital organs. This current histological classification of NE tumours of the prostate includes: (1) focal NED in conventional prostate adenocarcinoma; (2) carcinoid tumour (WHO well-differentiated NE tumour); and (3) small cell NE carcinoma (new WHO classification, poorly differentiated NE carcinoma) [56]. All PCa shows focal NED, although the majority only shows rare or sparse single NE cells. It is known that about 5-10% of prostatic carcinomas contain zones with a large number of single or

	PSA	NE Markers	Ki67
PCa.	Positive	Scattered + cells	Not increased in NE cells
PCa. with Paneth cell NE differentiation	Variably positive	Diffuse positive in Paneth cells	Few cases studied—not increased
Carcinoid-like tumor	Usually* positive	Positive	Not studied
Carcinoid tumor	Negative	Diffusely positive	Usually low Rarely increased (typically <5%–20%)
SC carcinoma	Usually negative or scattered positive cells	Positive in ~90% of cases	> 50%, typically >80%
LC NE carcinoma	Usually negative but may be positive	Diffusely positive	Usually >50%
Mixed NE (SC/LC) usual PCa.	Same as above for each component	Same as above for each component	Same as above for each component

*Results refer to carcinoid-like areas. Tumors usually associated with usual prostatic adenocarcinoma.

PCa. indicates adenocarcinoma; SC, small cell; LC, large cell.

Table 1.1: Classification of NED in Prostatic Tumours [51]

clustered NE cells detected by CHGA immunostaining. Besides 5-HT, positively stained proteins found in these NE cells include NSE, SYP, bombesin/ GRP and VEGF-A [56].

Although the WHO neuroendocrine classification is analogous to other organs, it does not account for the unique aspects of NED in PCa. With new clinical and molecular data emerging from patients overcoming hormone therapies, this highlighted a need for a refinement of diagnostic terminology to encompass the full spectrum of NED. In 2013, the Prostate Cancer Foundation assembled a working committee on the molecular biology and pathologic classification of NED in PCa. The re-defined pathological classification includes: (1) usual prostate adenocarcinoma with NE differentiation; (2) adenocarcinoma with paneth cell NE differentiation; (3) carcinoid tumour; (4) small cell carcinoma; (5) LC-NEC (large cell neuroendocrine carcinoma); (5) mixed (small or large cell) NE carcinoma - acinar adenocarcinoma [51,57].

The newly proposed classification of NE prostate carcinoma is outlined in table 1.1 [51], as well as the morphological features of each classification in Table 1.2 [57]. In current practice, NE cells are defined by IHC positivity for either SYP, CHGA, or CD56 (also known as NCAM1). Even though only about 10% of untreated usual prostate adenocarci-

WHO (2004)	Epstein *et al.*	
Histologic classification	Histologic classification	Morphologic features
Focal NED in conventional prostate adenocarcinoma	Usual prostate adenocarcinoma with NED	Usual acinar or ductal adenocarcinoma of the prostate in which NED is demonstrated by IHC alone
	Adenocarcinoma with Paneth cell NED	Intense eosinophilia with large cytoplasmic granules
Carcinoid tumor	Carcinoid tumor	Uniform appearance of well-differentiated cells; rare mitoses
Small cell NE carcinoma	Small cell carcinoma	Sheets of uniform cells, frequent mitoses, high nuclear/ cytoplasmic ratio
	Large cell NE carcinoma	Large cells, extensive
	Mixed (small or large cell) NE carcinoma—acinar adenocarcinoma	Biphasic carcinoma with distinct admixed components of NE (small cell or large cell) carcinoma and usual conventional acinar adenocarcinoma; rarely, the adenocarcinoma component may have ductal or other variant features

NED, Neuroendocrine differentiation; IHC, immunohistochemistry; NE, Neuroendocrine.

Table 1.2: Morphological Features of NED [57]

nomas shows focal NED, it is a highly heterogenous phenotype, specifically in PCa. The *de novo* NE tumours of the prostate, which are composed of exclusively NE tumour cells without history of prostate adenocarcinoma are very rare. The tumours that fit into this category include the aforementioned carcinoid tumour, small cell carcinoma, and large cell NE carcinoma of the prostate [57].

1.4.2 Models of Neuroendocrine Prostate Cancer

In the 1990's, a team of scientists created a transgenic mouse model of metastatic prostate cancer originating from NE [58]. At this time, experimental models to explore the role of NE cells in PCa were not available, with the majority of research being conducted by using human tissue samples, human cell lines, and animal models of sporadic naturally occurring disease. Garabedian, et al., were able to develop a new transgenic mouse model in which SV40 T-Ag was produced in members of the NE cell lineage resulting in metastatic PCa. By using a rat probasin gene promoter in the transgenic adenocarcinoma mouse prostate (TRAMP) model, they were able to restrict expression of SV40 T-Ag to secretory cells in the dorsal and lateral lobes of the prostate. What they found was that progression of PCa generated by SV40 T-Ag in mouse NE cells did not require androgens

Name or characteristic	Origin of cells	Histology	Evidence of plasticity
Cell line			
NCI-H660	Lymph node metastasis from a patient with small-cell prostate cancer	NA	Dependency on EZH2
GEMMs			
Rb1 deletion and *Pten* loss	Mouse prostate epithelium	Mixed adenocarcinoma and NEPC (SYP^+) cells	EZH2 inhibition reverses antiandrogen (enzalutamide) resistance
Tp53 deletion and *Pten* loss	Mouse prostate epithelium (luminal cells)	Divergent differentiation, including squamous, sarcomatoid, and small-cell NE-like (SYP^+CHGA^+) cells	Lineage tracing demonstrates that luminal adenocarcinoma cells give rise to NE tumours in response to antiandrogen (abiraterone) treatment
Mycn induction and *Pten* loss	Mouse prostate epithelium	Foci of poorly differentiated carcinoma with divergent differentiation, including sarcomatoid and small-cell NE ($CHGA^+$) cells	Upregulation of AR-regulated genes following EZH2 inhibition
Xenografts			
MYCN induction and *AKT* activation	Human prostate epithelium	Divergent differentiation, including small-cell NE and mixed NE–acinar adenocarcinoma ($SYP^+CHGA^+NCAM1^+$) cells	Upregulation of epigenetic regulators (EZH2 and DNMT1); CSC features
PDX			
LTL331R	PDX adenocarcinoma (LTL331)	NEPC ($SYP^+CHGA^+CD56^+$) cells	Rapid emergence of NE tumour following castration

Table 1.3: Plasticity in NEPC Models [14, 36, 59–63]

and that the FVB/N CR2-T-Ag mice provided a model of NE cancer whose progression could be followed from initiation to advanced metastatic disease [58].

In an extensive review, Davies, et al. summarized an up-to-date review of the various accepted models used to study neuroendocrine prostate cancer (NEPC) [59], as seen in table 1.3. Notably, data from *in vitro* and *in vivo* human PCa models, as well as genetically engineered mouse models (GEMMs), support that lineage switch from epithelial cells to NE cells makes tumours less dependent on the AR, enabling them to escape inhibition of the AR pathway.

There are two hypotheses addressing the origin of NEPC: one suggesting that normal NE cells undergo oncogenic mutation, and the other suggests that adenocarcinomas undergo lineage conversion to the NE phenotype via genetic or epigenetic dys-regulation. Irrespective of their origins, the models were shown to share consistent molecular or epigenetic features.

Some of the common molecular features include:

- low or absent AR signalling [14,51,57,64,65]
- *RB1* loss (70-90%) [14,66]
- *TP53* loss (56-67%) [39,66]
- *MYCN* amplification (40%) [39]
- *ERG* rearrangements (50%) [67]
- up-regulation of *BRN2* [68], *SOX2* [69,70] and *PEG10* [71]
- down-regulation of *REST* [72,73]

Some of the common epigenetic features include:

- up-regulation of DNA methyltransferases and altered DNA methylation [14];
- up-regulation of enhancer of zeste homologue 2 (EZH2) and Polycomb-mediated gene silencing [14,74].

Researchers generally agree that lineage plasticity contributes to the acquisition of the CSC phenotype, but its involvement in the emergence of NEPC is still under debate. No direct evidence supports that NEPC arises from the expansion of resident CSCs and /or NE cells within a heterogeneous tumour (as would be expected for a hierarchical model) or from the transdifferentiation of adenocarcinoma cells via a CSC intermediate (as would be expected for a dynamic transdifferentiation model) as seen in Figure 1.8.

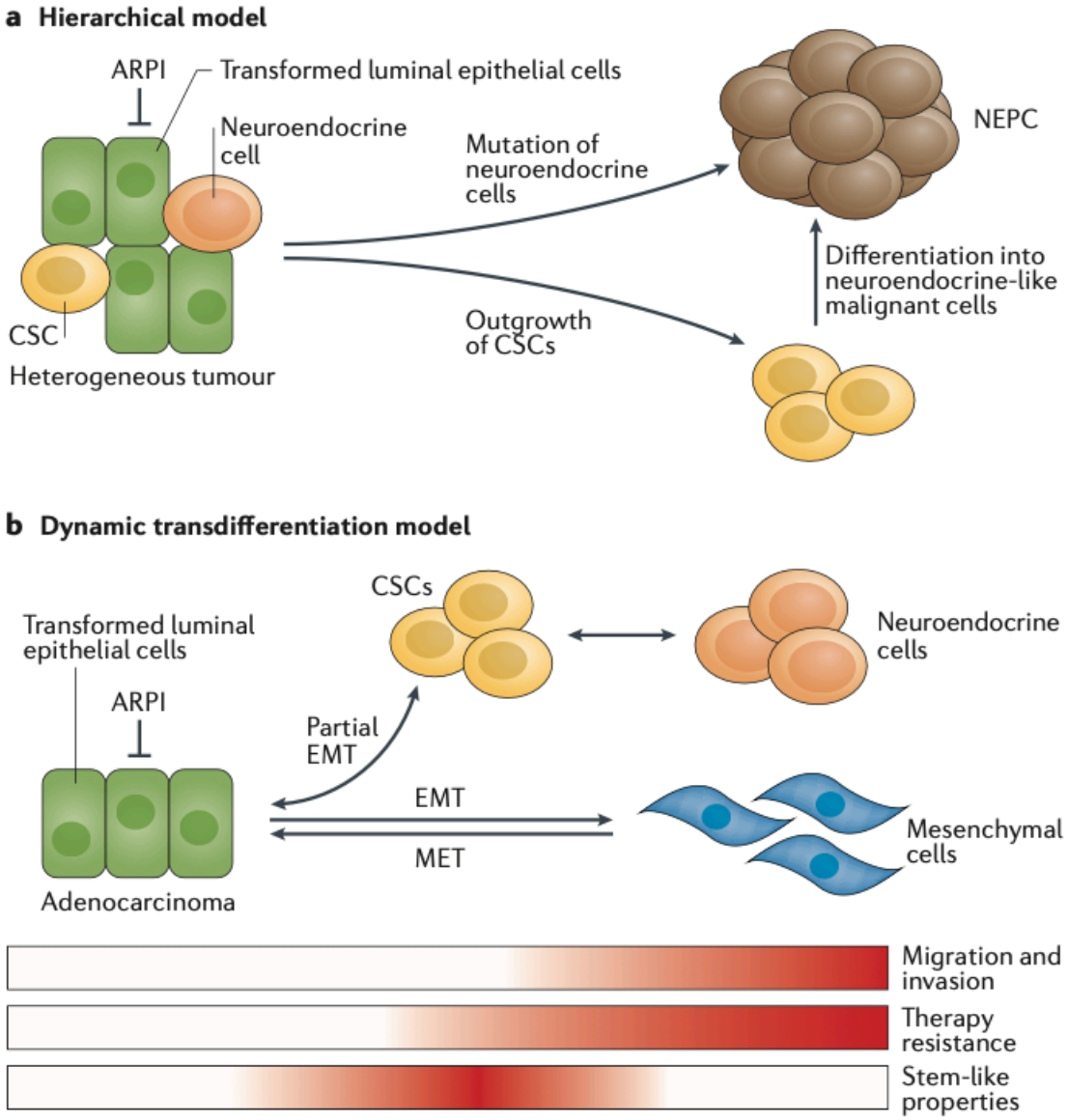

Figure 1.8: Hypothetical Models of NED in response to AR Pathway Inhibitors [59]
(a) The hierarchical model, showing heterogeneous tumour cells containing a varying mixture of stemness and/or proliferative abilities; (b) The dynamic transdifferentiation model shows that under pressure from the ARPIs, the luminal epithelial cells can be reprogrammed into NE cells. The ability for migration and invasion, extent of therapy resistance, and extent of stem-like properties vary over the spectrum of adenocarcinoma to NE transdifferentiation (red indicates a high level). [59]

In the hierarchical model, androgen receptor inhibitors (ARIs) can reduce tumour burden by eliminating the highly proliferative AR-driven cells (the luminal epithelial cells) but not the relatively dormant AR-in-different cells (the cancer stem-like cells (CSCs) and/or NE cells). The tumorigenic CSC population expands following ARIs treatment. The plasticity of these cells enables them to differentiate into NE-like malignant cells, which constitute NEPC. However, other mechanisms such as the acquisition of new mutations in pre-existing NE cells could also drive the emergence of NEPC. In the dynamic transdifferentiation model, the pressure of ARIs can cause luminal epithelial cells to be reprogrammed into NE cells. Activation of a partial EMT endows cells with a plastic phenotype to further progress via a transient pluripotent and stem-like state to generate CSCs [59].

1.5 Neuro-Products and Their Potency on Cell Function

As previously mentioned, mCRPC patients that have progressed on ADT and onto further lines of therapies have a higher prevalence of NED in their tumour composition, resulting in adverse clinical outcomes [75]. Further evidence shows that NED in mCRPC patients is significantly increased in LN metastases compared to the primary tumours [76]. There are many NE-products, or intrinsic NE molecules used to detect NE components, as previously mentioned. The main biomarkers used are CHGA, SYP, NSE, and neural cell adhesion molecule (NCAM1).

CHGA, also known as secretory protein is an acidic protein encoded by the *CHGA* gene in humans. Elevated CHGA expression levels in tissues and blood are correlated with disease burden and poor outcomes of PCa [57, 77, 78]. CHGA appears to be the most sensitive marker from literature, and is most widely used for detecting NED either at the tissue level or in the general circulation [79–82]. acSYP, also known as P38, is an acidic calcium binding glycoprotein closely associated with synaptic structure and function, and is an integral membrane protein of synaptic vesicles [83]. It has been reported

that the expression level of SYP is higher in malignant prostate tissue, compared to benign. Moreover, high SYP levels in tumours are associated with poor survival of patients with prostate metastases to the bone [84–86]. In a systematic literature review by Muoio et al., authors looked at the role of NSE in PCa progression [69]. Regarding the correlation between blood NSE and PCa stage, only 3 studies demonstrated that increased PCa stage was associated with higher NSE serum levels, especially in metastatic versus localized PCa [87–89]. In light of this literature review, NSE might have a prognostic value, but any definitive conclusion is currently not possible [90]. Lastly, NCAM1 or CD56, is a membranous marker that plays a key role in cell-to-cell interactions [57]. Over-expression of NCAM1 has been reported in various metastatic cancers as a promoter of cell migration, including in neuroblastoma, small cell lung carcinoma, renal cell carcinomas and PCa [91].

1.5.1 NE Transcripts and NE-products Circulating in Liquid Biopsies

Obtaining solid biopsies at advanced stages of PCa has remained problematic in clinical practice due to the invasiveness of the procedure. Liquid biopsy refers to the analysis of blood or other bodily fluids to obtain clinically or biologically relevant information about a solid malignancy, analogous to information obtained from a traditional tumour biopsy [92]. It encompasses a broad spectrum of approaches aimed at characterizing different fluid components including CTCs, circulating tumour DNA (ctDNA), circulating RNA, microRNAs, and extracellular vesicles (EVs) as seen in Figure 1.9.

Some of the advantages of a liquid biopsy compared to the conventional tissue biopsy is that it could help with the early intervention and diagnosis of a disease, risk assessment of BCR, and treatment selection based on the presence of certain biomarkers [94]. Liquid biopsies (blood in particular) are easy to access, less invasive than surgical removal of a tissue biopsy, and can offer a more comprehensive cross-sectional molecular profile of primary tumours and metastases during each patient trajectory. Some of observable characteristics like RNA over-expression, DNA abnormalities, variation in protein expressions

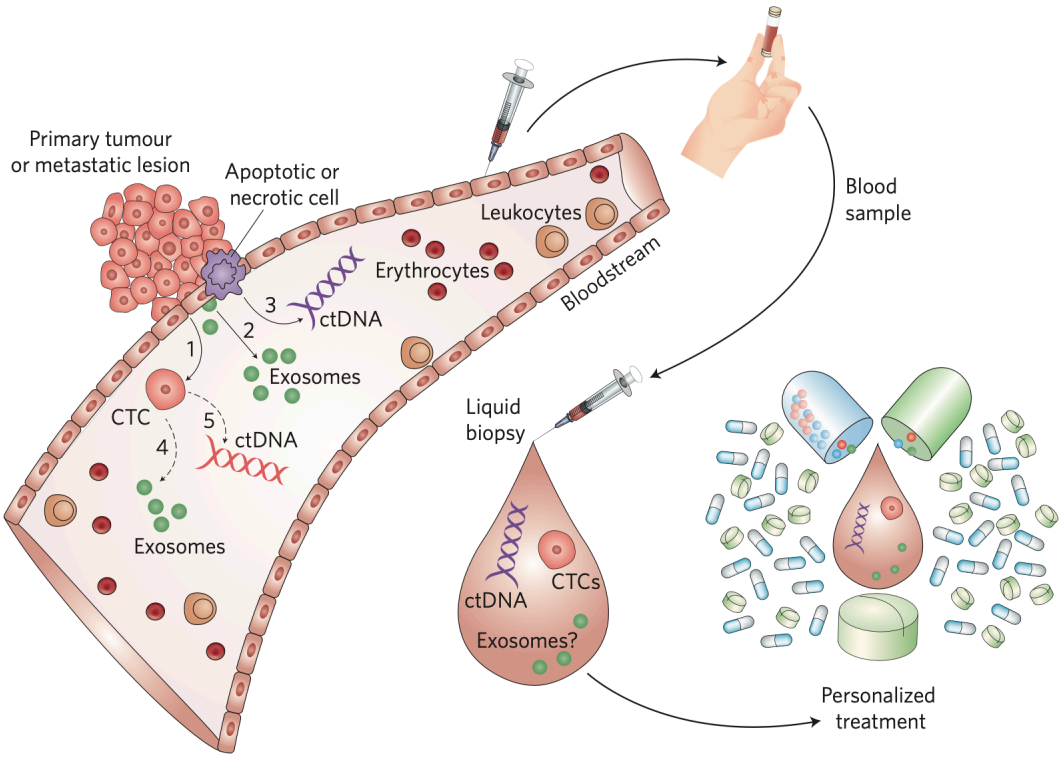

Figure 1.9: Various Components in Liquid Biopsy [93]

A subset of aggressive tumour cells can enter the bloodstream from the primary tumour and/or metastatic lesions. Exosomes are released by viable tumour and normal cells. Apoptotic or necrotic tumour cells release ctDNA into the bloodstream. CTCs can further contribute to the pool of circulating exosomes and ctDNA [93].

could all be found in a drop of patient blood and could be used to increase knowledge about the underlying disease (e.g. tumour burden and heterogeneity), ultimately translating to improved cancer diagnosis, therapy guidance and disease surveillance. One may also repeatedly draw blood throughout the patients' disease for better stratification, monitoring of therapeutic efficacy, identifying new therapeutic targets, and detect the emergence of possible resistance mechanisms [93]. CTCs are cancer cells that are shed by primary tumours or metastates into the blood stream. It is commonly known that an increase in CTC enumeration is correlated with prognosis and disease burden in mCRPC patients [95–98].

In a study done by Khan et al., the authors investigated epithelial cell adhesion molecule (EpCAM) expression and CTC detection in patients with metastatic neuroendocrine tumours (NETs) and evaluated the potential of CTCs to predict radiological progression. To their knowledge, this was the first systematic analysis showing EpCAM expression and CTC detection in NETs. They concluded that the CTCs were associated with progressive disease and may provide useful prognostic information given the variable survival rates of patients with NETs [99]. They also highlighted the diversity of NE-products in CTCs, with 82% being positive for SYP and 21% for CD56 (NCAM1) [99]. Another study done by the same group showed a significant correlation between the number of CTCs and an elevated serum CHGA level [100]. The first limitation of studying CTCs is the rarity of these cells in the bloodstream, usually around one CTC per billion of blood cells [101]. This challenge has been addressed by new technologies.

CellSearch (Menarini Silicon Biosystems Inc., Bologna, Italy) is the only FDA-cleared and clinically available assay for CTC enumeration. CellSearch is an affinity-based assay that uses immuno-magnetic beads targeting EpCAM to enrich CTCs. It is based on the assumption that most CTCs, which are epithelial by origin, express EpCAM, whereas white blood cells (WBCs) do not. The enumeration of CTCs is performed based on staining for DAPI (a nuclear marker), CK (cytokeratin 7/8, an epithelial marker), and CD45 (a WBC marker). DAPI+/CK+/CD45- cells are counted as CTCs. However, solely relying on EpCAM expression for CTC enrichment has been recognized to have critical limitations due to the fact that EpCAM expression is heterogenous or even not expressed in some cancer cell subtypes and CTCs.

In a review done by Lampignano et al., authors look at enrichment, isolation and molecular characterization of EpCAM-negative CTCs [102]. Reports showed that CellSearch is unable to detect CTCs in about 36% of metastatic breast cancer patients [103], and similar data are also published for lung cancer as well [104–106]. The second limitation would be that some CTCs do not express EpCAM. Examples of undetected cells are those undergoing EMT due to the loss of epithelial characteristics such as the expression

of EpCAM and E-cadherin, and gain some mesenchymal traits such as the expression of vimentin. Eventually, cells lose their adhesive properties and gain motile and invasive features [102, 107].

Several studies have looked at CTC phenotypes as prognostic biomarkers in metastatic PCa. Some have reported that CTCs with very small nuclei were significantly elevated in patients with visceral rather than non-visceral metastatic PCa [108]. Similar observations were also reported using the Epic platform, which showed that CTCs from patients with a NE phenotype were smaller in size [97]. The Epic Sciences platform is a non-selection-based platform that characterizes all nucleated cells and identifies CTCs based on a multi-parametric digital pathology process identifying abnormal cells among the normal WBCs utilizing protein expression and cell morphology [109–111]. This technique has demonstrated the ability to identify distinct CTC populations including traditional (CK+,CD45-), apoptotic, CK-negative, and CTC clusters [112]. A very interesting study done by Beltran et al., was able to demonstrate that CTCs from patients with NEPC have distinct characteristics by utilizing the Epic platform. Neuroendocrine PCa tumour cells were predominantly of smaller size, demonstrated lower AR-expression and abnormal nuclear and cytoplasmic features [97]. When testing an independent cohort, they found that up to 10% of CRPC patients also harbored similar NEPC CTC subpopulations and their presence was associated with aggressive clinical features (i.e., visceral metastases and high CTC burden) [97]. Further studies are still required to validate the clinical utility of CTCs for early detection of NEPC patients as well as potential prognostic impacts in predicting response to AR-directed therapies in CRPC [97].

1.5.2 Previous Work Done in the Host Lab

The host lab interest for NED dates back to the 1990's. Studies range from the functional outcome of various NE-products and the role they play on human PCa cell lines to their expression in prostate NE cells in tissues in terms of cancer cell motility and hormone

ablation, respectively. More recently, a pilot study was launched to analyze four NE transcripts in the blood of mCRPC patients.

a. Bombesin Activation of PCa Cell Motility Through FAK

The host lab had identified the focal adhesion kinase (FAK) transcript through the use of phosphotyrosine antibodies to screen an expression library generated from the RNA of immature prostate cells in primary culture [113]. In searching for its potential role in PCa, they observed the up-regulation of pp125^{FAK} expression, its activation by phosphorylation on tyrosine and its association with paxillin, a FAK partner than connects integrins to the extracellular matrix (ECM) proteins, and p50^{CSK} in PCa tissues from patients with metastases [113]. The normal and localized PCa tissues showed undetectable or low levels of both FAK mRNA and protein and an absence of pp125^{FAK} complexes. An increase in expression and activation of pp125^{FAK} in metastatic PCa tissues were also corroborated in PCa human cell lines, from the most tumorigenic and androgen-independent AR-negative PC-3, followed by DU145 and then the androgen-responsive and AR-positive LNCaP [113].

This was an integral finding that shed light on the signalling pathway for motility of the NE-product, bombesin. Bombesin is an analog of GRP and contains the same active sequence, however it is isolated from frog skin and is not a human protein. In previous findings, the host lab had already demonstrated that while bombesin acts through the GRP receptor to induce intracellular calcium mobilization in PC-3 cells, it does not stimulate their proliferation [114].

The lab then expressed an interest in the bombesin/ GRP signalling pathway involving pp125^{FAK}, integrins and other associated proteins. A link was established between pp125^{FAK} and bombesin signalling pathways by showing that inhibition of protein tyrosine kinases (PTKs) and protein kinase C (PKCs) alters PC-3 motility triggered by bombesin, while not affecting adhesion to ECM proteins. They reported that bombesin

triggers tyrosine phosphorylation of some integrin and integrin- associated proteins coupled to pp125^{FAK} in PC-3 cells [115].

In subsequent studies on FAK in cells undergoing bombesin-induced motility, it was shown that bombesin treatment resulted in the re-localization of FAK in focal contacts concomitantly with its tyrosine phosphorylation on residue 397 and with the formation of actin lamellipodia [116]. Furthermore, the motility of bombesin-induced cells was significantly reduced in the presence of FAK inhibitors, microinjected in PC-3 cells, and thereby reducing cell motility. Altogether, these observations point towards a critical role for FAK in the action of bombesin/GRP on PC-3 cell motility [116].

b. VEGF-A, a NE-product Activator PC-3 Cell Motility

With a growing interest in the VEGF family and their expression in PCa, it was noted that not only was vascular endothelial growth factor A (VEGFA) detected faintly in tumour and normal epithelial cells, but also that the highest levels were observed in the NE-cell subtype [54]. This was achieved through IHC testing, with sparse prostate cells staining positively for VEGF-A in accordance with CHGA and 5-HT stains [54].

The screening of the prostate cDNA library had also identified vascular endothelial growth factor receptor 1 (FLT1), one of the VEGF receptors, as an active tyrosine kinase in prostate epithelial cells. This puzzling observation in non-endothelial cells prompted the host lab to investigate and demonstrate that VEGF-A activates its receptor, FLT1 in PC-3 cells through similar FAK signalling, resulting in enhanced cell motility [54]. Thus VEGF-A like bombesin/GRP activate their receptor signalling through FAK to enhance cell motility. Similarly to bombesin, VEGF-A had no effect on PC-3 cell division (unpublished results).

The findings are supportive of the paracrine role of NE cells in PCa. The direct action of VEGFA on signalling through FLT-1 and FAK in PC-3 cells, as well specific VEGFA binding to cell surface proteins, and stimulation of cell migration, adds to the concept that the aggressive nature of prostatic tumour cells may be attributed to NE cell-mediated

progression [54]. This observation was the first to demonstrate direct effects of VEGFA on human PCa cells.

c. Calcitonin A (CALCA) Involvement on Motility in LNCaP Cells

Although not published yet, the host lab also showed that CALCA increases FAK activation and the motility, but not the growth of LNCaP cells. CALCA had no effect on PC-3 motility and growth. Conversely, bombesin and VEGFA had no effect on LNCaP cell motility, nor growth. These observations suggest that NE-products may exert differential effects on cancer cells displaying distinct features in tumours. Furthermore, their action on motility supports a role in the migration of cancer cells and establishment of metastases.

d. Serotonin (5-HT) Expression Post Hormone Castration

The canine prostate has the tendency to spontaneously develop hyper-plastic and neoplastic changes with increasing age, similarly to the human prostate and is seen as the most reliable model to study these diseases, not naturally observed in most other mammalian species [117]. It has been a model of choice for the host lab for years and was used to test the relation between NED and hormone treatment. The host lab compared prostatic NE cells in both patients and dogs given androgen-ablation therapy, pharmacologically (ADT) and surgically (castration), respectively. In both models, NE cells were stained for 5-HT. The 5-HT positive NE cells were morphologically similar in dog and human prostates and identified in all groups, independent of their hormonal status [118]. Interestingly, the number of NE cells or density was within the same range in normal and hyperplastic dog prostates, but significantly higher after castration [118].

This confirmed that the dog may be a suitable animal model for studies regarding NE differentiation. In both dog and man, androgen ablation leads to a significant increase in 5-HT positive cell density. Moreover, once NED was induced, it was proven to be reversible in the steroid-supplemented castrated dogs, which were restored to the nor-

mal levels independently of basal cell growth and/or luminal differentiation [118]. This suggests that NED may be hormonally repressed in the prostate and that NE cells are regulated independently of basal cell growth and luminal/secretory cell differentiation and are possibly hormonally repressed [118].

Circulating NE Transcripts in PCa Patients

A pilot study that is currently under review, tested the presence of four NE transcripts, *SYP*, *NCAM1*, *VEGFA*, *ENO2* in the blood RNA of mCRPC patients. Overexpression of *SYP* was found to be associated with past abiraterone treatments, current treatments with a taxane, and more lines of therapy (Vesval, Wissing, Derderian et al., Molecular Oncology -under review, 2021). Furthermore, circulating *VEGFA* over-expression was found to be associated with patients who had received radiotherapy as their initial curative treatment. However, not all of the four NE transcripts were over-expressed or clinically significant. This study also highlighted the existence of 3 cell subtypes of the prostate in liquid biopsies.

1.6 HYPOTHESIS AND OBJECTIVES

As previously mentioned, reports by the host lab revealed the action of some NE products such as VEGF-A, bombesin/GRP and CALCA on human PCa cell lines, activating motility through FAK. Activation of cancer cell motility is a known contributor to tumour metastasis at several steps, including breaching of the basement membrane, escape from the primary tumour, migration to blood and lymphatic vessels, intravasation and extravasation and movement into distant organs. Further reports show persistence of 5-HT expression in NE cells post hormone therapy, independent of androgens.

The recent pilot study analyzing *VEGFA, SYP, ENO2* and *NCAM1* in the blood RNA of CRPC patients revealed a distinct signature, with some of the NE transcripts being significantly associated with anti-androgen, taxane or radiotherapy treatments.

Accordingly, we propose that circulating markers reflect the increasing contribution of NE cells during the progression of the disease and are traceable in liquid biopsies (whole blood), exemplifying extensive NE tumour heterogeneity.

Objectives were to:

1. Investigate NE cell subsets or populations in primary tumours.
2. Determine and select NE molecules of interest, and search for over expressed transcripts in published PCa datasets.
3. Further explore if more NE circulating transcripts are found in the blood of patients with advanced PCa.
4. Ascertain a potential NE signature of clinical relevance.

Chapter 2

Materials and Methods

2.1 Immunohistochemistry (IHC)

Studies on human tissues by IHC (BMD-10-1160) was approved by the ethics board of the research institute and renewed yearly. Formalin-fixed and paraffin-embedded blocks of prostate from patients (n = 10) who received neo-adjuvant hormone therapy for 3 months prior to RP were obtained from Dr. Gleave, Prostate Centre, Vancouver, BC. Consecutive sections (5um) stained with CHGA, NSE, SYP, CALCA, 5-HT antibodies were scanned using an Aperio Scanscope slide scanner at 20X. Slides were viewed and imaged by ImageScope software, and analyzed by a nuclear algorithm previously established by a pathologist (Dr. Eleonora Scarlata) in the host lab's server. Whole sections were analyzed searching for stained NE cells expressing at least one or more biomarkers. The ratio of stained cells to total cells in the whole tissue was determined for each biomarker in both benign glands and tumour foci and expressed as percentages. Clinical data was not available for these patients.

2.2 Human PCa Cell Lines and RNA Extraction

Androgen-responsive LNCaP (ATCC CRL-1740; AR-positive) and androgen-independent DU145 and PC-3 (ATCC HTB-81; ATCC CRL-1435; both AR-negative) were purchased from ATCC (Manassas, VA, USA). The NCI-H660 (ATCC CRL-5813; neuroendocrine, low AR) and 22Rv1 (ATCC CRL-2505; expressing AR and AR-V7) human PCa cell lines were generous gifts from Dr. A. Zoubedi (Prostate Centre, Vancouver, BC, CDN) and Dr M. Tremblay (McGill Goodman Cancer Centre, Montreal, QC, CDN), respectively. Cells were cultured and passaged according to standard procedures or recommendations. Declumping for the NCI-H660 was achieved by pipetting up and down 25 times at cell passages. RNA was extracted manually from cells at 70-80% confluence, following the miRNeasy kit and accompanying protocol (Qiagen).

2.3 Patients and Healthy Volunteers

This study (number MP-37-2017-3189) was approved by the Ethics Review Board of the McGill University Health Center (MUHC). All participants voluntarily signed an informed consent form. Blood was drawn from 15 patients (on 2nd and 3rd line therapies) from the MUHC at follow-up visits with oncologists and 8 healthy male volunteers of varying age with no prostate-related diseases in their lifetime. A unique coded ID was generated for each patient and volunteer to maintain blindness and ensure confidentiality.

2.4 Blood Processing and RNA Extraction

Blood samples were collected in PAXgene RNA tubes (4 x 2.5 mL, Qiagen) and kept at room temperature for 2 hours to allow cell lysis before being transferred to -20°C overnight and stored at -80°C. For RNA extraction, blood was thawed in the fridge (6-8°C), and processed using a PAXgene RNA extraction kit and an automated Qiacube, as per the manufacturer's protocol (Qiagen). RNA integrity (RIN), all above 8.0, was deter-

mined by the BioAnalyser 2100 (Agilent, Milcreek, ON, Canada) and concentration was determined by Nanodrop ND-1000 (Thermo Scientific, Waltham, MA, USA). 8-10 RNA aliquots (each with 500 ng total RNA) were made in 10uL of volume. RNA aliquots were stored at -80°C.

2.5 Gene Assays

All primers and probes were ordered from Thermo Scientific^{TM}. They were as follows for the 17 genes of interest: VEGFA (Hs00900055-m1), FLT1 (Hs01052961-m1), CHGA (Hs00900370-m1), CHGB (Hs01084631-m1), SCG2 (Hs01920882-s1), ENO2 (Hs00157360-m1), SYP (Hs00300531-m1), POU3F2 (Hs00271595-s1), CALCA (Hs01100741-m1), CALCR (Hs00156229-m1), SST (Hs00356144-m1), SSTR2 (Hs00265624-s1), GRP (Hs01107047-m1), GRPR (Hs01055872-m1), NCAM1 (Hs00941830-m1), MYCN (HS01041361), AURKA (HS00173978). Primers/probes for the 3 reference genes were: PGK1 (Hs00943178-g1), PPIB (Hs00168719-m1), RPLP0 (Hs00420895-gH)

2.6 RT-qPCR Assays in Cell Lines and Blood RNA

Gene assays were tested in each of the (5) human PCa cell lines using 200 ng RNA per cDNA reaction. Next, 200 ng of RNA from each PCa cell lines was combined to create a total of 1000 ng RNA, which was then serially diluted to generate standard curves for each assay. The serial dilutions also served as positive controls and inter-calibrators across various qPCR plates.

The first strand cDNA synthesis of RNA from both, whole blood and cell lines used the same reagents and protocol. 500 ng total RNA was reverse transcribed using Maxima H Minus First Strand cDNA Synthesis Kit, with dsDNase (Thermo Fisher Scientific) by following the manufacturer's protocol. Enzyme mediated dsDNA digestion was first performed on the RNA samples to ensure elimination of any contaminating genomic DNA.

Each total RNA sample was incubated for 2 min at 37°C with dsDNase (supplied with the kit) in a 10 μL total reaction volume. This was followed by heat-inactivation of the enzyme for 15 minutes at 65°C. To the same reaction tube, dNTP mix (10mM), oligo(dT)$_{18}$ primers (25 pmol), and nuclease free water were added for a total reaction volume of 15 μL. This was followed by incubation for 5 minutes at 65°C to remove RNA secondary structures. After the incubation, 4 μL 5X RT buffer and 1 μL Maxima H minus enzyme mix were added to the same tube for a final reaction volume of 20 μL. Reverse transcription was then carried out by incubation for 10 minutes at 25 °C followed by 15 minutes at 50 °C, and termination by heating for 5 minutes at 85°C. The synthesized cDNA was stored at -80°C until further use.

For each q-PCR reaction, 5 μL 2X TaqMan® Fast Advanced Master Mix (Thermo Scientific^{TM}, catalogue number: 4444963), 0.5 μL 20X TaqMan Assay, and 3.5 μL nuclease-free water (R0582) were combined with 1 μL of cDNA sample for a final volume of 10 μL. Triplicate reactions were run in 384-well plates, using CFX384 Touch Real-Time PCR System (Bio-Rad). After the initial Uracil N-glycosylase (UNG) incubation for 2 minutes at 50°C followed by polymerase activation for 20 seconds at 95°C, the reaction mixtures were subjected to 65 cycles of amplification following the sequence: 95°C for 3 seconds and 60°C for 30 seconds. Of note, the specific amplification of all NE transcripts were generally achieved after 40 cycles.

The CFX Maestro 1.1 software (v4.1.2433.1219) was used to quantify gene expression. The following calculation allows for copy number calculation from the serial dilutions of each gene assay:

$$\frac{\text{[(RNA conc. (ng) x Avogadro's Constant (6.022e23)]}}{\text{[Amplicon Length (bp) x Avg. molar mass of 1 bp in dsDNA (660) x 1x09 ng/1g]}}$$

For each gene assayed with the RNA mix of the 5 cell lines, the resulting slope of the standard curves and the sample's mean Cq were used to calculate absolute transcript copy numbers (CN) in each sample:

Log_2 Copies = [(Mean Cq - C)/m], where C = y-intercept, m = slope of the curve.

Geometric mean of CN from the three reference genes were used to normalize target gene CN in each sample including healthy controls. Relative fold change of target gene expression in each sample was then calculated by a ratio of normalized CN in the sample versus the average of normalized CN from all the healthy controls.

A sample maximization strategy was used to study all 17 genes of interest and 3 reference genes in the 15 patients and 8 controls, along with the serial dilution panel of PCa cell line RNA on each plate, with water as the negative control.

2.7 Statistical Analyses

All statistical analysis was performed in R studio.

For the IHC stained benign and cancer glands, the Fisher's Exact Test was used to determine statistical significance of each NE-biomarker moving from benign to cancer. IHC bar graphs were generated from Excel.

Published transcriptomic datasets (gene microarray and RNA sequencing) were accessed through Gene Expression Omnibus for the Stanford (GSE3933) [119], Cambridge (GSE70770) [120], MSKCC (GSE21032) [121] cohorts, and cBioportal for the SU2C [122], TCGA [123], Neuroendocrine [14] and Fred Hutchinson (GSE74695) cohorts [124]. For the Stanford dataset, normalization was carried out as described in the original paper [119]. Data retrieved from the other datasets were already processed and normalized (into z-scores). All over-expression was defined as being higher than the 99.5% confidence interval of the benign samples (for Stanford, Cambridge, and MSKCC), primary tumours (for SU2C), or relative to all samples (for Fred Hutchinson and Neuroendocrine datasets). Fisher's exact test was used to compare the percentages of cases over-expressing each gene based on category of sample type, or site of metastases. Transcriptomic dataset heat maps, hierarchical clustering dendrograms, Kaplan-Meier graphs, and box plots were generated by R studio. All significance was determined by a p value ≤ 0.05. Tests used: Fisher's Exact Test and Kruskal-Wallis test with Wilcoxon pairwise comparison. Kaplan

Meier survival curve analysis, combined with COX univariate and multivariate survival analysis were carried out for the MSKCC dataset. Hierarchical clustering for each gene of interest was performed per dataset through the advanced heat map R Studio coding of dendrograms.

The RT-qPCR bar graphs, standard deviations and heat maps were generated by Excel, boxplots were generated by R studio. Gene over-expression was determined by using a threshold of 2.58 standard deviations above the mean expression of that gene in blood RNA samples from volunteers, to ensure with 99.5% confidence that expression in controls was lower than this threshold.

To detect whether patients or treatment characteristics were associated with over-expression of individual markers, all the characteristics were dichotomized, and differences were evaluated using Chi-square tests in 2x2 tables. Survival analyses for disease progression and death were performed using the Cox proportional hazards model. If no event had occurred, patients were censored at the last date they were known to be alive and/or without disease progression, either clinical (worsening of symptoms: fractures, pain), biological (PSA rising in two subsequent measurements), or radiological (new lesion or increased size of existing lesions). Results with $p < 0.05$ were considered significant.

To analyze and rank the best possible NE signature or pattern found from the liquid biopsy and datasets, both frequency, intensity and mean values were weighted and used to score each NE transcript. Each cofactor holds different weights of importance: frequency (80%), maximum point intensity (10%), mean of intensity (10%).

Chapter 3

Epithelial Cells in Benign Glands and Cancer Foci Differentially Express NE-Related Products

3.1 Variation of expression in the NE cell subtypes

To assess the NED patterns in the prostate of patients, we analyzed consecutive sections from 10 hormone-treated patients prior to their RP. Sections had been stained for two to five NE-markers: CHGA, NSE, SYP, CALCA, 5-HT.

Five out of the ten patients (3, 5, 6, 7, 9) had consecutive slides stained for all the five markers; patient 8 had four stained for the same NE markers, excluding CALCA; patients 2 and 10 sections were stained for CHGA, NSE, and CALCA; patient 1 sections were stained for CHGA, NSE, and SYP; patient 4 sections were stained with CHGA and SYP.

All of the patients' slides were positively stained for at least one marker in either the benign gland or cancer foci. Interestingly, even though there were many similarly stained cells, there were no two stains that contained the exact same pattern. This suggests a variation in the phenotypes of cells belonging to the NE subtype, with some markers

being favourably expressed in certain NE cells. This is exemplified nicely in benign acini, illustrated in Figure 3.1, wherein two positively stained cells are seen in CHGA, but lost in NSE, SYP, CALCA, and 5-HT.

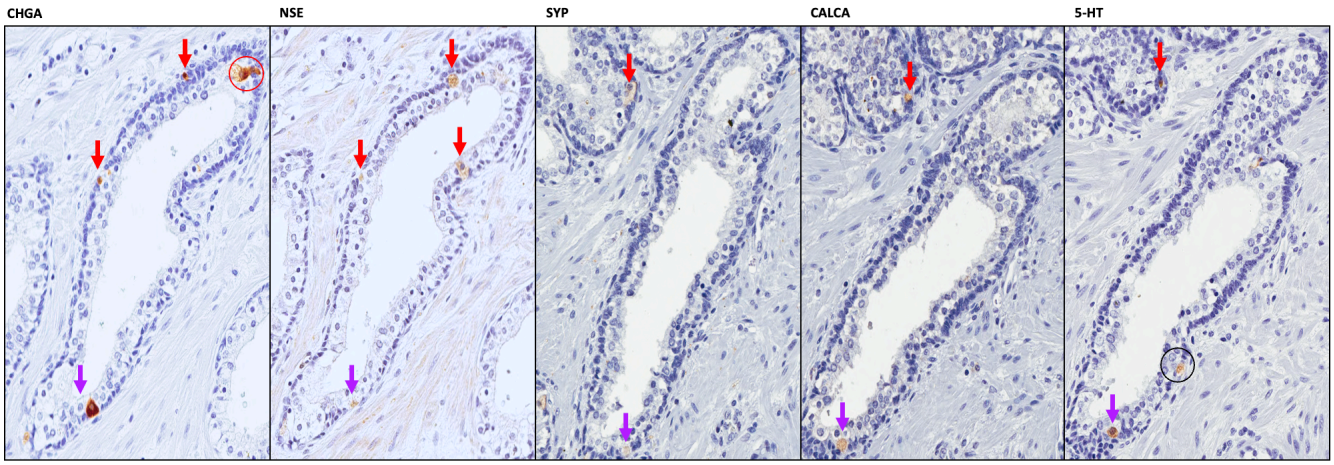

Figure 3.1: Example of consecutive benign glands exemplify NE cells of varying phenotypes

Patient 7 shows NED heterogeneity of benign areas from the same block. From left to right: CHGA, NSE, SYP, CALCA, 5-HT. Circled cells are unique, whereas the arrows show some of the similar cells in each marker.

Areas of stained cancer foci are shown in Figure 3.2 exemplifying sections from patient 4, whereby the NE cells in cancer foci express only a subset of known NE markers, creating various patterns. Several cells that are positively stained in the CHGA slide are found to be negative in the SYP slide. On the right, top and bottom panels, the cells exemplify this well. The 4 red circled cells in the top CHGA slide are almost completely negative for the SYP stain. This cancerous nest of NE cells is a notable example of the various NE cell subsets at the molecular level that exists within one patient's tumour foci.

Figure 3.3 shows the panel of all 5 of the NE-markers for patient 3. The aligned cancer cells are intensely stained for CHGA, NSE, SYP, but completely negative for CALCA and 5-HT. The circled cell on the right appears in CHGA and NSE, but is negative in SYP, CALCA, and 5-HT. These images further corroborate the NED intra-tumoural cell subtype found in prostate cancer from hormone-treated patients.

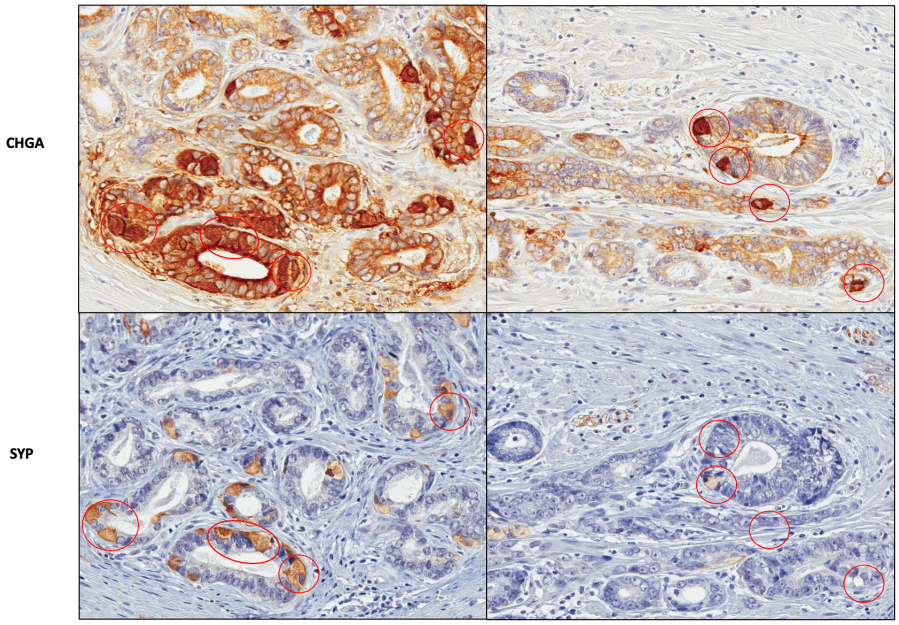

Figure 3.2: Consecutively stained cancer areas show NED heterogeneity

Patient 4 shows a variation of expression in NE cell subsets in consecutive cancerous sections from the same block. Top and bottom are consecutive slides, stained for CHGA and SYP. The red circles show similar positively stained cells.

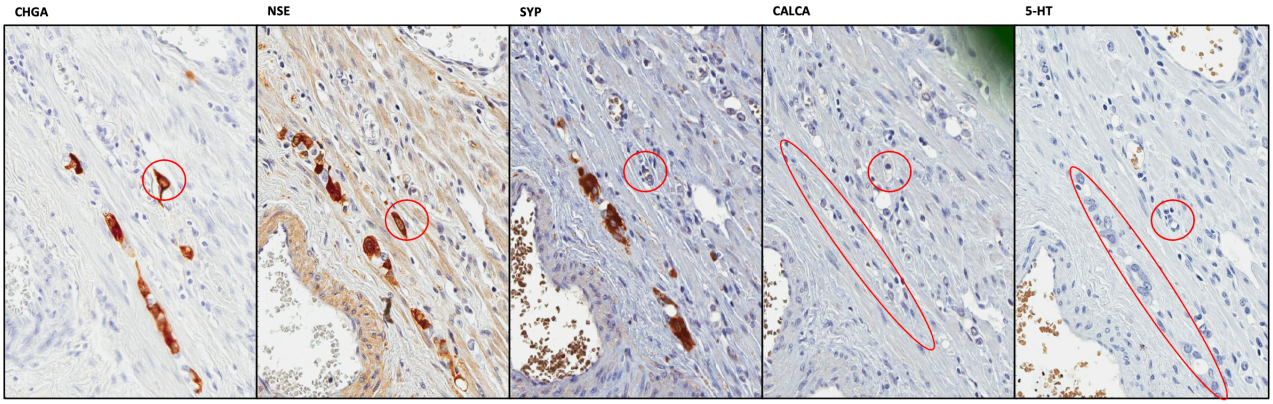

Figure 3.3: Heterogeneity in the expression of five NE markers

Patient 3 shows variation in cancerous stained NE cells of the same block. Consecutively stained slides from left to right for CHGA, NSE, SYP, CALCA, 5-HT expression. Red circle show positively stained NE CHGA+ and NSE+ cells in two sections; the red oval shows negatively stained CALCA and 5-HT cells in an intensely stained zone for the other three markers.

3.2 Unique NE patterns found in hormone-treated patients

Analysis with Fisher's Exact test highlighted the significance between each NE marker moving from benign glands to cancerous foci within each patient. Figure 3.4 shows a graphical representation of the percentage of positively stained NE cells found with each marker.

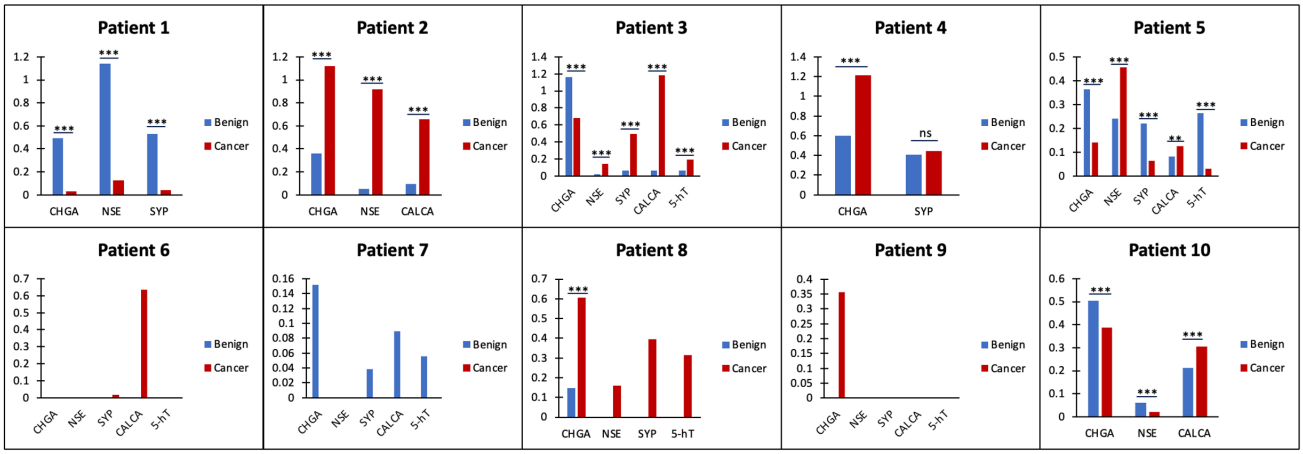

Figure 3.4: Comparison of the prostatic NE-cell patterns among patients

Patient Cases	Benign Gland	Cancer Foci
Patient 1	NSE > SYP > CHGA	NSE > CHGA = SYP
Patient 2	CHGA > CALCA > NSE	CHGA > NSE > CALCA
Patient 3	CHGA > SYP = CALCA = 5-HT > NSE	CALCA > CHGA > SYP > 5-HT > NSE
Patient 4	CHGA > SYP	CHGA > SYP
Patient 5	CHGA > 5-HT > NSE > SYP > CALCA	NSE > CHGA > CALCA > SYP > 5-HT
Patient 6	---	CALCA > SYP
Patient 7	CHGA > CALCA > 5-HT > SYP	---
Patient 8	CHGA	CHGA > SYP > 5-HT > NSE
Patient 9	---	CHGA
Patient 10	CHGA > CALCA > NSE	CHGA > CALCA > NSE

Table 3.1: NE marker expression listed by predominance in the 10 cases

Every patient portrayed unique NE marker cell patterns, with varying frequencies of expression between NE markers, as seen in summary Table 3.1. When looking at the cancer foci percentages of the 10 patients, we observed the frequency by which the NE markers came out the most expressed, with CALCA (n=2/7, 28.5%) > CHGA (n=2/10, 20%) > NSE (n=1/9, 11.1%) > SYP = 5-HT (0%). There were 10 unique profiles found with the expression of the 5 NE markers. No two patients contained the same frequency, or predominance of expression. We observed 9/10 (90%) patients expressing at least one of the NE markers in the cancer foci.

The pattern of NE marker predominance in benign glands was notably different. The most frequently expressed marker was CHGA (n=7/10 cases, 70%) > NSE (n=1/9, 11.1%). SYP, CALCA, and 5-HT were never the most expressed in any benign glands of cases. There were 8 unique profiles found in the expression of the 5 NE markers. We observed 8/10 (80%) patients expressing at least one of the NE markers in the benign glands.

These overall patterns are indicative of highly unique NE signatures in patients, and highlight the existence of multiple NE cell subsets. There was a significant differential expression ($p \leq 0.0005$) between benign glands and cancer foci. Of note, the NE marker expression in cancer foci was not always higher than that of the benign. For instance, patient 1 shows a significant differential expression for NSE (p=3.6e-168), > CHGA (p=1.28e-96) > SYP (p=4.33e-93) in NE cells in benign vs. cancer foci. Interestingly, this patient's benign glands were more positively stained than the cancerous cells. NSE proved to be the most effective marker (1.14% positively stained) for identification ofNE cells in this particular prostate block. Conversely, patient 2 exhibits an inverse pattern, with significantly more NE-stained cells in all the cancer foci compared to the benign, expressing NSE (p=3.42e-232), CALCA (p=4.49e-107), and CHGA (p=2.03e-82). CHGA was the best NE marker present in both cancer foci and benign glands, comprising 1.1% of positively stained cells.

When looking at patient 3 in Figure 3.4, there is a significant differential expression for four of the five NE markers in cancer foci vs. benign glands, CALCA (p= 2.61e-92)

$>$ SYP (p=7.46e-28) $>$ NSE (p=9.95e-09) $>$ 5-HT (p=4.17e-06). For this patient, the most positively stained NE cells in cancer were expressing CALCA (1.18%), while the most positively stained benign cells were CHGA+ (1.16%). Both patients 3 and 6 had CALCA as the highest expressed NE marker in the cancer foci.

Patient cases 3, 5, 6, 7 and 9 were tested with all 5 NE markers, and each contain a unique signature of NE markers in both the benign and cancer areas. When looking at Figure 3.4, patient 7 has a contrasting signature to that of patients 6 and 9. All of patient 7's expression falls in the benign glands, whereas all of patients 6 and 9's expression falls in the cancer foci. Extrapolating from this, we can see the versatility of the NE cell phenotypes that exist within the prostate from hormone-treated cancer patients. NE cells are not exclusively found in cancer foci, or benign glands, nor are they mutually dependent on each other. Patient 4 was the only case in which there was no differential significance found within the SYP marker moving from benign to cancer cells, however CHGA still proved to be significant (p=1.56e-60).

Overall, the most percentage of positively stained cells in all the benign glands of the 10 patients were CHGA (1.16%) $>$ NSE (1.14%) $>$ SYP (0.53%). The most percentage of positively stained cells in all the cancer foci of the 10 patients were CHGA (1.21%) $>$ CALCA (1.18%) $>$ NSE (0.91%). Altogether these findings demonstrate that NE cells are present in all prostate tissues included in this study, coming from 10 patients who received neo-adjuvant therapies prior to RP. NE cells are detected in cancer and benign areas of 9 vs. 8 cases, respectively. As a whole, they constitute up to 1.5% of epithelial cells present in prostate sections and all five selected markers are detected. Inclusive of both the benign and cancer cells combined, the most predominant markers were CHGA, followed by NSE, CALCA, SYP and 5-HT. The use of a single marker is not sufficient to study this prostatic cell subtype, displaying extensive subsets of cells expressing diverse NE markers with varying combinations.

Chapter 4

In-depth Literature Review to Select NE Markers

Based on the above observations on prostatic NE cells expressing one or several combined markers, we carried out a systematic literature review to identify NE markers of interest and further to mine PCa specific transcriptomic datasets, and investigate the most relevant genes in patient liquid biopsies. Illustrated in Figure 4.1 is a flow chart of steps by which markers were selected. In the identification process, the nine NE-products previously studied in the host lab (*CHGA, GRP, GPRR, FLT1, VEGFA, CALCA, ENO2, SYP, NCAM1*) were included along with the aforementioned key words, yielding a total of 600 records to screen. Screening comprised of databases such as PubMed (n=561), NIH clinical trials (n=20), and cBioPortal (n=7). Strict exclusion criteria ensured relevance and comprehensibility during the screening process. Overall, 26 eligible NE transcripts were noted. By adding the 9 NE markers studied in the host lab, a total of 35 NE-related transcripts were chosen to conduct our search in datasets.

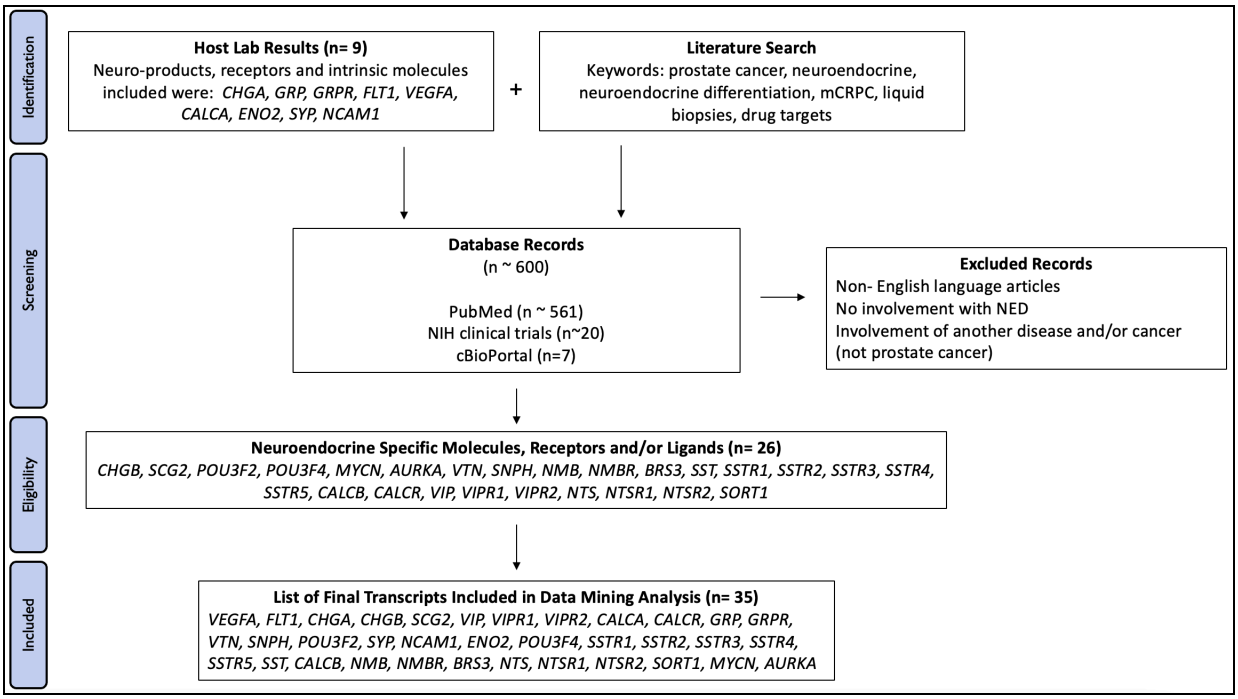

Figure 4.1: Flow Diagram of Literature Search and Inclusion Process

NE Gene Acronyms	NE Gene Full Name
VEGFA	Vascular Endothelial Growth Factor A
FLT1	FMS Related Receptor Tyrosine Kinase 1
CHGA	Chromogranin A
CHGB	Chromogranin B
SCG2	Chromogranin C (Secretogranin 2)
VIP	Vasoactive Intestinal Peptide
VIPR1	Vasoactive Intestinal Peptide Receptor 1
VIPR2	Vasoactive Intestinal Peptide Receptor 2
CALCA	Calcitonin A
CALCR	Calcitonin B
GRP	Gastrin Releasing Peptide
GRPR	Gastrin Releasing Peptide Receptor
VTN	Vitronectin
SNPH	Syntaphilin
POU3F2	POU Class 3 Homebox 2
SYP	Synaptophysin
NCAM1	Neural Cell Adhesion Molecule 1
ENO2	Neuron Specific Enolase
POU3F4	POU Class 3 Homebox 4
SSTR1	Somatostatin Receptor 1
SSTR2	Somatostatin Receptor 2
SSTR3	Somatostatin Receptor 3
SSTR4	Somatostatin Receptor 4
SSTR5	Somatostatin Receptor 5
SST	Somatostatin
CALCB	Calcitonin B
NMB	Neuromedin B
NMBR	Neuromedin B Receptor
BRS3	Bombesin Receptor Subtype 3
NTS	Neurotensin
NTSR1	Neurotensin Receptor 1
NTSR2	Neurotensin Receptor 2
SORT1	Sortilin 1
MYCN	MYCN Proto-Oncogene
AURKA	Aurora Kinase A

Table 4.1: An inclusive list of all the genes of interest, including their acronyms and full gene name

4.1 Mining of transcriptomic datasets reveals a correlation between NE gene over-expression and progression of disease

In order to gain insights on the most over-expressed NE-related genes in PCa development and stage of disease, we mined three microarray datasets, known as Stanford [119], Cambridge [120], and MSKCC [121] comprising 141 benign prostates, 310 primary tumours removed at RP, 14 primary tumours from trans-urethral resections of the prostate (TURP) in advanced hormone-treated patients (Cambridge), 9 lymph node (LN) metastases removed at RP (Stanford) and 20 miscellaneous metastases (MSKCC). To deal with PCa progression, we analyzed the RNA-seq dataset from the SU2C metastatic cohort of advanced PCa patients [122], which include 81 metastases to LNs, 83 to bones, 16 to soft tissues/adrenals, and 27 to the liver. For each dataset, the over-expression of a gene was determined based on the 99.5% confidence interval of the mean expression level in the benign samples (Stanford, Cambridge, MSKCC) or primary tumours (SU2C; n=6). The last two datasets, the Fred Hutchinson [124] and Neuroendocrine dataset [14] did not contain samples from the benign prostate or primary tumours, and samples were then analyzed as relative to each other. Heat maps show unique patterns of over-expression moving from benign to primary to metastases in the Stanford, Cambdrige, MSKCC, and SU2C datasets, respectively. The related dendrograms help to cluster together NE genes of similar patterns of over-expression.

In the Stanford gene microarray dataset, comparisons between the benign glands and primary tumour samples show significant over-expression in two transcripts in cancer, notably *SSTR1* (p = 1.39e-08) and *AURKA* (p = 6.0e-05) in 47% and 34% of the patients, respectively. The majority of NE-transcript over-expressions within primary tumours were in the 20-40% range, as seen in Figure 4.5. LNs resected at RP significantly over-expressed five transcripts, *AURKA* (p=4.0e-09) in all 100% of patients, *SSTR1* (p=1.39e-08) in 67%,

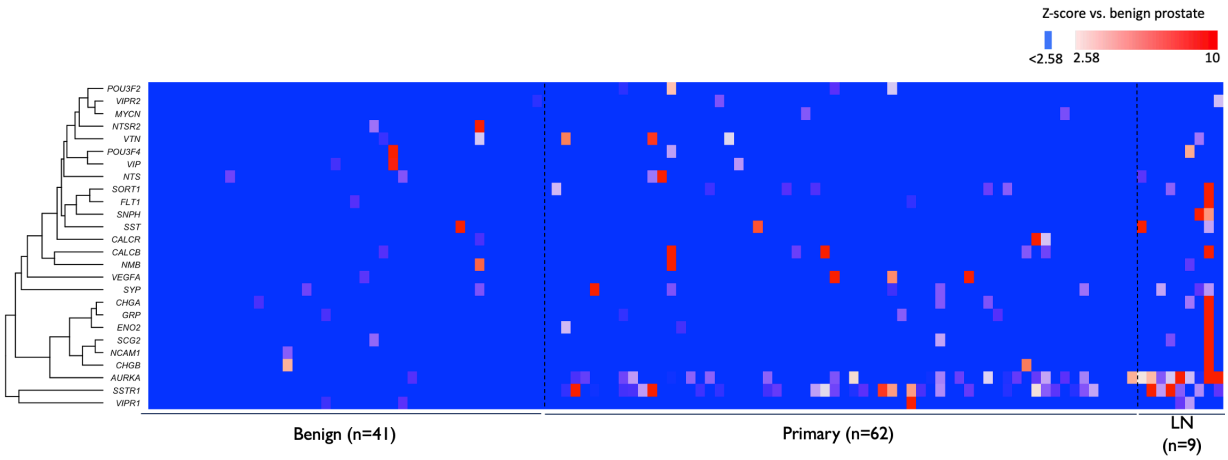

Figure 4.2: NE Gene Overexpression in the Stanford Transcriptomic Dataset
In the Stanford cohort, 9/35 NE transcripts of our list were missing: *GRPR, NMBR, BRS3, SSTR2, SSTR3, SSTR4, SSTR5, CALCA, NTSR1.*

SNPH (p=0.01) in 40%, *SYP* (p=0.02) in 38% and *SORT1* (p=0.03) in 22% compared to benign glands. As shown by the dendrogram on the left of the heat map, the two predominant transcripts *AURKA* and *SSTR1* in LNs cluster together with *VIPR1*, although less expressed. The general trend in the Stanford dataset shows more over-expression of NE transcripts as you move from benign to primary tumours to LN metastases.

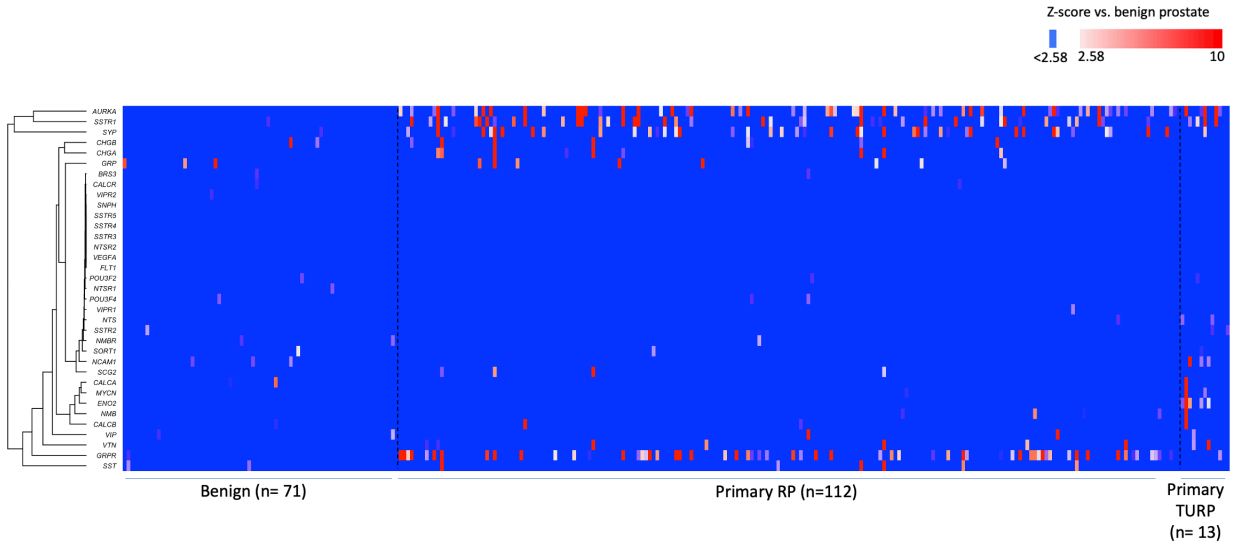

Figure 4.3: NE Gene Overexpression in Cambridge Transcriptomic Dataset

In the Cambridge gene microarray dataset, comparisons between the benign samples and primary tumours show significance in the same NE transcripts as the Stanford dataset (*AURKA* (p=1.56e-08) in 26% of the patients and *SSTR1* (p=3.26e-05) in 20%), as seen in Figure 4.5. However, the *GRPR* transcript (p=3.58e-08) ranked first, being over-expressed in 29% of tumours and *SYP* (p=1.81e-05) in 20%. In primary tumours from more advanced patients undergoing transurethral resection of the prostate (TURP), *AURKA* ranked first, being significantly over-expressed in 38% of cases ((p=3.70e-05), similarly to *ENO2* (p=3.70e-05) $>$ *SSTR1* (p=0.001) in 31%. Based on the dendrogram in Figure 4.3, there are two clusters of closely related NE-genes. The first cluster includes *AURKA, SSTR1, SYP*, while the second cluster includes *VTN, GRPR, SST*. The first cluster is similar to the cluster in Stanford, also enforcing the importance of *AURKA* and *SSTR1* over-expression in primary tumours of patients with advanced disease. The general trend in the Cambridge dataset shows more over-expression of NE transcripts as you move from the benign to primary tumours from untreated patients and to advanced TURP cases.

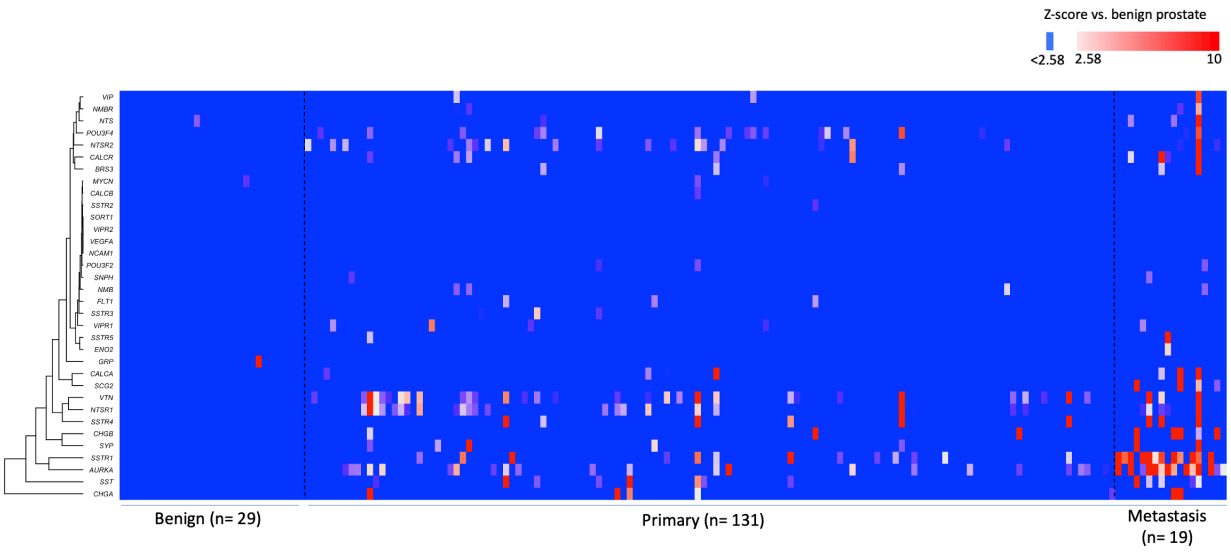

Figure 4.4: NE Gene Overexpression in MSKCC Transcriptomic Dataset

In the MSKCC dataset (gene microarray), comparisons between the benign and primary samples show significance for NE transcripts in cancer such as *NTSR1* (p=0.015) over-expressed in 18% of primary tumours, followed by *AURKA* (p=0.015) in 17% and *NTSR2* (p=0.045) in 16%. The metastatic samples displayed significantly more over-expressed NE transcripts compared to benign tissues with *AURKA* (p=2.41e-08) and *SSTR1* (p=7.23e-07) being predominant in 74% and 63% of cases, respectively. The additional NE-transcripts being over-expressed were *NTSR1, SST, CHGB* (p=0.006) in 26%, followed by *SCG2*, and *CALCR* (both at p=0.019) in 21%. Based on the dendrogram in Figure 4.4, there is one main cluster of over-expressed NE transcripts in metastases with *SSTR1, AURKA* and *SST*. In the primary tumours, *VTN, NTSR1* and *SSTR4* are closely related as well. The general trend in the mSKCC dataset is similar to the previous ones, showing an increase in over-expression moving towards advanced cases: starting with the lowest number of cases and minimal expression in the benign, followed by an increasing proportion of patients expressing NE genes in their primary tumours, and lastly the highest proportion of cases over-expressing more elevated NE transcripts in metastases growing in diverse locations.

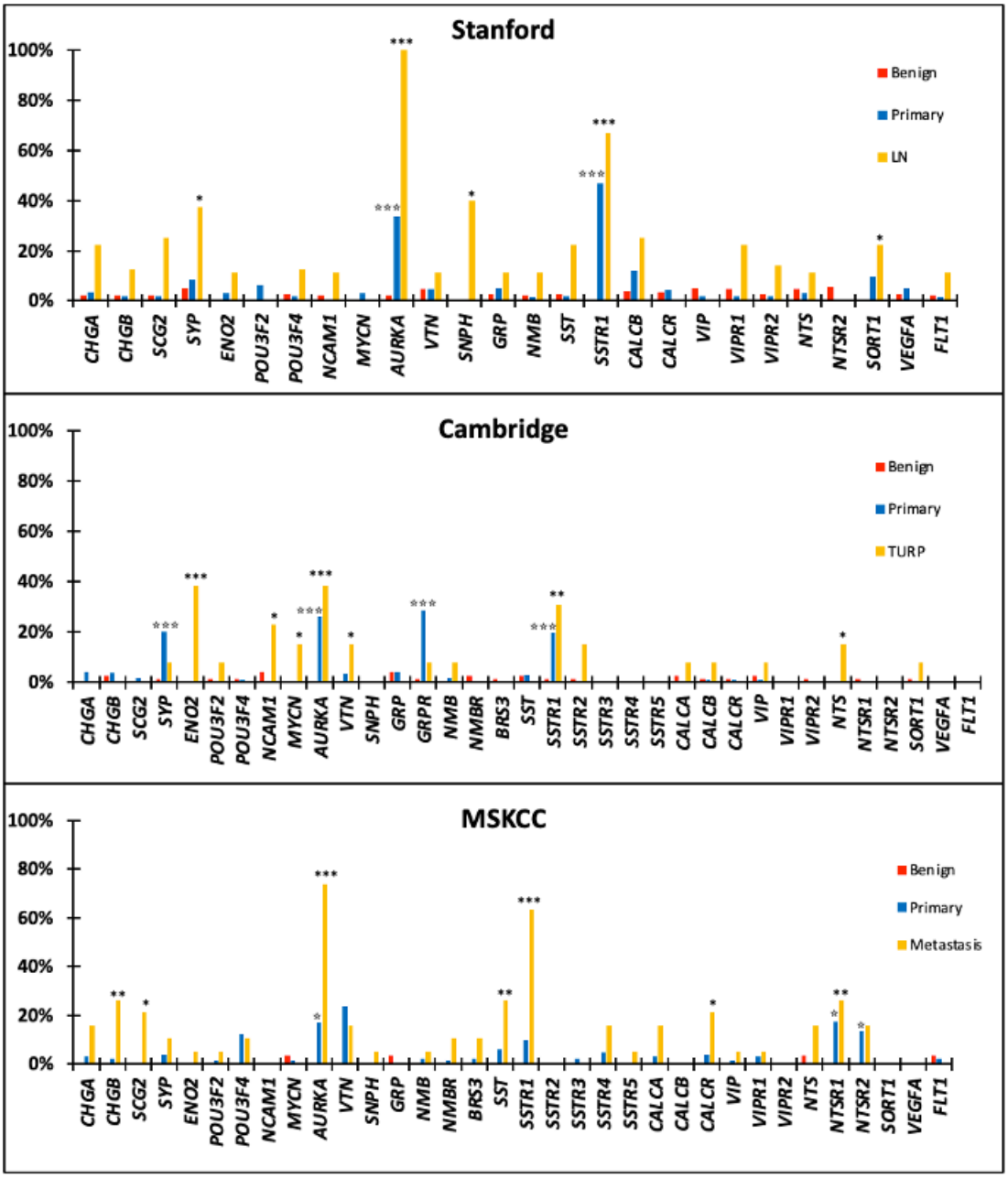

Figure 4.5: Percentage of patient over-expressing NE genes in samples included in the Stanford, Cambdrige, and MSKCC cohorts and datasets

When comparing the three previously described datasets, each contains a comparatively similar cohort of primary tumours. Figure 4.5 shows similarities between the percentages of patients over-expressing NE genes in the samples analyzed. The most commonly NE transcripts that come up often in the three cohorts are $AURKA > SSTR1 > SYP$.

Each of these three cohorts also contained samples related to more advanced cases (Stanford= LN metastases, Cambridge = TURP, MSKCC = multiple metastases of un-ifentified locations), in which some of the over-expressed NE transcripts are also similar. For example, all of the advanced cohorts contain *AURKA* > *SSTR1* as the highest over-expressed transcripts. The TCGA (RNA sequencing) dataset did not provide insightful information, as they had only one cohort of patient samples, being all primary. Our NE markers were over-expressed by less than 10%. No statistical analyses were performed for this specific cohort.

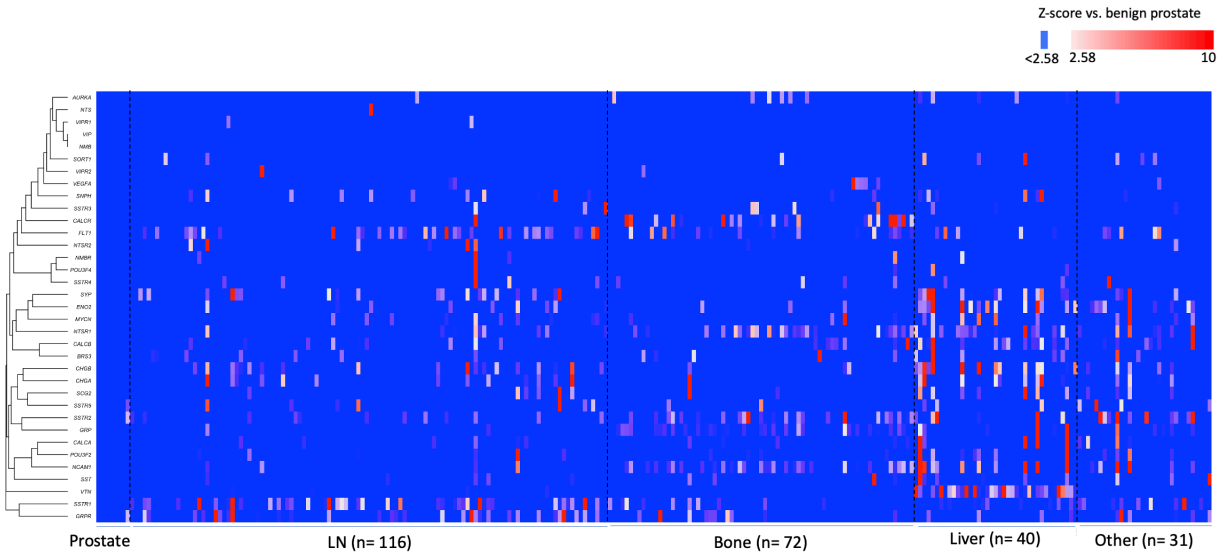

Figure 4.6: NE Gene Overexpression in SU2C Transcriptomic Dataset

In the SU2C dataset (RNA sequencing of metastases from patients with advanced disease), overall relative comparisons were made between the diverse sites of metastases (bone, liver, LN, and other soft tissue). For each site of metastasis, the most over-expressed NE marker was *VTN* ((p=2.2e-16) at 95% in the liver, *GRP* (p=1.30e-10) at 44% in the bone, and *SSTR1* (p=0.02) at 35% in both the LN, and other soft tissues. Looking at all the metastatic sites as a whole, most of the chosen NE transcripts (n= 33/35, 94%) were over-expressed in at least one of the locations. The two transcripts that were not found to be over-expressed by any site was *NMB* and *VIP*. Of the selected NE transcripts, the sites where they were most over-expressed were the LNs for 94% of the genes (33/35), in

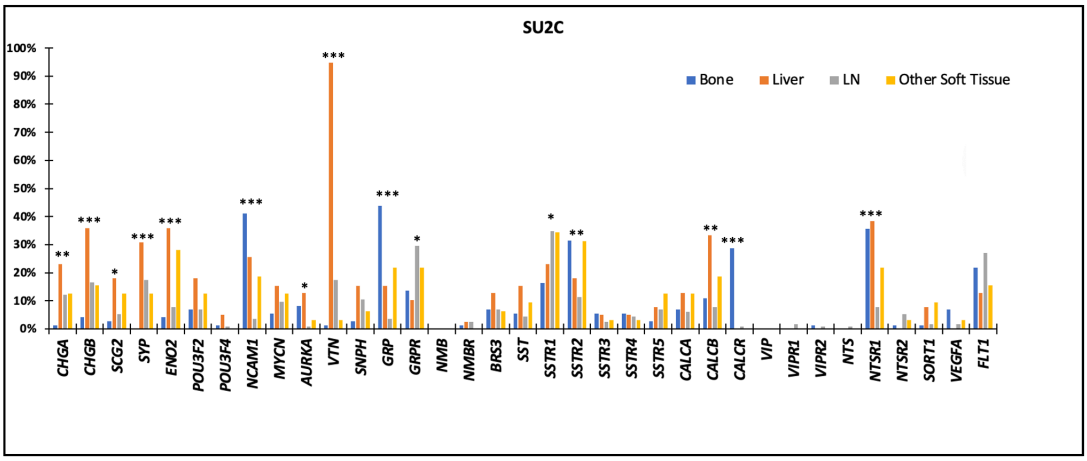

Figure 4.7: Percentage of patients over-expressing each NE transcript in SU2C cohort
P-values from left to right: *CHGA* (p=0.003), *CHGB* (p=0.003), *SCG2* (p=0.03), *SYP* (p=6.71e-05), *ENO2* (p=4.64e-06), *NCAM1* (p=8.69e-10), *AURKA* (p=0.01), *VTN* (p=2.2e-16), *GRP* (p=1.29e-10), *GRPR* (p=0.02), *SSTR1* (p=0.02), *SSTR2* (p=0.003), *CALCB* (p=0.003), *CALCR* (p=4.20e-10), *NTSR1* (p=1.9e-06).

bones for 85.7% (30/35), in soft tissues for 80% (28/30) and lastly in the liver with 77% (27/35) of the NE transcripts. Based on the aforementioned percentages, the metastatic site that contained the most frequent amount of over-expression was LN. In like to the Stanford dataset, the *SSTR1* is the most over-expressed transcript found in the LN.

The dendrogram displayed in Figure 4.6, shows multiple clusters. One cluster that stood out the most as being highly over-expressed was between *SSTR1* and *GRPR*. Also, the main cluster in the middle containing *SYP, ENO2, MYCN, NTSR1, CALCB, BRS3* are all highly over-expressed in the liver and other soft tissues. Interestingly, *AURKA, NTS, VIPR1, VIP, NMB* cluster together at the top, and are all not highly over-expressed at any metastatic site. As previously seen in the primary cohorts, *AURKA* and *SSTR1* seemed to be a predominantly important NE transcript for the primary samples, however we see it less when moving towards the metastatic samples. Of note, the most significant NE genes over-expressed in this series of metastases also differ from the predominant genes observed in the small series of metastases of the MSKCC cohort.

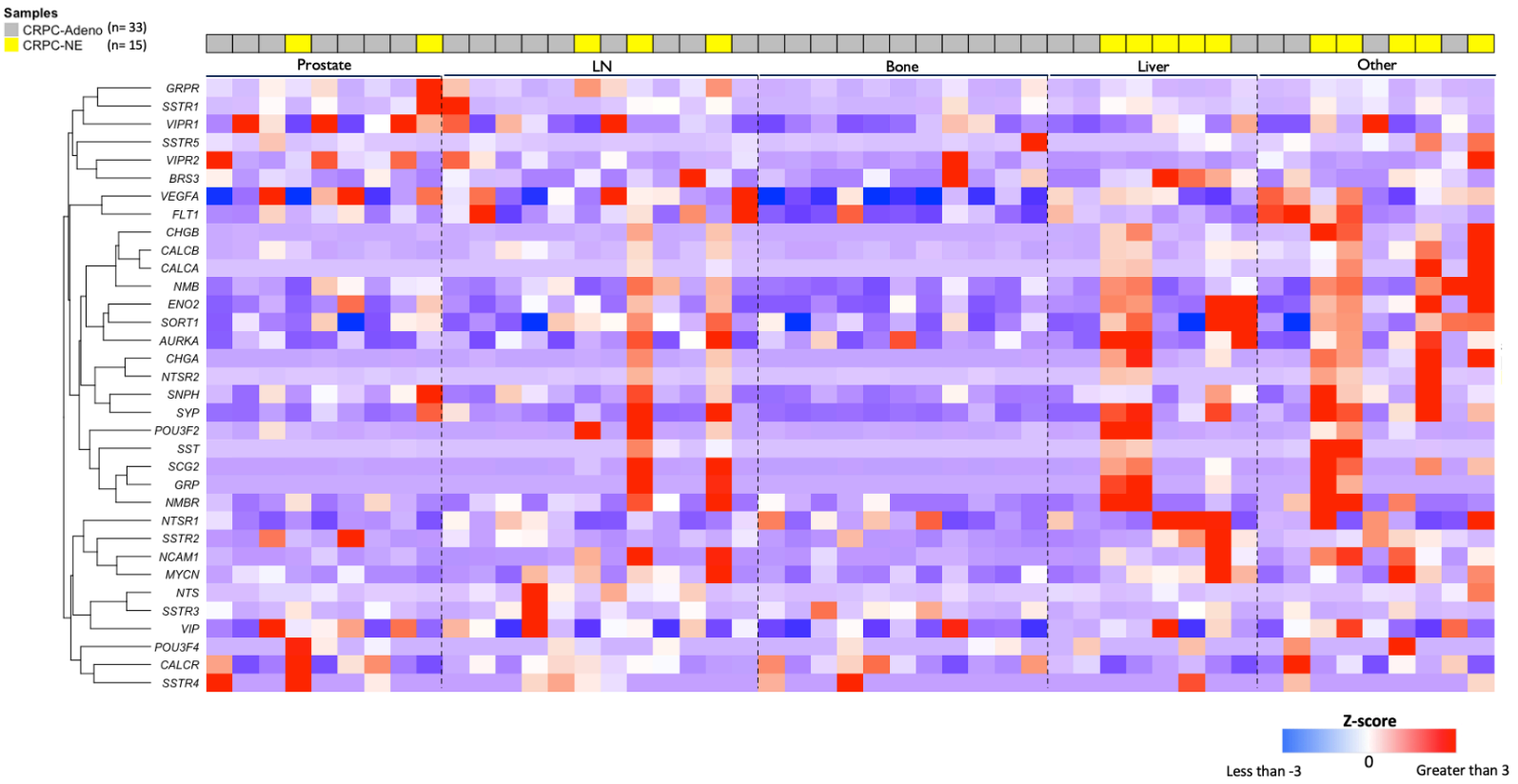

Figure 4.8: NE Gene Overexpression in Neuroendocrine Transcriptomic Dataset

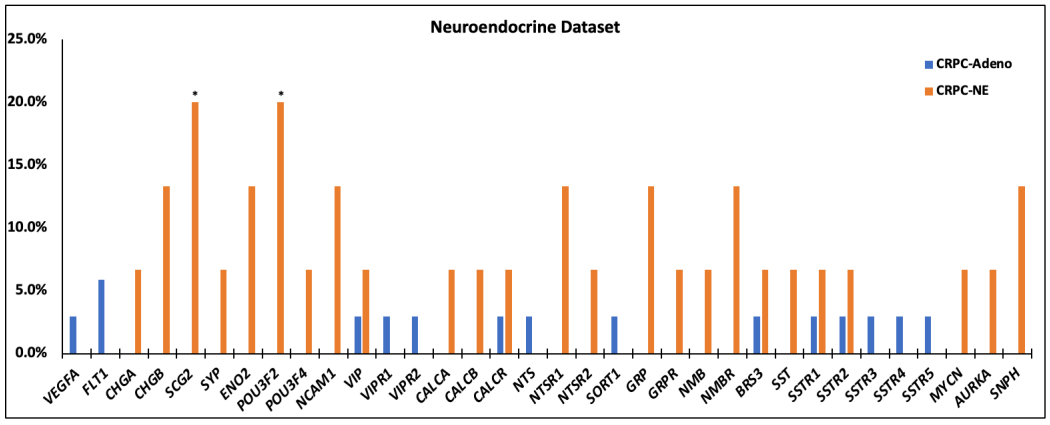

Figure 4.9: Percentage of patients over-expressing each NE transcript in the neuroendocrine dataset

The RNA sequencing dataset by Beltran et al., [14] classifies PCa patients into conventional adenocarcinoma (CRPC-Adeno), or neuroendocrine like CRPC (CRPC-NE) based on pathological morphology guidelines [51]. No benign samples were provided in this dataset, however there were prostate samples and varying sites of metastasis (LN, bone, liver, others). Over-expression was based on the relative comparison of z-scores, and not towards the primary prostate samples because of the low sample number (n=9). In the heat map illustrated in Figure 4.8, the samples are categorized by site of metastases: LN, bone, liver, and other soft tissues. Interestingly, the highest proportion of expressed transcripts was in the CRPC-NE liver metastases (62.5%), followed by soft tissues (55.5%), prostate (22.2%), LN (25%), Bone (0%). Furthermore, and as expected, the majority of NE genes that were the most expressed were seen in the CRPC-NE cases, with a significant differential over-expression of *CHGA* (p=0.02), and *POU3F2* (p=0.02), both at 20% in Figure 4.9.

An interesting observation made with this dataset was that 14/35 (40%) of the selected NE genes were over-expressed in the metastatic CRPC-adeno cases. This is a substantially different result compared to the previous SU2C and MSKCC dataset. In the previously mentioned datasets, almost 100% of the selected NE genes were found to be over-expressed in various sites of metastasis (with very few exceptions). When looking at the dataset by Beltran, et al., very few of the selected genes (14.2%) were found in both CRPC-adeno and CRPC-NE cases. This confirms that with disease progression towards a CRPC-NE state, more NE genes are exclusively over-expressed, compared to the conventional CRPC-adeno cases.

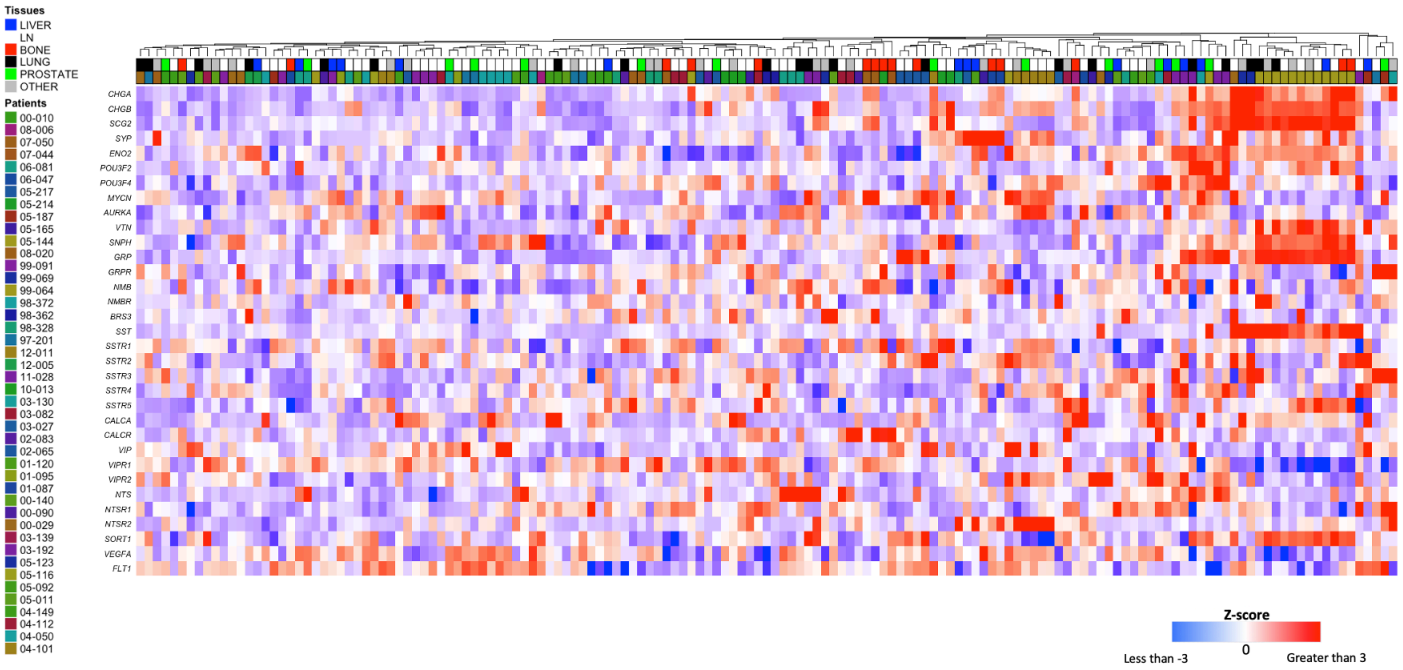

Figure 4.10: NE Gene Overexpression in Fred Hutchinson Dataset

The Fred Hutchinson dataset provides patient samples that contain multiple metastases, of which we verified if paired metastases might express the same NE gene pattern or signature. The cohort contains a total of 171 tumour samples collected at autopsy of 63 treated mCRPC, whose death was identified as PCa-specific [124]. We focused on the 44 patients who had at least two lesions and up to 14 in one patient. The heat map, Figure 4.10, shows the hierarchical clustering of the diverse metastases for the 35 NE genes. Of note, two main patterns were observed:

(1) a single patient may have lesions displaying a highly homogenous gene signature in multiple metastases to one site (as seen in the LN mets of patient 06-081) or else, metastases to various sites clustering together (patient 04-101, with 12 different metastases to 6 different sites).

(2) a single patient may contain lesions displaying a highly heterogeneous gene signature in multiple metastases to one site (as seen in the LN mets of patient 11-028). Moreover, we observed that metastases to the same site from different patients also clustered together (bone metastases from 07-050,01-010, and 07-044).

Looking at the heat map for this cohort, we can express the amount of positive relative z-scores as percentages. The most expressed NE transcripts found were *FLT1* (55%) > *VEGFA* (54%) > *SSTR1* (53%) > *VIPR1* (52%).

Collectively, these findings are in support of prostatic NE cells differentially expressing specific transcripts, according to types of lesions, e.g. primary tumours vs. metastases at various sites, and stages of disease. Moreover, the number of over-expressed NE transcripts also increases with progression, being often differentially expressed and more abundant in the various metastases of more advanced cases than in primary tumours from RP cases. A conclusive pattern was that NE genes in the primary tumours from TURP cases were closely related to metastases of advanced cases, whereas those LNs from RP cases are closer to the primary tumours from RP.

The two summary Tables below summarize the main findings on patterns found in the various datasets. When analyzing the datasets, we wanted to determine how often each of the 35 NE transcripts were expressed, and by how much they were over-expressed. Table 4.2 presents the most frequently over-expressed NE transcripts based on samples analyzed in each dataset or cohort (sample), whereas Table 4.3 presents them based on the most intense over-expression.

There are many similarities between frequency and intensity of over-expression. Within the primary tumour samples: *SSTR1, SYP, AURKA, SST*, are the most common to both Tables in the RP cohorts, *SSTR1* is common in the TURP primary tumour samples and also appears highest in frequency and intensity. However, when looking at the LNs from Stanford, the top five most frequent and most intense NE transcripts are not similar. *AURKA* is the only similar transcript that appears both frequently and intensely in the LNs resected at RP. Within the metastatic samples, there exists a high variation of over-expression. This variety of expression of NE marker transcripts enforces the conclusion that there exists multiple cell phenotypes in the NE subtype.

Datasets	Primary Tumours		Metastases				
	RP	TURP	LN/ RP	CRPC/ mixed locations			NEPC/ mixed locations
Stanford: Gene microarray, 2004	SSTR1> AURKA> CALCB> SORT1>SYP		AURKA >SSTR1 > SNPH >SYP >CALCB				
MSKCC: Gene microarray, 2010	VTN> NTSR1> AURKA> NTSR2> POU3F4			AURKA>SSTR1> CHGB =SST =NTSR1			
TCGA: RNA Seq., 2015	AURKA=GRP= SST> SYP						
Cambridge: Gene microarray, 2015	GRPR> AURKA> SYP= SSTR1	ENO2= AURKA> SSTR1> NCAM1> SSTR2					
Neuroendocrine: RNA seq., 2016				FLT1			SCG2=POU3F2> CHGB=NCAM1= GRP
Hutchinson: Gene microarray, 2016				FLT1 > VEGFA > SSTR1 > VIPR1			
SU2C: RNA Seq., 2019				**LN:** SSTR1 > GRPR > FLT1 > SYP >CHGB	**Bone:** GRP > NCAM1 > NTSR1 > CALCR > FLT1	**Liver:** VTN > NTSR1 > ENO2 = CHGB = CALCB	**Other Soft Tissue:** SSTR1 > SSTR2 > ENO2 > GRPR = NTSR1

Table 4.2: Frequency of the most over-expressed NE transcripts in published prostatic datasets

Datasets	Primary Tumours		Metastases				
	RP	TURP	LN/ RP	CRPC/ mixed locations			NEPC/ mixed locations
Stanford: Gene microarray, 2004	VIPR1 > SYP > NMB > VEGFA > SSTR1		CHGA > GRP > ENO2 > NCAM1 > AURKA				
MSKCC: Gene microarray, 2010	SST > AURKA > SSTR4 > VTN > CHGA			CHGA > SSTR1 > CALCA > AURKA > BRS3			
TCGA: RNA Seq., 2015	NTSR2 > VIP > SST > POU3F2 > CALCB						
Cambridge: Gene microarray, 2015	AURKA > NMB > VTN > SSTR1 > CALCA	SST > SSTR1 > SYP > VIP > VTN					
Neuroendocrine: RNA seq., 2016				NTS > SSTR3 > SSTR5 > SSTR1 > SSTR4			NTSR2 > GRPR > CALCB > CALCA >POU3F4
Hutchinson: Gene microarray, 2016				VTN > NCAM1 > POU3F2 > SST > CALCR			
SU2C: RNA Seq., 2019				**LN:** NMBR > POU3F4 > NTSR2 > SSTR4 > SSTR3	**Bone:** SST > SCG2 > MYCN > SSTR2 > VEGFA	**Liver:** GRP > BRS3 > CALCB > CHGA > CALCA	**Other Soft Tissue:** NTSR1 > MYCN > SYP > SSTR2 > NCAM1

Table 4.3: Intensity of the most over-expressed NE transcripts in published prostatic datasets

Chapter 5

Over-expression of Circulating NE-related Transcripts in PCa

5.1 NE-related transcripts are expressed in human PCa cell lines

Out of the 35 NE-related transcripts analyzed in the published datasets, 17 of the most representative over-expressed genes were chosen to continue studying in cell lines and patient blood. Based on a compromise between the levels of over-expression in both intensity and frequency (Tables 4.2, and 4.3), the chosen NE-related transcripts were: *CHGA, CHGB, SCG2, SYP, ENO2, NCAM1, POU3F2, MYCN, AURKA, GRP, GRPR, VEGFA, FLT1, CALCA, CALCR, SST, SSTR2*. These NE-related genes were each found to be either the most frequently expressed, or most intensely expressed in the dataset analyses.

Figure 5.1 illustrates the NE transcripts expression levels in each cell line, AR-positive LNCaP and 22Rv1, and AR-negative PC-3, DU145, NCI-H660. The chromogranin family of transcripts (*CHGA, CHGB, SCG2*) showed similar expression, in that they were all highly expressed in the NCI-H660 cell line, and somewhat expressed in the 22Rv1 cell line. Other intrinsic molecular NE markers like *POU3F2, SYP, ENO2, AURKA, MYCN*

were also seen in the NCI-H660 cell line. All of these aforementioned NE transcripts were also expressed, but at low levels in the PC-3 cells. Interestingly, *AURKA* was mostly expressed in DU145, compared to NCI-H660.

When looking at the lower panel of Figure 5.1, we see NE-product transcripts and their respective receptors. Out of all the NE-transcripts presented in this panel, *VEGFA* and *SSTR2* are the only two markers present in all the five PCa cell lines, while the others are not. We also see more variation here in the most expressive cell lines. *VEGFA* and *CALCR* are most commonly expressed in DU145, while *GRPR* was found highly expressed in PC-3 cells. Overall, most of the cell gene expression was found in the AR-independent cell lines.

Even though NCI-H660 is the most expressive cell line, some NE genes are predominant in other cell lines. Figure 5.2 shows the mixture of all cell lines in a serial dilution, with the corresponding R^2 values, and slopes. Equal fifths of each PCa cell line was represented during the dilutions. All 17 NE genes of interest, as well as 3 reference genes *RPLP0, PGK1, PPIB* were successfully detected in each of the mixed cell line serial dilutions, providing a positive inter-calibrator between the qPCR plates.

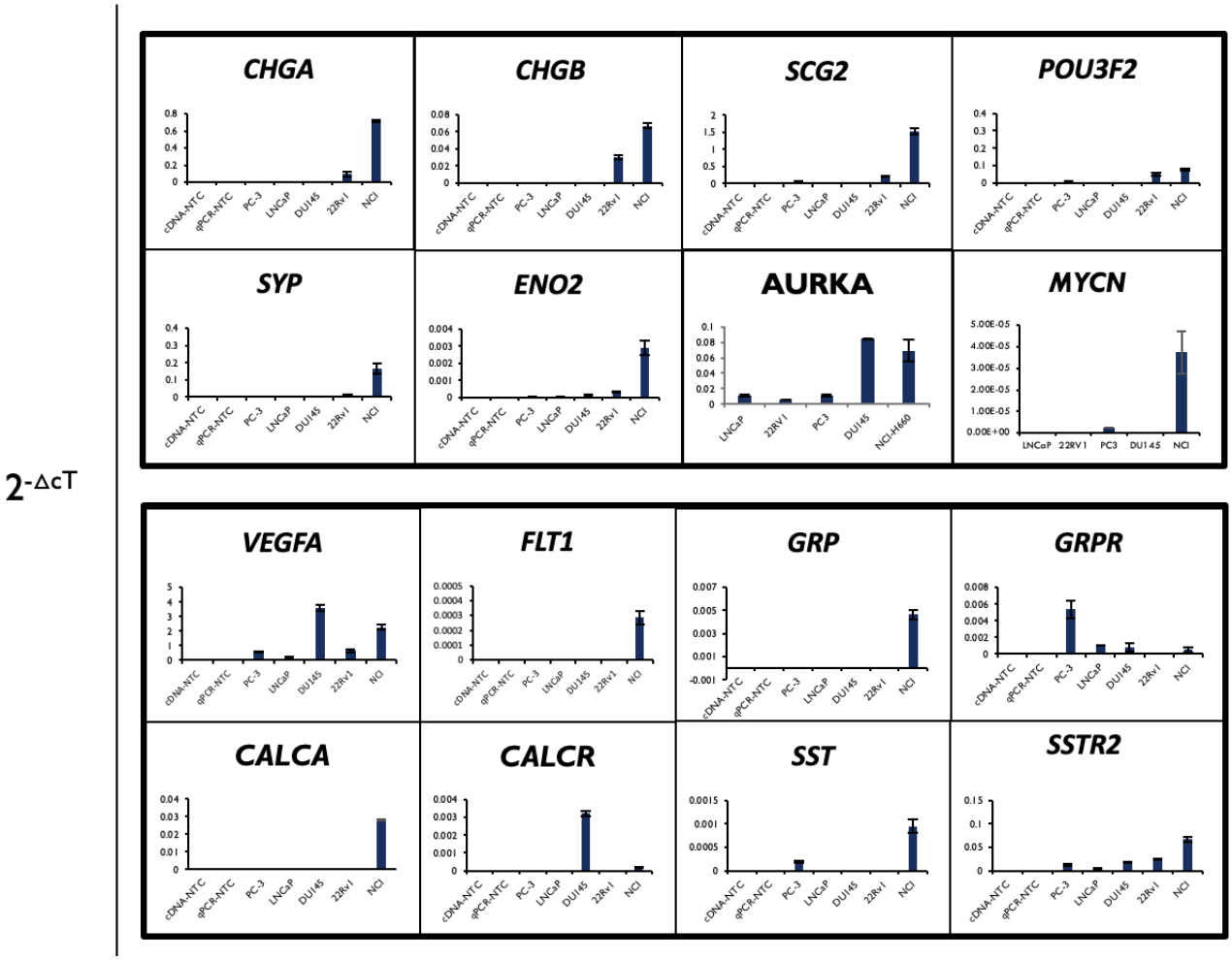

Figure 5.1: Optimization of RT-qPCR assays in 5 Human PCa Cell Lines

16 NE genes of interest; note: *NCAM1* assay testing in cell line was previously done in a prior project, by another colleague, and is not included here.

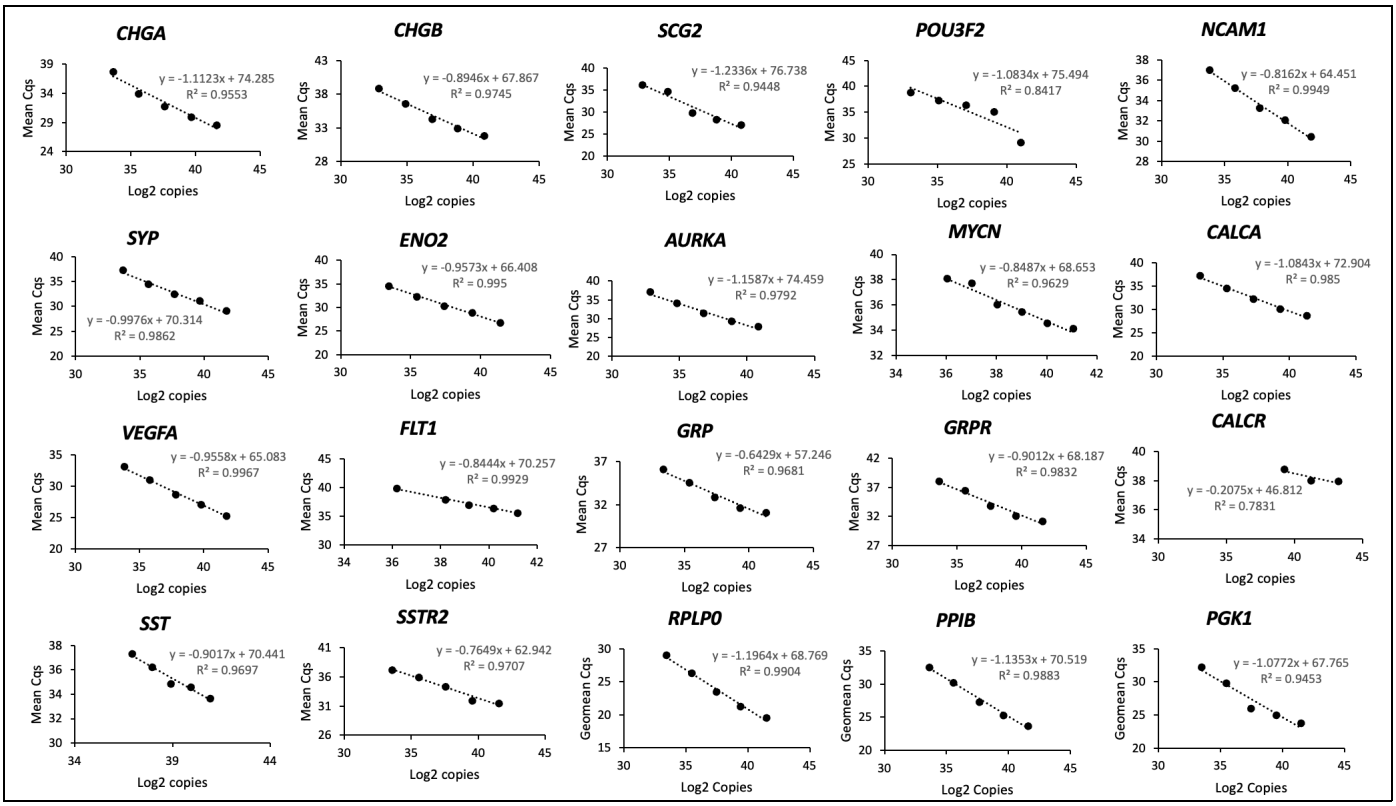

Figure 5.2: Serially Diluted Mixed Cell lines represented in each of the 17 NE genes of interest and 3 references genes.

5.2 Clinical characteristics of patients

The characteristics of patients enrolled in this stsudy are displayed in Table 5.1. The 15 mCRPC patients were all advanced cases with 5 on second line therapies and 10 on third lines therapies. 7/15 (46.6%) of patients were already metastatic at diagnosis, whereas 8/15 (53.3%) had received initial curative treatments (62.5% surgery, and 37.5% radiation). Metastases were primarily found in bones (14/15, 93.3%) and LNs (6/15, 40%).

All of the patients were on systemic therapies against mCRPC: 6.6% received only ADT, while 33.3% received Abiraterone as well. Other treatments included 9 patients on chemotherapy (comprising 66.6% Docetaxel and 33.3% Cabazitaxel).

Parameters			**mCRPC Patients (n=15)**
Age, median (range), years			71 (52-85)
PSA, median IQR, ng/mL			20.23 (1.2-38.8)
Gleason score at biopsy	6		0 (0%)
	7		4 (26.6%)
	8		1 (6.6%)
	9		6 (40%)
	10		2 (13.3%)
	Not reported		1 (6.6%)
Treatment of initially localized disease (n=8)	Surgery		5 (62.5%)
	Curative Radiotherapy		3 (37.5%)
Treatment of initially metastatic disease (n=7)	ADT		7 (100%)
	ADT + palliative RT		2 (28.6%)
	ADT + CT		2 (28.6%)
Time, median IQR, in months	Time diagnosis to CRPC		30 (12-87)
	Time CRPC to inclusion		22.5 (12-33)
Metastatic Site	None		0 (%)
	Bone		14 (93.3%)
	Visceral		2 (13.3%)
	LN alone		6 (40%)
	LN + Bone		5 (33.3%)
Current Line of mCRPC Therapy	2nd line		5 (33.3%)
	3rd line		10 (66.7%)
Current Treatment	ADT only		1 (6.6%)
	AR inhibitors	Abiraterone	5 (33.3%)
		Enzalutamide	0 (0%)
	Taxanes	Docetaxel	6 (40%)
		Cabazitaxel	3 (20%)
Progressive Disease			8 (53.3%)

Table 5.1: Baseline clinical features of 15 mCRPC patients

5.3 Over-expression of NE-related transcripts in the blood of 15 mCRPC patients and 8 healthy controls

Upon verification of expression in all 5 human PCa cell lines, the 17 NE genes were then tested in the blood RNA of mCRPC patients (15) and (8) healthy controls of varying age. Important to note and as shown for each gene in Appendix 1, the normalized expression of NE transcripts did not correlate with age of controls. These mean normalized expression values of controls were used to determine the threshold of over-expression for each gene as presented in Table 5.2. Appendix 1 shows the normalized expression of all NE transcripts within the blood RNA of the 15 patients. There were five NE genes for which there was no signal in both the controls and patients (*CHGA, GRP, CALCA, CALCR* and *SST*), leaving a remainder of 12 expressed NE genes of interest. Each boxplot below in Figure 5.3, shows the relative normalized gene expression, with the over-expression threshold defined above for each gene. *VEGFA* was the most frequently over-expressed, namely in 26.6% (n=4/15) patients, followed by *SYP, AURKA, FLT1, SSTR2* in 20% (n=3), *NCAM1, POU3F2, MYCN* in 13% (n=2/15), and *CHGB, GRPR* in 6% (n=1). *SCG2* was not over-expressed in these 15 mCRPC patients. Hence, altogether, 10 out of the 17 NE genes selected were found over-expressed in the blood RNA of a majority of mCRPC patients compared to controls.

NE Transcript	Normalized Threshold Values
AURKA	1.08e+11
MYCN	1.76e+11
FLT1	2.18e+13
SCG2	2.01e+10
CHGB	1.52e+10
ENO2	6.88e+11
NCAM1	7.90e+11
POU3F2	3.04e+10
SSTR2	5.19e+11
SYP	5.59e+10
GRPR	2.22e+11
VEGFA	9.57e+10

Table 5.2: Threshold values for each NE gene of interest
An over-expression threshold was defined for each gene by the mean in controls + 2.58 SD (standard deviations) for a confidence interval of 99.5%.

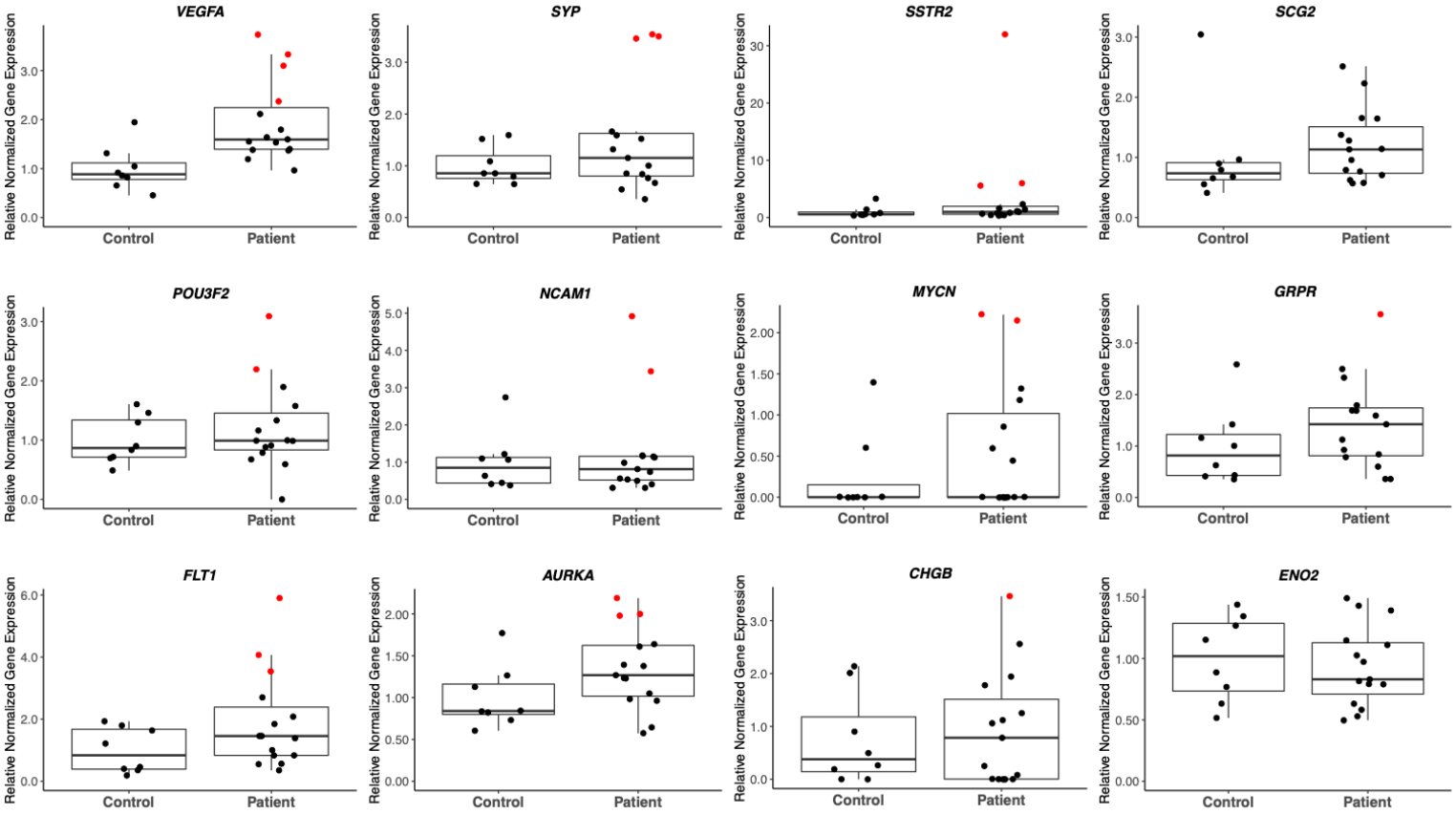

Figure 5.3: Relative normalized gene expression of 12 NE transcripts in patients vs. controls.

Given the data above on circulating genes in patients, a heat map was constructed to illustrate the distribution of circulating NE-related transcripts in each patient, as seen in Figure 5.4. The heat map below reveals a high level of heterogeneity among patients with over-expressed NE genes in the blood. At least one gene was over-expressed in 66.6% (n=10) of patients. No patient over-expressed all of the NE transcripts, suggesting that the NE subtype is represented by cells of different phenotypes. Overall, there exists 9 different NE signatures, with the exception of those patients with similar signatures: (R2 =R6), (R4=R20). Five patients (R1, R5, R7, R10, R22) did not over-express any of our NE genes. Interestingly, R27 over-expresses the highest number of our 12 NE genes, giving a signal at 67% (n=8/12). Altogether these findings on circulating NE transcripts support a high differential NE gene expression between patients. They also substantiate the existence of several cell subsets, exhibiting different phenotypes within the NE-cell subtype, as frequently observed in advanced PCa.

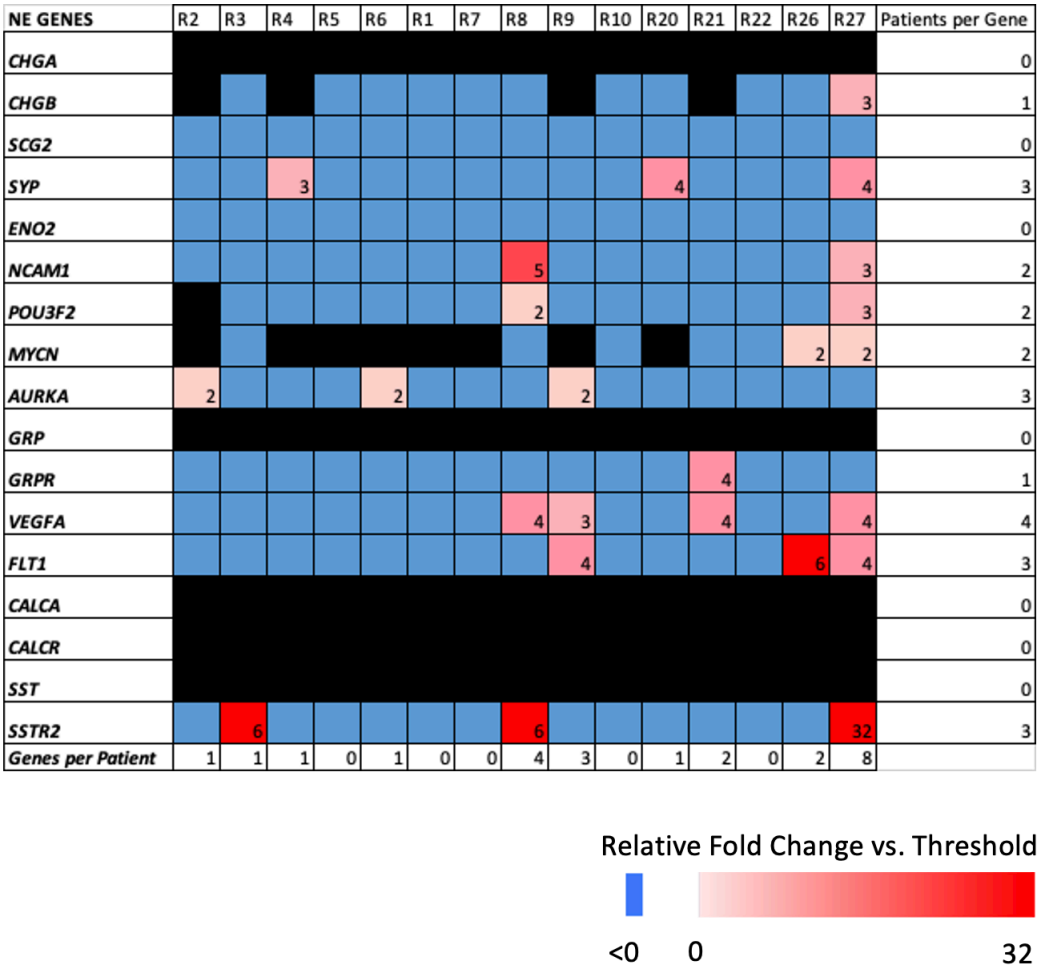

Figure 5.4: Over-expression heat map representative of the 17 NE transcripts in mCRPC patients

The black squares show no signal in the RT-qPCR assays. Blue squares show expression at the threshold or lower, and the pink to red squares are over-expression values up to 32 fold.

Chapter 6

Proposition of a Short-hand Unique NE Gene Signature

Throughout the mining of transcriptomic datasets, and the results from liquid biopsies, there exists much overlap in the most intense and frequent NE transcripts. Our results showing a highly differential expression of NE markers in prostate tissues, as well as mining transcriptomic datasets, led us to further explore the potential of their over-expression in circulating blood, by which a specific NE signature could be indicative of advanced disease. To our knowledge, there have been no studies to provide such a signature, or pattern, given the extreme clinical heterogeneity of the disease, as well as the variation in NE cell subtype.

Table 6.1 shows a colour-coated summary of similar genes found in the blood of our cohort of patients, as well as the cohorts in each of the transcriptomic datasets. The top 12 NE genes of each dataset were ranked, as well as the 12 detectable transcripts in circulation. One observation was that *SSTR1* and *VTN* were commonly seen at 79% (n=11/14). Although these two transcripts were not yet tested in patient blood, they are prospects for future experiments when more NE genes will be added.

When looking at specific NE genes, *SYP* and *CHGB* are the transcripts most seen in every dataset and in the blood at 88%. Following this would be *AURKA* seen in 63% of

datasets and blood. *SSTR2*, *POU3F2* and *ENO2* were equally seen in 50% of the datasets and blood. Based on the number of times any NE gene was seen in the top 12 ranks, a signature containing the most relevant genes in circulation can be proposed. The NE pattern or signature with the most prevalent genes would be composed of: *SYP* > *CHGB* > *AURKA* > *SSTR2* > *POU3F2* > *ENO2*. We see that these NE transcripts are ranked the best and most in all of the datasets + blood.

In the aforementioned results of each individual dataset, we saw that *SYP* was most represented by the primary tumour samples, and less so in the metastases. The four primary datasets (Stanford, TCGA, MSKCC, Cambridge) all over-express *SYP* in primary tumours of RP and TURP samples, as well as in some mets (LNs at RP). *CHGB* was previously seen frequently in the mixed metastatic samples as well as in NEPC mets. We see it comes up as well in the dataset containing primary samples, although it is not ranked in the top five of all transcripts. *AURKA* was very commonly seen in the databases. It was often over-expressed in the primary tumours (RP, TURP), as well as in the LNs resected at RP. Furthermore, it was also found in the mixed locations of metastases. *SSTR2* is different from the previous NE transcripts because it is exclusively found to be over-expressed in the metastatic samples. It is highly ranked in the neuroendocrine, Hutchinson, SU2C, and patient blood samples. In the SU2C dataset, *SSTR2* was most intensely expressed in the bone, and other soft tissue. Both *POU3F2* and *ENO2* were not very important when looking at the liquid biopsies, however *POU3F2* was commonly over-expressed in the mixed NEPC and CRPC mets. *ENO2* was found frequently in the primary tumours of RP and in TURP samples, as well as in metastatic samples from the liver and soft tissues.

The genes not yet tested in the blood, such as *SSTR1* and *VTN*, which are both commonly seen in both primary and metastatic samples, will be added on for future endeavours of this project. Based on the overall combination of results with the datasets and blood, we feel that the aforementioned NE genes (*SYP, CHGB, AURKA, SSTR2, POU3F2, ENO2*) would be the most important to test in liquid biopsies of advanced PCa patients. Additionally, NE markers that are known drug-targets in clinical trials, and that ranked

high in liquid biopsies (*VEGFA*, *FLT1* and *GRPR*) would also be the most important to include in tests.

By combining literature studies on clinical trials, transcriptomic datasets, and liquid biopsy testing, the final list of NE-genes proposed would include 8 markers: *VEGFA, FLT1, GRPR, AURKA, SSTR2, SYP, CHGB, POU3F2*.

Ranked NE Transcripts	Stanford	MSKCC	TCGA	Cambridge	Neuroendocrine	Fred Hutchinson	SU2C	Patient Blood
1	*SSTR1*	*VTN*	*GRP*	*GRPR*	*SCG2*	*SST*	*SSTR1*	*VEGFA*
2	*AURKA*	*AURKA*	*VIP*	*AURKA*	*POU3F2*	*SYP*	*VTN*	*SSTR2*
3	*SYP*	*NTSR1*	*VTN*	*SSTR1*	*SSTR1*	*NTSR2*	*NTSR1*	*FLT1*
4	*CHGA*	*SSTR1*	*SST*	*SYP*	*SSTR2*	*POU3F2*	*GRPR*	*SYP*
5	*GRP*	*NTSR2*	*AURKA*	*SST*	*CHGB*	*VTN*	*FLT1*	*AURKA*
6	*VIPR1*	*POU3F4*	*POU3F2*	*VTN*	*BRS3*	*SSTR2*	*SSTR2*	*NCAM1*
7	*CALCB*	*SST*	*CHGB*	*GRP*	*CALCR*	*CALCA*	*GRP*	*POU3F2*
8	*VEGFA*	*CHGA*	*SSTR3*	*CHGB*	*NCAM1*	*SCG2*	*NCAM1*	*MYCN*
9	*ENO2*	*SSTR4*	*SSTR1*	*CHGA*	*SNPH*	*NMBR*	*CHGB*	*GRPR*
10	*NMB*	*CHGB*	*CALCB*	*VIP*	*GRP*	*CALCR*	*CALCB*	*CHGB*
11	*SORT1*	*CALCA*	*SYP*	*NMB*	*FLT1*	*VIPR2*	*SYP*	*ENO2*
12	*CHGB*	*SYP*	*NTSR1*	*CALCB*	*ENO2*	*POU3F4*	*ENO2*	*SCG2*

Table 6.1: Ranking of most important genes gathered from all transcriptomic datasets and patient blood data

The ranking of NE markers was analyzed with cofactors such as: intensity of over-expression, frequency, and mean of over-expressed values. Each corresponding NE transcript over-expressed in the blood is colour coated, and matched with those in the dataset. Both *SSTR1*, *VTN* are the same colour, representative of genes to be tested. NE genes in grey (*CHGA, GRP, SST, CALCA, CALCR* contained no signal in the blood of this small series of patients).

Chapter 7

Clinical Relevance of the NE subset of cells

An important aspect of this research is to find out if our findings are clinically relevant and may help to predict recurrence of the disease (BCR) after curative therapy as well as response to therapies. They could also be used as a basis to better manage patients at advanced stage of the disease.

7.1 Survival analyses show the predicative value of circulating NE transcripts

To ascertain the predicative value of our findings, we accessed the MSKCC database, which was the only one to provide the patients' clinical data regarding BCR after RP and survival. Therefore, we tested different combinations of over-expressed NE transcripts in this dataset and performed Kaplan-Meier survival analyses based on BCR, complemented by Cox univariate and multivariate tests.

In the first set of analyses (Fig. 7.1), cases over-expressing at least one NE gene experienced earlier BCR (p=0.0024). This was supported by both the univariate and multivariate Cox analyses (Table 7.1). Results are relatively similar for cases over-expressing

two NE genes, (p=0.0029), and even more pronounced when five or more NE genes are over-expressed (p=0.00039).

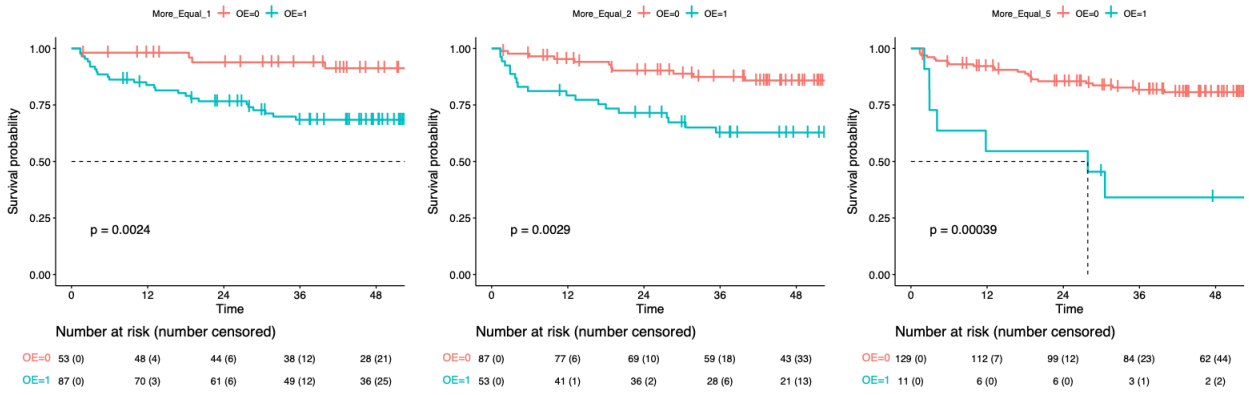

Figure 7.1: Kaplan-Meier survival analysis
Left to right: At least 1 NE gene OE, At least 2 NE genes OE, At lease 5 NE genes OE.

With regards to over-expression of specific NE transcripts, we looked at the top 17 ranked NE genes in the MSKCC dataset (same ranking as previously listed in Table 6.1: *VTN* > *AURKA* > *NTSR1* > *SSTR1* > *NTSR2* > *POU3F4* > *SST* > *CHGA* > *SSTR4* > *CHGB* > *CALCA* > *SYP* > *CALCR* > *SCG2* > *BRS3* > *NTS* > *VIPR1*). From this list, we compiled our next set of survival analyses, starting from the top ranked gene, then adding each gene in succession, and so forth. It is noteworthy that some of the NE genes ranked in our list were chosen for their predominance in metastases datasets, but not necessarily in primary tumours. This process was able to show us at what point there was no predicative increase in the event of a BCR. One pattern we saw was that cases over-expressing any of the top 17 ranked NE genes overall experienced an earlier BCR (Figure 7.2). Interestingly, in the analyses between the top 7, 8, and 9 NE genes, there was no increase in hazard ratio, nor significance. This was supported by the univariate analyses, but lost in some instances during the multivariate analyses (Table 7.1).

In the middle right panel of (A.) in Figure 7.2, the cases that over-expressed the top 4 ranked NE transcripts (*VTN*, *AURKA*, *NTSR1*, *SSTR1*) experienced an earlier BCR ($p<0.0001$). This combination of top ranked NE genes proved to hold the most significance, with 63 cases in the over-expressed group, and 77 cases that were not over-expressed, with a HR

of 4.0 (Table 7.1). A trend that was seen in these results was that there seemed to be a peak by which the addition of genes no longer added any effect of the event of an earlier BCR. After the addition of the top 4 NE genes, the hazard ratios decreased, meaning that there was less of a significant effect between the over-expressed and non over-expressed cases. After the addition of the top 14 NE genes (Figs. 7.2 B, C), there were no changes in the survival outcome, p-value remained (p=0.004), and no change to the hazard ratios. Overall, having an increasing amount of select NE genes is indicative of experiencing an earlier BCR.

A.

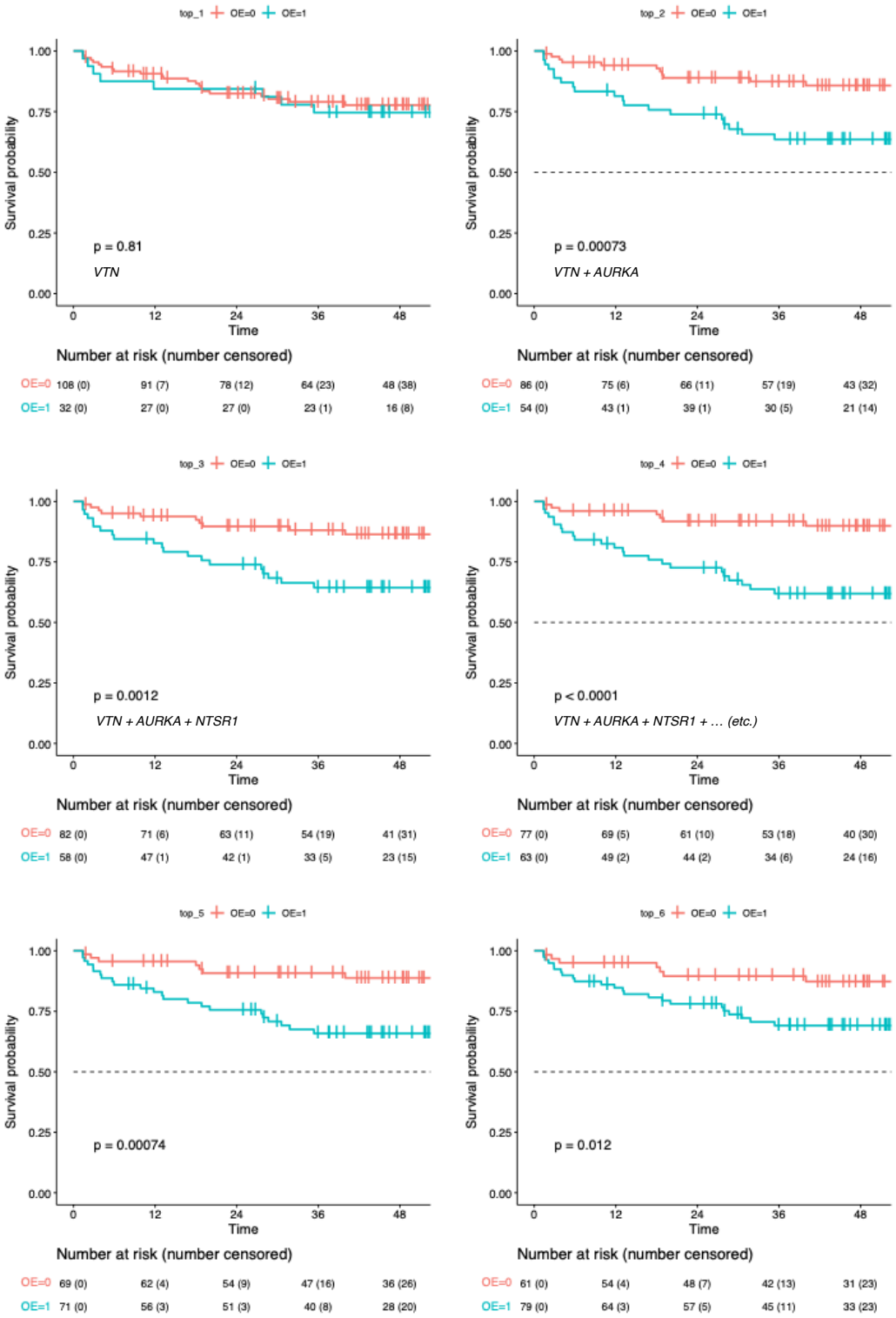
top_1 OE=0 OE=1
Survival probability
1.00
0.75
0.50
0.25
0.00
p = 0.81
VTN
0
12
24
36
48
Time
Number at risk (number censored)
OE=0 108 (0) 91 (7) 78 (12) 64 (23) 48 (38)
OE=1 32 (0) 27 (0) 27 (0) 23 (1) 16 (8)
top_2 OE=0 OE=1
p = 0.00073
VTN + AURKA
OE=0 86 (0) 75 (6) 66 (11) 57 (19) 43 (32)
OE=1 54 (0) 43 (1) 39 (1) 30 (5) 21 (14)
top_3 OE=0 OE=1
p = 0.0012
VTN + AURKA + NTSR1
OE=0 82 (0) 71 (6) 63 (11) 54 (19) 41 (31)
OE=1 58 (0) 47 (1) 42 (1) 33 (5) 23 (15)
top_4 OE=0 OE=1
p < 0.0001
VTN + AURKA + NTSR1 + … (etc.)
OE=0 77 (0) 69 (5) 61 (10) 53 (18) 40 (30)
OE=1 63 (0) 49 (2) 44 (2) 34 (6) 24 (16)
top_5 OE=0 OE=1
p = 0.00074
OE=0 69 (0) 62 (4) 54 (9) 47 (16) 36 (26)
OE=1 71 (0) 56 (3) 51 (3) 40 (8) 28 (20)
top_6 OE=0 OE=1
p = 0.012
OE=0 61 (0) 54 (4) 48 (7) 42 (13) 31 (23)
OE=1 79 (0) 64 (3) 57 (5) 45 (11) 33 (23)

B.

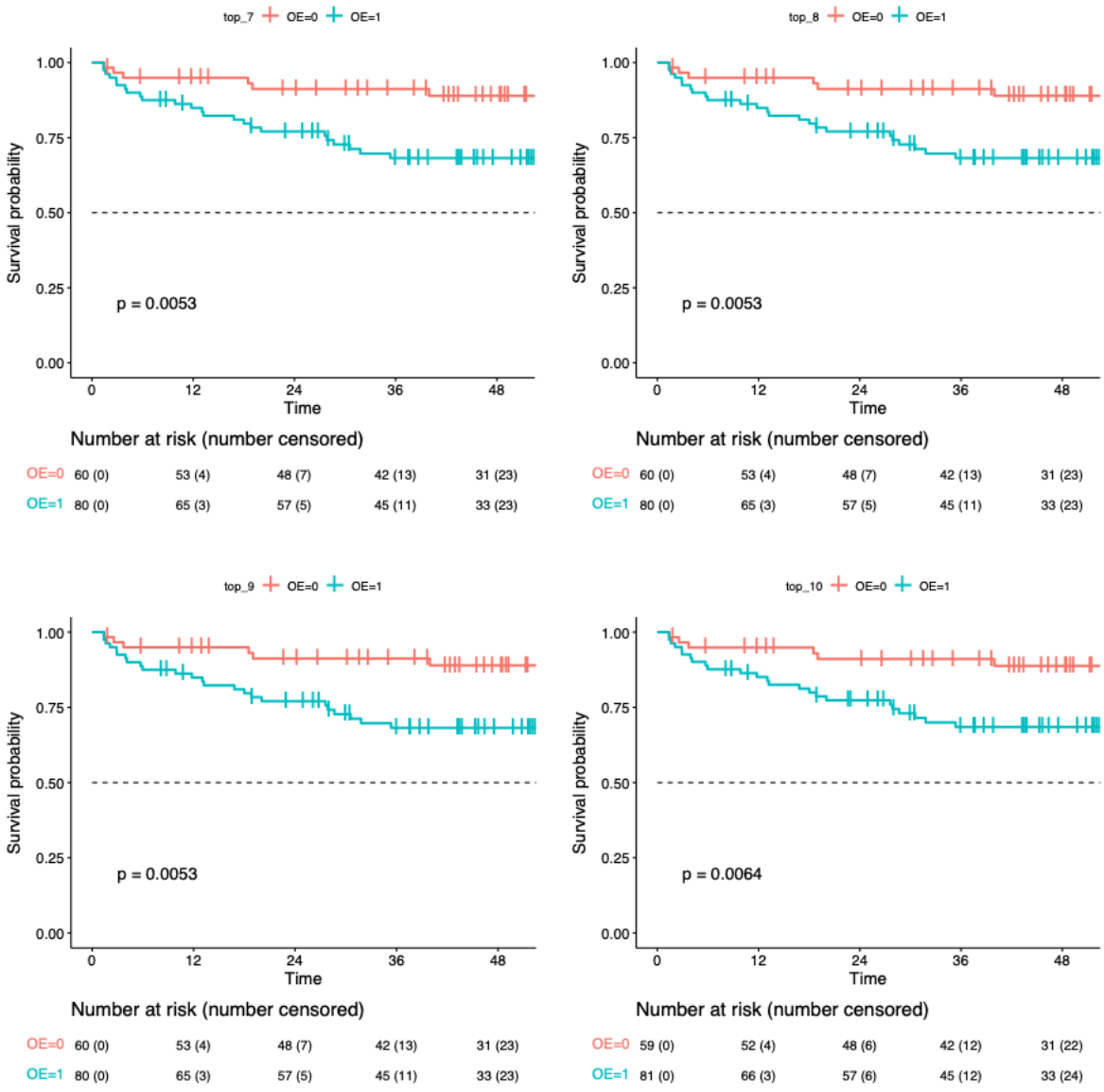
top_7 OE=0 OE=1
Survival probability
1.00
0.75
0.50
0.25
0.00
p = 0.0053
0 12 24 36 48
Time
Number at risk (number censored)
OE=0 60 (0) 53 (4) 48 (7) 42 (13) 31 (23)
OE=1 80 (0) 65 (3) 57 (5) 45 (11) 33 (23)
top_8 OE=0 OE=1
Survival probability
1.00
0.75
0.50
0.25
0.00
p = 0.0053
0 12 24 36 48
Time
Number at risk (number censored)
OE=0 60 (0) 53 (4) 48 (7) 42 (13) 31 (23)
OE=1 80 (0) 65 (3) 57 (5) 45 (11) 33 (23)
top_9 OE=0 OE=1
Survival probability
1.00
0.75
0.50
0.25
0.00
p = 0.0053
0 12 24 36 48
Time
Number at risk (number censored)
OE=0 60 (0) 53 (4) 48 (7) 42 (13) 31 (23)
OE=1 80 (0) 65 (3) 57 (5) 45 (11) 33 (23)
top_10 OE=0 OE=1
Survival probability
1.00
0.75
0.50
0.25
0.00
p = 0.0064
0 12 24 36 48
Time
Number at risk (number censored)
OE=0 59 (0) 52 (4) 48 (6) 42 (12) 31 (22)
OE=1 81 (0) 66 (3) 57 (6) 45 (12) 33 (24)

C.

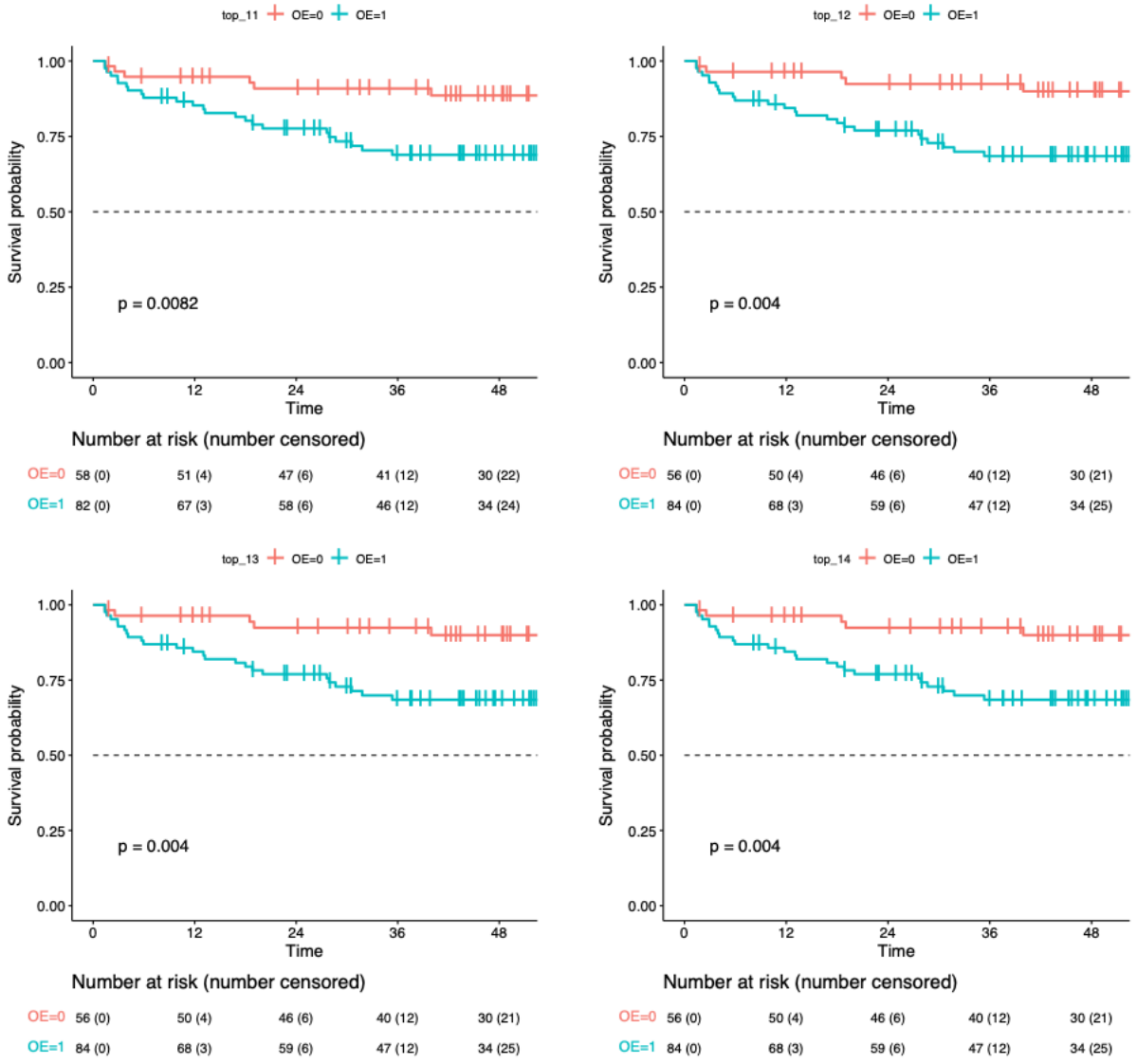

Figure 7.2: Kaplan-Meier survival analysis of the most important NE transcripts we had ranked and known to be over-expressed in the MSKCC dataset

Graphs are placed in order of most relevant NE gene being over-expressed, then adding in succession, the rest of the list of over-expressed NE genes one at a time. The list of the 17 genes includes: *VTN* > *AURKA* > *NTSR1* > *SSTR1* > *NTSR2* > *POU3F4* > *SST* > *CHGA* > *SSTR4* > *CHGB* > *CALCA* > *SYP* > *CALCR* > *SCG2* > *BRS3* > *NTS* > *VIPR1*. (A) shows the succession of the top 6 NE genes (B) shows the succession of the top 10 NE genes (C) shows the succession of the top 14 NE genes.

Over-expressed Genes from MSKCC	Hazard Ratio (confidence interval)	
	Univariate	Multivariate
At least one NE gene	**3.6 (1.5-8.6)**	**2.6 (1.0-6.8)**
At least two NE genes	**2.6 (1.4-5.1)**	1.5 (0.7-3.4)
At least five NE genes	**4.0 (1.8-9.2)**	1.1 (0.3-3.5)
Top 1 NE genes	1.1 (0.5-2.3)	1.1 (0.5-2.7)
Top 2 NE genes	**3.1 (1.5-6.1)**	2.2 (0.9-5.3)
Top 3 NE genes	**3.0 (1.5-5.9)**	**2.4 (1.0-5.8)**
Top 4 NE genes	**4.0 (1.9-8.4)**	**3.5 (1.4-8.7)**
Top 5 NE genes	**3.4 (1.6-7.3)**	**3.0 (1.2-7.2)**
Top 6 NE genes	**2.5 (1.2-5.4)**	2.1 (0.9-5.1)
Top 7 NE genes	**2.9 (1.3-6.4)**	2.0 (0.9-4.9)
Top 8 NE genes	**2.9 (1.3-6.4)**	2.0 (0.9-4.9)
Top 9 NE genes	**2.9 (1.3-6.4)**	2.0 (0.9-4.9)
Top 10 NE genes	**2.8 (1.3-6.3)**	2.0 (0.8-4.9)
Top 11 NE genes	**2.8 (1.3-6.1)**	2.0 (0.8-4.8)
Top 12 NE genes	**3.2 (1.4-7.2)**	2.2 (0.9-5.5)
Top 13 NE genes	**3.2 (1.4-7.2)**	2.2 (0.9-5.5)
Top 14 NE genes	**3.2 (1.4-7.2)**	2.2 (0.9-5.5)
Top 15 NE genes	**3.2 (1.4-7.2)**	2.2 (0.9-5.5)
Top 16 NE genes	**3.2 (1.4-7.2)**	2.2 (0.9-5.5)
Top 17 NE genes	**3.2 (1.4-7.2)**	2.2 (0.9-5.5)

Table 7.1: Univariate and Multivariate Cox analyses

Multivariate analyses for over-expressed genes, with pre-operative PSA, Gleason score, and T stage as cofactors. Confidence intervals are within 99.5% (+/-2.58 SD) and significant hazard ratios (HRs) are bold.

7.2 Circulating NE transcripts in patients' liquid biopsies are clinically relevant

We next investigated whether the over-expression of circulating NE genes in our 15 patients were associated with clinical parameters. Note, the 9 highest ranking over-expressed NE genes from (Table 6.1) were: *VEGFA, SSTR2, FLT1, SYP, AURKA, NCAM1, POU3F2, MYCN, GRPR*. There was not a lot of significance seen in general, regarding baseline features. Patients who received radiotherapy seemed to show an increase of NE detection, however no specific transcripts reached significance. Studying individual NE genes that were over-expressed, Figure 7.3 showed that *SSTR2* detection was increased in patients who did not receive any current mCRPC therapies (p=0.038). Furthermore, the same significance was seen in *NCAM1*, and *POU3F2*. Interestingly, *MYCN* over-expression was significantly associated to patients receiving Abiraterone (p=0.032).

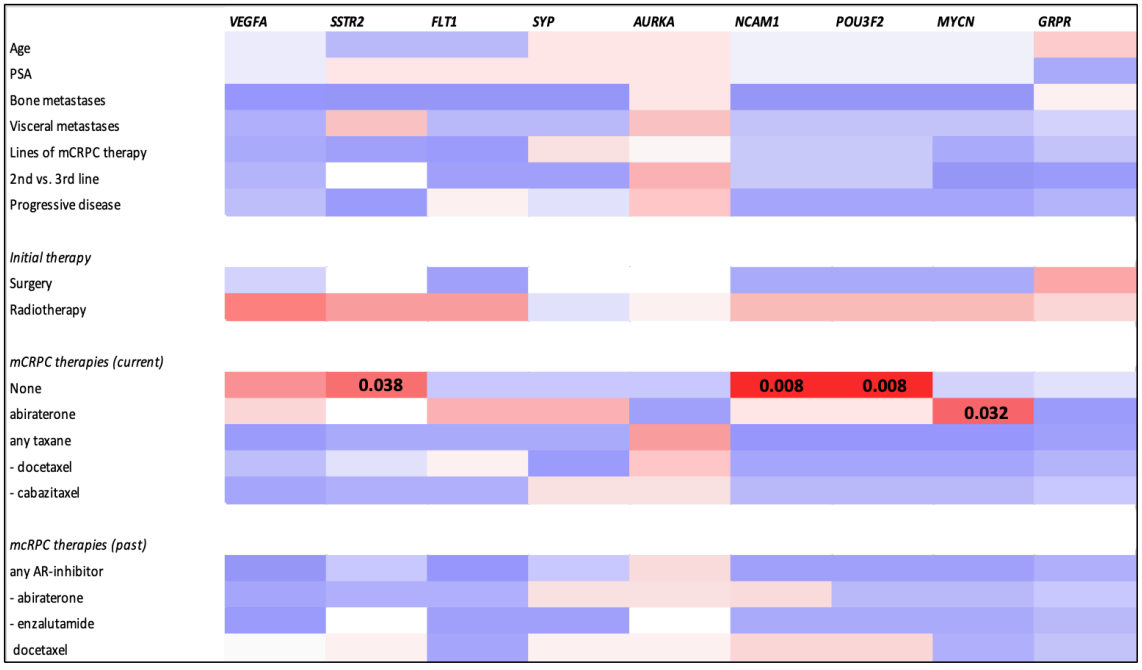

Figure 7.3: Patient and/or treatment characteristics and the association with over-expressed NE markers

Characteristics were dichotomized, and differences were evaluated using Chi-square tests. Significance is indicated when applicable, $p \leq 0.05$.

Survival analyses were conducted for disease progression and death (Table 7.2). Of note, 2 patients had died during the period of this study. No statistical significance was reached for disease progression and/or death but certain patterns or trends were observed for specific NE markers. For instance, over-expression of *SYP* (HR 1.02) or *AURKA* (HR 3.00) both have an increased risk for disease progression. The same NE markers: *SYP* (HR 7.35) and *AURKA* (3.83) each have an increased risk for death.

Taken together, this data suggests the NE cell subtype over-expressed in liquid biopsies of patients with advanced disease are clinically relevant, correlating with outcome, despite the low number of cases enrolled in this study during the pandemic. This substantiates the proposed concept of the NE subtype consisting in a variety of cells differentially over-expressing NE markers, at least in the advanced stage of disease.

NE Gene	Disease Progression	Death
SYP	1.02 (0.12-8.49)	7.35 (0.45-119.17)
VEGFA	0.33 (0.04-2.67)	NA
SSTR2	0.35 (0.04-2.85)	NA
GRPR	NA	NA
NCAM1	NA	NA
MYCN	NA	NA
FLT1	0.42 (0.05-3.42)	NA
AURKA	3.00 (0.67-13.52)	3.83 (0.24-61.27)
POU3F2	NA	NA
At least one marker	0.64 (0.17-2.40)	NA
Increasing of markers	0.68 (0.27-1.24)	0.91 (0.33-2.55)

Table 7.2: Over-expression of circulating genes is associated with disease progression and patient death

Hazard ratios and 99.5% confidence intervals for disease progression and death in patients over-expressing the select circulating markers. HRs and respective 99.5% CIs were calculated using Cox proportional hazard models. NA: non-applicable. No HRs show significance.

Chapter 8

Discussion

This study highlights the concept of NED in a multitude of ways: (1) Inter-patient heterogeneity; (2) intra-patient heterogeneity; (3) inter-tumoural heterogeneity; (4) intra-tumoural heterogeneity. The significance of NED in relation to progression is especially seen through the analysis of multiple cohorts in the transcriptomic datasets. The commonality of transcript over-expression from the published datasets and liquid biopsies enforces a strong shorthand signature for cells of the NE subtype to be studied and used as possible biomarkers for prognosis of PCa. Clinical relevance substantiates the importance of the NE cell subtype when looking at the most advanced PCa cases.

8.1 NED in benign glands and cancer foci of primary tumours

The intent of this part of the study was to demonstrate the inter-patient and intra-tumoural NED in a small series of RP specimens from 10 patients that were stained by IHC with five different NE markers. As predicted, all of the 10 patients exemplified a different NE signature or pattern within their benign glands as well as their cancer foci.

While focusing on the NE-stained cells in the benign glands, we found out that CHGA was the most positively expressed NE-marker and that less that half of the cases expressed

CHGA more in the cancer foci compared to the benign glands. This observation was surprising because CHGA is well-known in literature and accepted as the main marker expressed by NE cells in prostatic primary tumours [77, 78]. Contrary to this, CHGA expressed the highest percentage of positively stained cells in the benign area of all 10 patients (1.16%), and was most frequently expressed in 7 patients (70%). While these findings highlight the importance of CHGA to detect NE cells in the primary tissue of the prostate, they also indicate that CHGA might not be the best NE marker in this series of cases (received neo-adjuvant ADT prior to RP). The tissues do not represent the situation of patients who have had hormonal therapies for long periods of time and have progressed to the mCRPC and more advanced stage, however they do remain meaningful to reflect the effect of ADT on the NE subtype. When looking at the consecutive slides in benign glands (Figure 3.1), the CHGA stain contains positive cells that are missing in the NSE, SYP, CALCA, and 5-HT-stained slides. Within all of the benign glands of the patients, there were 8 unique profiles, which suggests a high inter-patient complexity regarding NED.

This study also confirms that there exists different subsets of NE-cells within each tumour environment. Indeed, shifting sights to the positively stained NE-cells in the cancer foci, CALCA was the most positively expressed. As previously mentioned, CALCA was studied in the host lab and proved to enhance LNCaP motility through FAK activation (unpublished). Therefore, the finding of its presence at high frequencies in the cancer foci is of interest and in line with the fact that the receptor calcitonin receptor (CALCR), is involved in PCa invasiveness, and possible relationship with metastases to the bone [125]. Within the cancer foci of all cases, no two patients contained the same frequency of NE markers, nor did they have the same predominance of NE expression. Through our observations, 90% of the patients expressed at least one of the NE markers. Furthermore, our NE markers were representative of the varying cells displaying NE phenotypes that exist within each cancer foci.

Another interesting finding was that not all of the NE markers were similarly expressed. For example, in patients 6 and 9, one NE marker had such a high predominance of positive expression, while the other 4 NE markers were not expressed in the benign nor in the cancer foci. When thinking in terms of clinical relevance, the knowledge of a high NE content could affect the efficacy and efficiency of therapies. This result proves that even though patients receive the same hormone treatment, and are at the same stage of their disease, they do not express similar ligands and/or receptors at the same levels. Due to the fact that there is high inter-patient heterogeneity, this sheds light on the urgent need for a more precision based medicine.

In the above example specifically, patient 6 only expresses CALCA, with very minimal SYP, in comparison to patient 9 who only expresses CHGA in its NE cells. If patient 6 and 9 were given the same CALCA or CALCR-targeted therapy, only patient 6 would benefit. There were also patients in which there was no NE marker expressed in cancer foci expression, and instead was only found to be positive in the benign glands (patient 7). This could also be due to the fact that NE protein might be expressed later in the disease, once a patient is metastatic. Considering that these IHC stained tissues are from the primary tumours of RP cases, the cells might not have acquired a heavy NED phenotype. Overall, we see a highly diversified NED between patients, within the same patient, and even within the same tumour of the same patient in the primary tumour foci and benign glands.

Among some limitations of the tissue NE marker analysis was that we did not have the clinical data to perform further statistics on the patients, nor did we have access to TURP primary tumours from advanced cases. Another aspect to consider is the additional studies of NED in normal and hyper-plastic prostates from organ donors and patients having no PCa. Unknown external characteristics like age, Gleason score, or PSA level might have correlated to varying expression levels of the NE markers. Another limitation was that all 10 of these patients received neo-adjuvant hormone therapy prior to RP, and that no comparison was made with prostate tissues from untreated (hormone-naive) patients.

It would have been interesting to see an increase in the expression of NE markers, while comparing before and after hormone-therapy, but diagnostic biopsies were not available. It is important to mention that neo-adjuvant ADT prior to RP is not as frequent as in the 1990s. A major disadvantage was the difficulty to properly grade primary tumours due to hormonal effects on more differentiated and hormone-dependent cancer cells, while not providing sufficient benefits for surgeons. Deeper studies of tissue comparisons and scoring of multiple NE stains are needed in future studies. An alternative strategy to analyze several markers on the same slide could be done by immunofluorescence with multiple antibodies. Since this tissue material was pre-stained years ago, no additional multiplex staining was done. Nonetheless, it is conceivable that based on our observations summing up all the positive cells expressing different NE markers, they would reveal a wider contribution of NE cells and their products to the prostate physiopathology, notably in PCa.

8.2 Transcriptomic analysis reveals NE gene over-expression in relation to progression

To better understand the relationship between NE phenotype, NE heterogeneity, and progression of the disease, several published RNA sequencing and microarray data were analyzed. Each dataset contained samples from diverse cohorts of patients moving from benign to primary tumours of RP cases removed in the weeks following diagnosis as well as advanced TURP cases, to LN metastases resected at RP, or distant metastases from patients with advanced disease.

When looking at the dataset analyses of mostly primary tumours of the Stanford, Cambridge, MSKCC cohorts, there exists a high inter-patient heterogeneity of NE genes being over-expressed that increases with progression of disease. When moving from RP to TURP primary tumours and to metastases, we observe a significant association with increased NE transcripts. When comparing these three datasets, each were very similar in

the over-expression of certain NE transcripts (*AURKA, SSTR1, SYP*). Each of these transcripts were important in the RP, and advanced TURP cases. In like with literature, SYP is a long-standing intrinsic NE marker used for identification of the NE-cell subtype. It is no surprise that it's commonly over-expressed in primary tumour tissues [8, 15]. Furthermore, the elevated levels of *AURKA* is worth mentioning since the protein has generated interest, being involved in the progression of the disease. Our findings on its over-expression in the various cohorts is of clinical significance given that there are currently drug-targeted therapies for *AURKA* in clinical trials. The demonstration of the Somatostatin family receptors (*SSTR1, SSTR2*) being over-expressed is also of great importance, as these receptors are currently being targeted as therapies and used for molecular imaging of metastases containing malignant NE cells [126–128].

The remaining metastatic datasets (Fred Hutchinson, Neuroendocrine, and SU2C) contained various metastatic samples to different sites of the body. There were less similarities found for NE genes over-expressed in these metastatic datasets, compared to the many similarities found in the primary datasets and cohorts. This may imply that as the disease progresses and becomes more advanced, and eventually mCRPC, mechanisms controlling NED lead to some divergences. This would allow some NE cells to develop their own unique set of genes with phenotypes that may not be similar between sites of metastases and between patients. In the SU2C cohort specifically, metastases to the LN, liver, bone, and other soft tissues each contain a very different pattern of over-expressed NE genes.

Results show preferential NE over-expression of NE genes in the liver metastases, followed by bone, then LN and other soft tissue (Fig. 4.6). No two sites of metastases contained the same intensity or frequency of NE transcripts. When taking a closer look at the composition of NE transcripts over-expressed in respective liver mets, the two datasets contained very different patterns. In the SU2C cohort, *VTN* was the most frequently seen transcript, while in the NE cohort, *MYCN* was the most frequent at this site. The difference in NE gene over-expression, even at the same site is indicative of inter-tumoural

heterogeneity. It also enforces the notion that there exists multiple cell phenotypes within the NE-subtype. The NE dataset has also illustrated and confirmed that the panel of 35 NE genes selected were more commonly found in the CRPC-NE patients compared to the conventional CRPC-adeno patients. Within this NE dataset, some CRPC-NE patients exhibited as high as 70-80% of our genes over-expressed. With these results in mind, we were confident that moving forward with the testing of certain NE transcripts in the blood of patients was a promising avenue.

The Hutchinson dataset was especially different because it contained multiple metastases biopsied from warm autopsies.The dendrogram from Figure 4.10 illustrates that patients containing multiple metastases to the same site could still present with a high diversity of NE markers. This is an important and relevant finding because it enforces caution when trying to image or treat the various metastases, since they are not all identical in their molecular and cellular composition. Conventional tissue biopsies are not always the best representative of the cancer as a whole, and instead would only provide one piece of information or insight into a particular metastasis, while neighbouring metastases could be comprised of different cell subsets and/or gene patterns. Furthermore, in addition to inter-patient heterogeneity of gene over- expression in primary tumours and metastases, we identified remarkable intra-patient heterogeneity in metastases located at different sites, and even to the same site. It is thus conceivable that cells of diverse phenotypes not only contribute to the development and stage of PCa, but also respond differently to certain drugs, thus leading to further progression and death from this disease.

There were some limitations for the analysis of the datasets. One of them was that not all genes were found in each dataset; 9 of 35 NE transcripts selected were not included in the Stanford dataset, 1 in the SU2C, and 1 in the Hutchinson series. Furthermore, clinical follow up data were not provided in most of them, and as such, we were able to asses clinical relevance of our over-expressed NE genes solely with the MSKCC dataset.

8.3 Traceability of NE genes in blood RNA of advanced patients

To better understand the expression of the NE genes in PCa progression, we shifted sights their potential presence in the circulation, in whole blood. We chose 17 specific NE genes of the 35 initial list because they were highly over-expressed in the publicly available datasets, as well as found to be important in literature studies. A handful of the chosen transcripts were also specific targets for therapy in clinical trials. We successfully showed that the selected 17 NE transcripts (*CHGA*, *CHGB*, *SCG2*, *SYP*, *ENO2*, *NCAM1*, *POU3F2*, *MYCN*, *AURKA*, *GRP*, *GRPR*, *VEGFA*, *FLT1*, *CALCA*, *CALCR*, *SST*, *SSTR2* were measurable in 5 different human PCa cell lines (Fig. 5.1). The fact that the majority of NE gene expression was seen in the more aggressive AR-independent cell line, NCI-H660, known as a NE model, confirms the suitability of this model. High expression of NE genes in other AR- negative cell lines also suggests that the NE phenotype is related to progression of the disease. Further, it supports the theory that NED is an enabler of resistance to hormone-therapy. Indeed, cancer cells that can function independently of AR will not be affected by androgen-deprivation therapies.

An interesting finding in cell line expression was that *GRPR* is predominantly expressed in the PC-3 cell line. As previously mentioned, the host lab was the first to prove that GRP/bombesin binding to the GRPR is involved in the activation of PC-3 cell motility through FAK [114, 115]. Reaching the same conclusion for GRPR at the RNA level coupled to the protein level, substantiated the importance and presence of gastrin-releasing peptide receptor (GRPR) as a key NE transcript in more aggressive PCa cells. Literature also places great value on the GRPR, for molecular imaging of metastases [129] and is currently being studied in clinical trials. A few NE-related genes like *CALCR*, *VEGFA*, *AURKA* were more expressed in other cell lines, notably *CALCA* in the DU145 cell line. It is worth mentioning that the host lab has previously demonstrated that CALCA activates LNCaP cell motility via FAK activation (unpublished data). However, the expression of

its receptor had not yet been assessed. These findings support that NE-products and related receptors may also act through paracrine mechanisms.

After optimization of assays , we then wanted to verify the traceability of our selcted 17 NE genes in the blood RNA of 15 mCRPC patients and 8 healthy controls. The RT-qPCR results first showed that 5/17 NE genes were not expressed in either the controls or the patients. The expression of the 12 remaining genes was also not significantly associated with age of healthy volunteers, whose ages for some of them overlap the age of the patients. The mean of these values has allowed us to define the threshold for each gene, enabling us to state on NE gene over-expression with a 99.5% confidence interval. As predicted, we observed a wide diversity between patients, creating 9 unique signatures or patterns based on the heat map generated in Figure 5.4. We hope that with the addition of more patients to our cohort, all 17 NE genes would eventually be expressed. Surprisingly, *CHGA* was not detectable in the liquid biopsies of our mCRPC patients in their 2nd or 3rd line therapies. Therefore, it is conceivable that *CHGA* may not always be the best NE-marker traceable in our mCRPC patients. Based on the IHC results, CHGA was primarily seen in the benign glands of the prostate tissue compared to cancer foci. These two results are in line with each other in that CHGA might not be the most important marker in NE cells of advanced disease and instead be a useful marker in primary tumours, or in cases that have not yet had treatments. This was also suggested by analyses of transcriptomic datasets of prostatic tumour tissues (RP and TURP) and metastases of patients with advanced disease.

From the 12 NE transcripts that we successfully detected in liquid biopsies, the most over-expressed genes were *VEGFA, AURKA, SYP, FLT1* and *SSTR2*. All of the aforementioned NE transcripts, except *SYP* are current targets for drugs in clinical trials. It was not surprising that these were the most frequently over-expressed NE transcripts from the blood RNA results, given their clinical involvement. As previously mentioned, *GRPR* is known to be involved with molecular imaging of metastases, and *VEGFA* is known to be targeted in combination with *FLT1*, its receptor. *AURKA* is known to interact with *MYCN*,

causing downstream effects leading to a more aggressive NE phenotype. Both *SCG2* and *ENO2* had no over-expression, even though they were expressed at threshold level. This was surprising given that *ENO2*, the transcript for the NSE protein, was highly seen in cancer foci (but of RP cases) in the IHC slides. In like with CHGA, NSE is also a known NE-marker and is likely important at the early stages of the disease, in primary tumours.

As previously mentioned, high patient heterogeneity is illustrated by these results, especially given the fact that there were only two instances by which patients' had the same over-expressed transcripts. We were successfully able to trace NE transcripts in the whole blood, and concluded that there exists several cell subsets displaying NE phenotypes in advanced PCa.

An important limitation in this project, and for this part of the thesis specifically, is the small cohort size. Due to the COVID-19 pandemic, I was limited with backordered reagents for my RT-qPCR reactions, as well as limited with patient access. Patients only came to their in person visits if necessary for medical reasons/problems not solved by speaking to their physicians through telemedicine, while blood PSA tests could be done locally and close to home through their CLSC. Bio-banking was completely put to a stop, thus limiting the number of liquid biopsy material available for analysis. Consequently, statistical analyses for the clinical data of our patients have a limited statistical power based on our small cohort size of 15 patients and 9 healthy controls. Expansion is planned to increase our cohort size, and categories of patients enrolled. Some longitudinal follow-ups are to be continued to trace these NE genes, along with other categories of makers.

8.4 A Short-hand preliminary NE Signature and Clinical Relevance

When looking at the combined results from the primary tumours, datasets, and liquid biopsies, there is no doubt that NED in PCa is related to progression of the disease. We have demonstrated a high heterogeneity of the NE markers inter- and intra- patient as

shown in cancer foci and benign glands. The mining of the list of our 35 genes in datasets revealed that these NE genes are associated with progression, being primarily observed in prostatic metastases from diverse locations, followed by primary tumours from advanced cases and lymph nodes resected at radical prostatectomy. Based on a combination of how frequent a gene appeared, and both the maximum and average intensity by which it was over-expressed, we were able to rank the genes. Out of all 7 datasets (primary cases, primary advanced cases, metastatic cases), and whole blood RNA, we obtained a list of the top 12 transcripts. Given our top 6 found in liquid biopsies, as well as important therapeutic targets, we propose a NE-signature composed of 8 markers: *VEGFA, FLT1, GRPR, AURKA, SSTR2, SYP, CHGB, POU3F2*. This is a preliminary list that would be expanded based on the addition of more patients, and more NE genes of interest, like *VTN* and *SSTR1*. We have confidence that patients over-expressing top NE genes would benefit from a precision medicine approach, due to the aggressive features of the NE phenotype during disease progression.

Survival analyses performed on RP patients confirm that expressing at least one or more NE gene(s) are predicative of an earlier BCR. This was possible through the clinical data provided by the MSKCC dataset. Interestingly, after the addition of the top 4 NE genes ranked from the MSKCC dataset, there was less of a significant effect between the over-expressed and non over-expressed cases. This may have decreased in significance due to the fact that the groups were more un-even after the addition of four over-expressed NE genes. The fact that cases over-expressing two or more NE genes experienced an earlier BCR, supports the notion that NE cells displaying several phenotypes may render a patient less responsive to ADT. This would have caused an indiscrepancy in the significance of the varying cohorts. In line with this is the demonstration that NE transcripts are more likely to be expressed in the most aggressive and androgen-independent types of PCa cells. Further statistical analyses were provided by Cox univariate and multivariate analyses. Hazard ratios in all instances showed an increased risk of experiencing a BCR in any given scenario, however this was not significantly supported by the multi-

variate analyses, which included cofactors such as pre-operative PSA, Gleason score, and T stage.

In order to see the specific patient characteristics in association to over-expression of individual NE markers, a Chi Square test was performed. Surprisingly, not a lot of significance came out of this analysis. This might be explained by the very small sample size of only 15 patients. Interestingly, there were significant associations with *SSTR2, NCAM1, POU3F2*. These transcripts all showed increased over-expression in patients receiving no current current mCRPC therapies. *MYCN* was the only NE transcript associated with patients treated with Abiraterone. Another pattern observed (although not significant) was that *AURKA* over-expression was affected by all clinical parameters, as well as past and current therapies. This is presented in Figure 7.3. Survival analyses (including disease progression and death) were also performed for the same over-expressed genes. There was a slight increased risk of having disease progression if a patient over-expressed *SYP*, however no significance was found. More information, follow ups, and longitudinal studies are needed for a more conclusive clinical significance.

In line with the specific NE-products tested in host lab's results, the clinical findings are consistent with previous work. Even though there was no association between any single NE product and risk of relapse, there was sufficient results from both the IHC and RNA datasets to accept the notion of NE-products stimulating cancer cell motility. We would reserve our hypothesis that NE-products are important for progression because they affect motility. Along these lines, the host lab has shown that both AR positive and AR negative cell lines are sensitive to NE-products. Interestingly, not all NE-products are equally expressed within the cell lines, meaning that NE-products can have a differential action on their neighbouring cells, depending on their expression. An increase in amount of over-expression of our genes in the Taylor cohort is revealing of having a significantly earlier recurrence of disease. Furthermore, the literature datasets show an increase in over-expression, in the most advanced or progressed samples of the disease. Based on these findings, it supports the relationship between NE-products, progression

in the datasets, and PCa. This same finding may have not been seen in the blood biopsy experiments due to a lack of large sample size. However, given the strong evidence thus far from the IHC and dataset analyses, having a larger sample size would make the blood results likely follow suit.

Speculating on the aforementioned findings of NE-products relating to progression of PCa, the results argue for an increase in both the presence of NE cells, as well as an increase in expression of NE genes within tumours. What is shown by the IHC results and literature is an increase in the number of NE cells. However, this is not mutually exclusive of the fact that there also can exist an increase in expression of NE genes in these cells. It seems that some NE-products are more expressed in the NE cells of advanced disease, compared to the primary. There also exists a pattern of these NE genes that render them more aggressive, therefore being able to produce products that are negatively affecting their environment and motility. From the dataset results, we know that NE cells are also found in metastasis, meaning that these cells may have left the initial cancer site as a stem cell and differentiated into a NE-like cell. Otherwise, it could be an expression of NE-products on neighbouring cells. Due to plasticity from the stem cells, it is conceivable that the gene patterns of a patient is constantly evolving. An increase in the number of NE cells may occur simultaneously with the over-expression of some NE genes in particular cells.

Overall, there is a clinical relevance of the NE-cell subtype in advanced PCa patients. PCa continues to be a clinically challenging disease because of the androgen-independent state by which there seems to be an increase in the NE cell-phenotypic diversity.

Chapter 9

Conclusion

Metastatic castration resistant PCa patients remain un-curable, due to a high tumour heterogeneity and the clinically challenging, unpredictable biological nature of the disease. There are no successful curative treatments for the 30% of patients that experience BCR after initial curative therapies. Additionally, there is also no successful curative treatments for those diagnosed with a metastatic disease, whose disease rapidly re-appears after an initial favourable response. With increasing evidence of a supporting role for NED in PCa, and correlating to the progression of the disease, it becomes imperative to address certain underlying mechanisms. Plasticity, EMT, phenotypic diversity, and resistance to hormonal therapies are all inter-related mechanisms that guide a cell towards the NE phenotype. Once transformed prostate cells and their progeny gain NE characteristics, and androgen-sensitive cells adapt, the overall tumour cells may become androgen-insensitive and AR-independent. These cells would continue to thrive, despite therapeutic efforts of the metastases from different categories of patients, and liquid biopsies (blood RNA) from advanced patients. Within the primary tumour tissues, we witnessed high inter- and intra- patient heterogeneity, resulting in 10 unique patterns of our ten cases. Each dataset contained varying cohorts of patients, showing an increased overexpression of NE genes from benign, to primary tumours from RP, to primary tumours from advanced TURP and LNs resected at RP, and finally to multiple sites of metasta-

sis. Unique molecular patterns of over-expressed NE genes were observed in 60% of our patients' whole blood, illustrating inter-patient heterogeneity and the urgent need for precision medicine. An increasing amount of NE transcripts are clinically relevant, predictive of earlier BCR and found to be associated with disease progression. A short-hand NE signature was suggested in our discussion, however further research is required to enforce this signature. Particularly, serial longitudinal studies could be useful to narrow down a specific testable liquid biopsy NE signature. The incorporation of liquid biopsies to test for possible NE biomarkers predictive of progression would be a key step towards precision medicine and the development or refinement of curative therapies.

Chapter 10

Appendices

10.1 Appendix 1

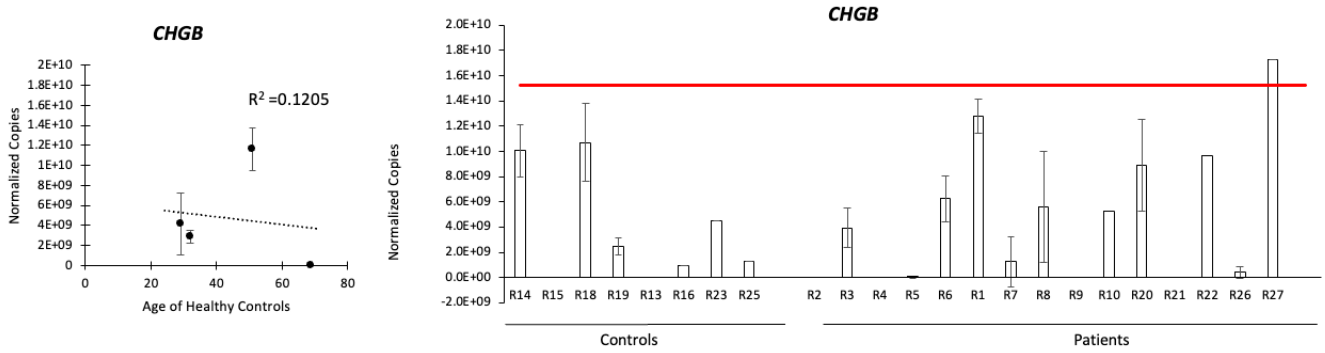

Figure 10.1: Normalized Expression of CHGB

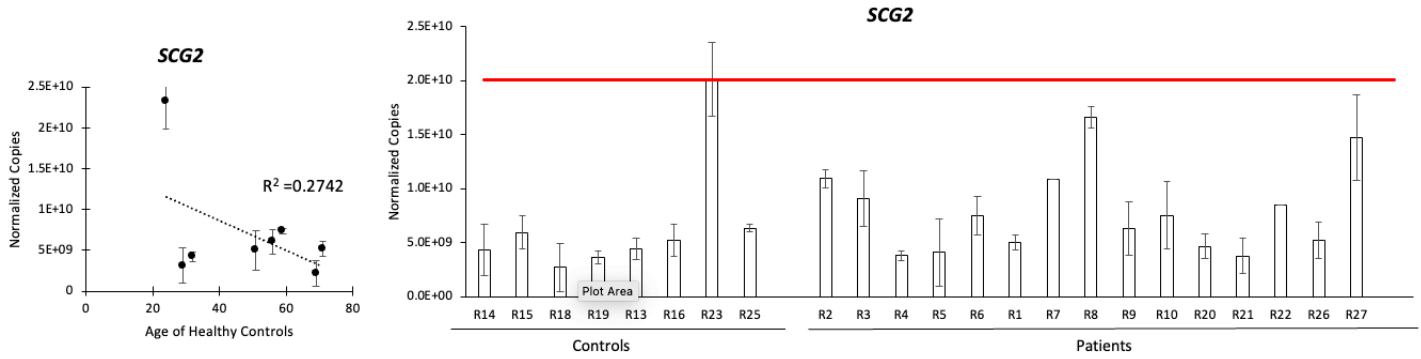

Figure 10.2: Normalized Expression of SCG2

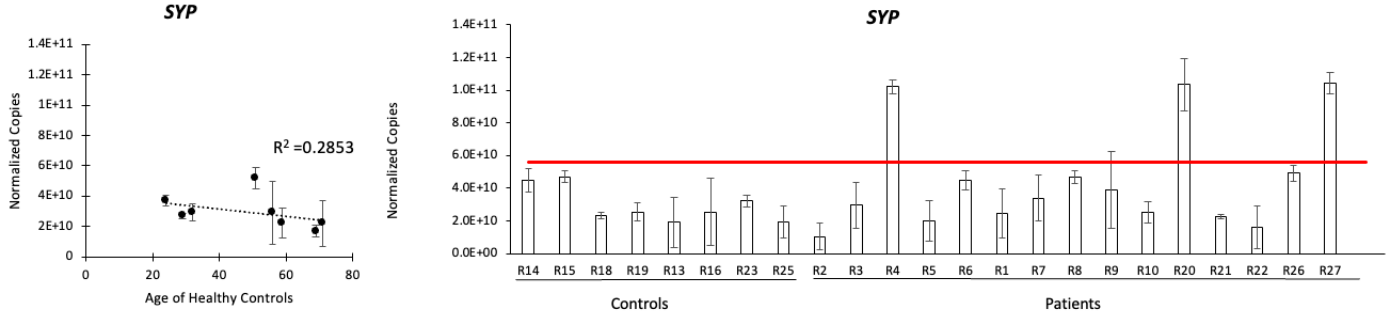

Figure 10.3: Normalized Expression of SYP

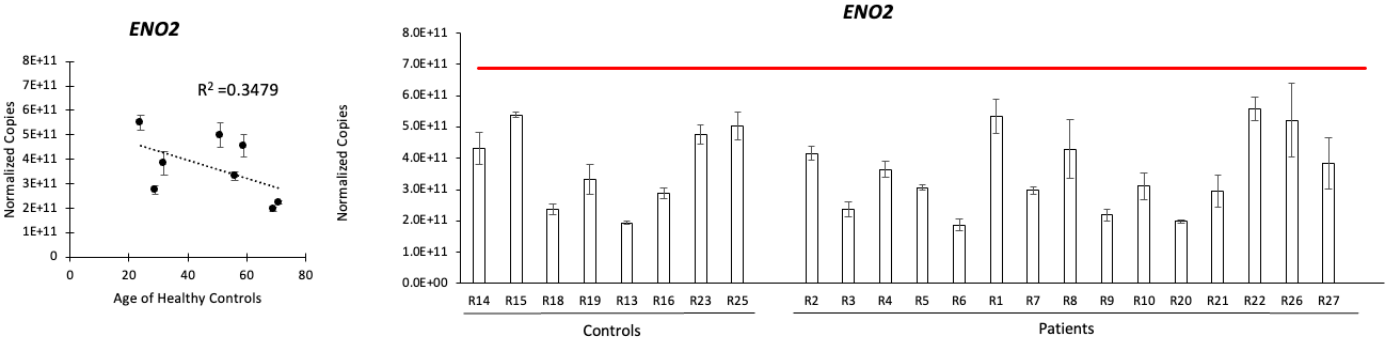

Figure 10.4: Normalized Expression of ENO2

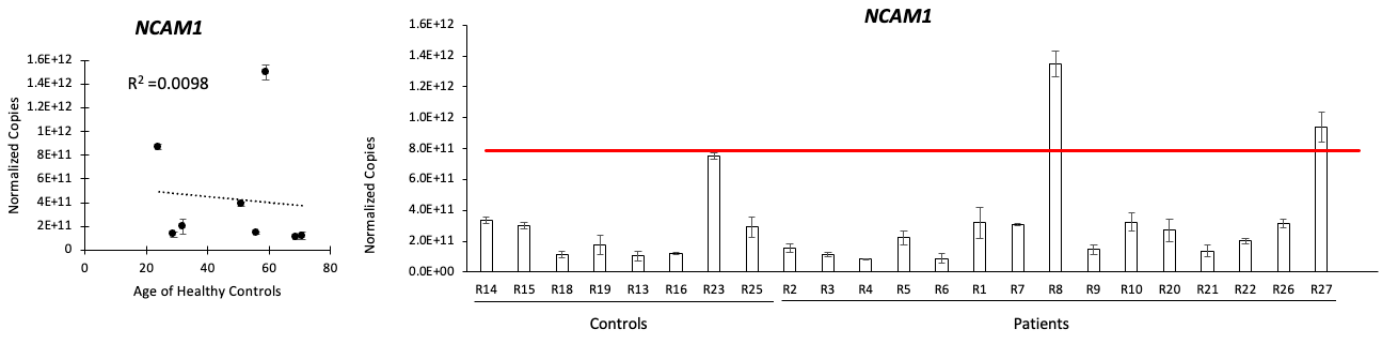

Figure 10.5: Normalized Expression of NCAM1

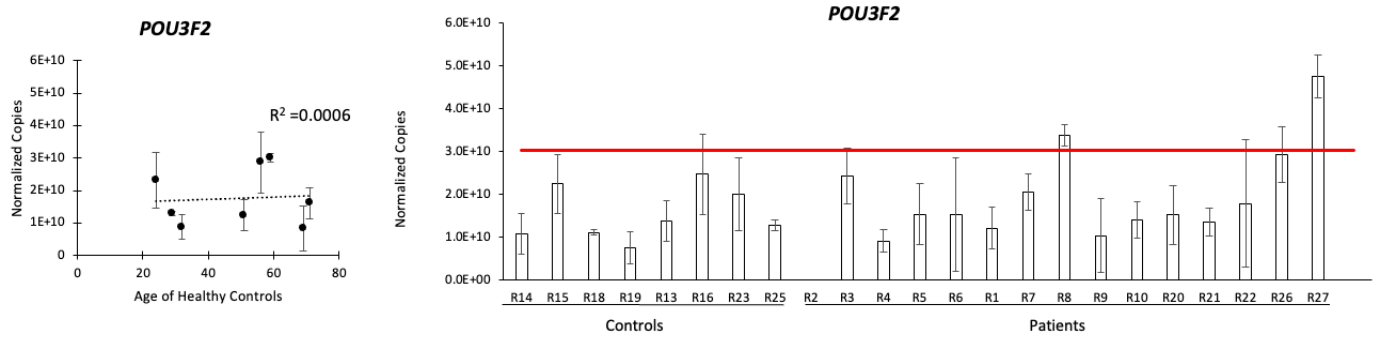

Figure 10.6: Normalized Expression of POU3F2

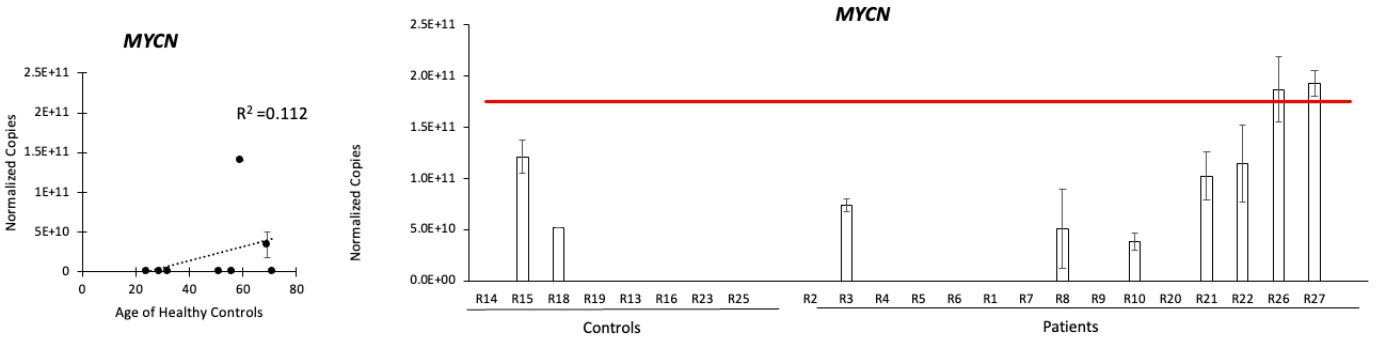

Figure 10.7: Normalized Expression of MYCN

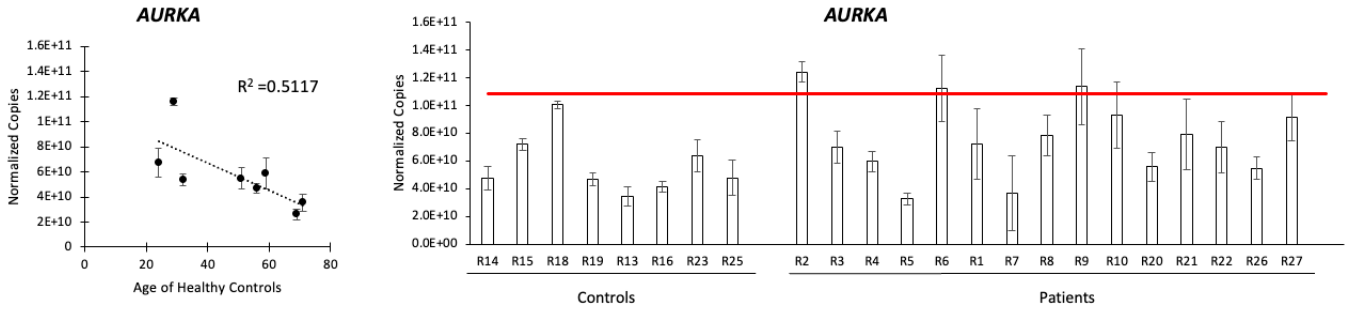

Figure 10.8: Normalized Expression of AURKA

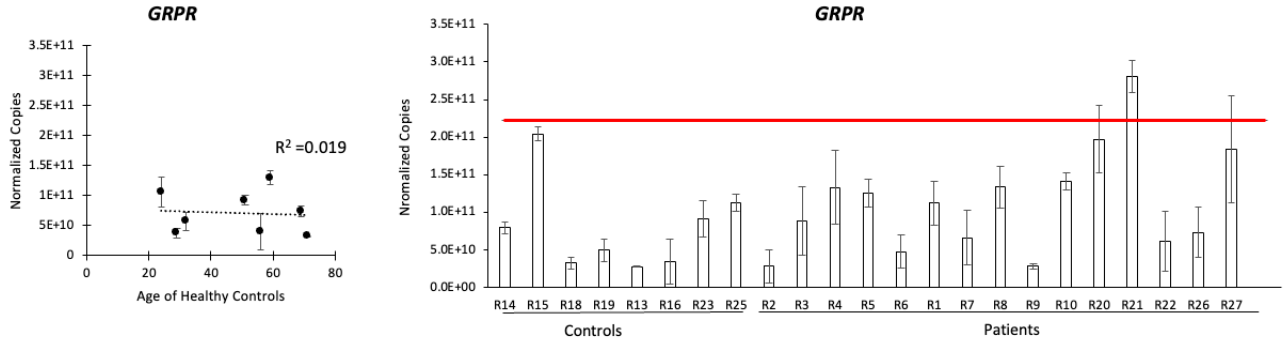

Figure 10.9: Normalized Expression of GRPR

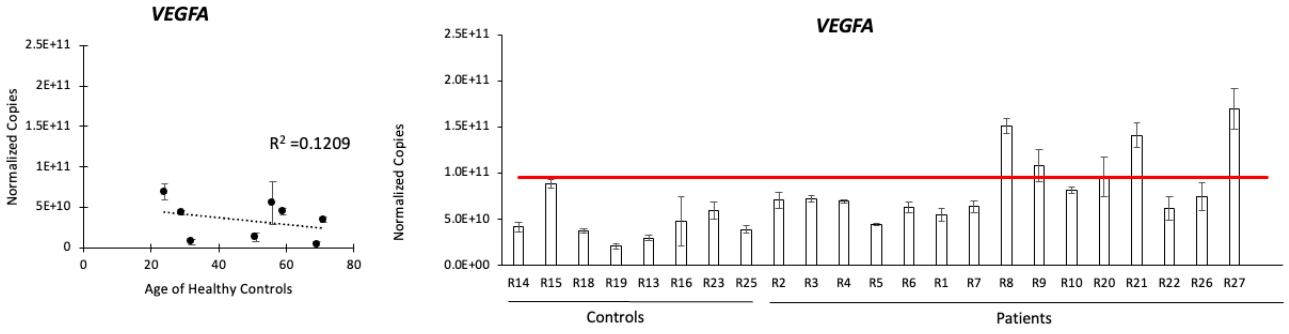

Figure 10.10: Normalized Expression of VEGFA

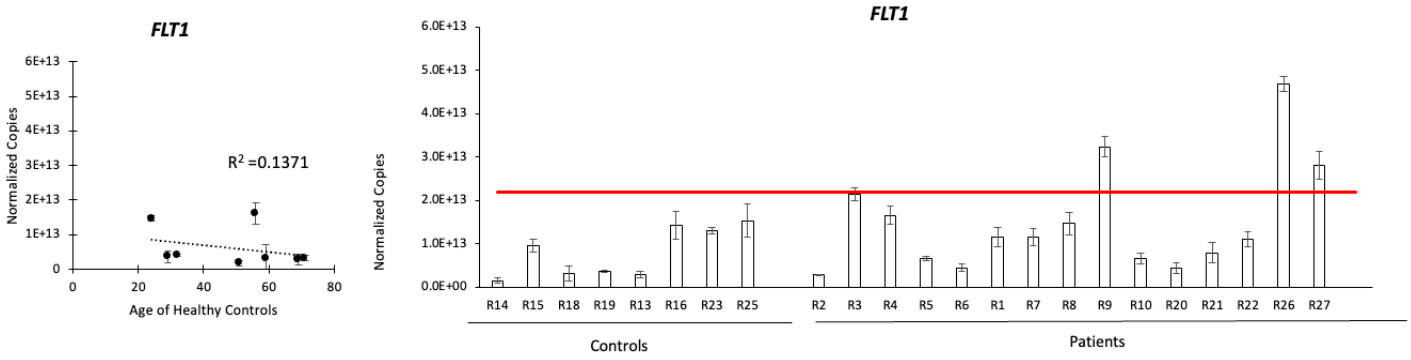

Figure 10.11: Normalized Expression of FLT1

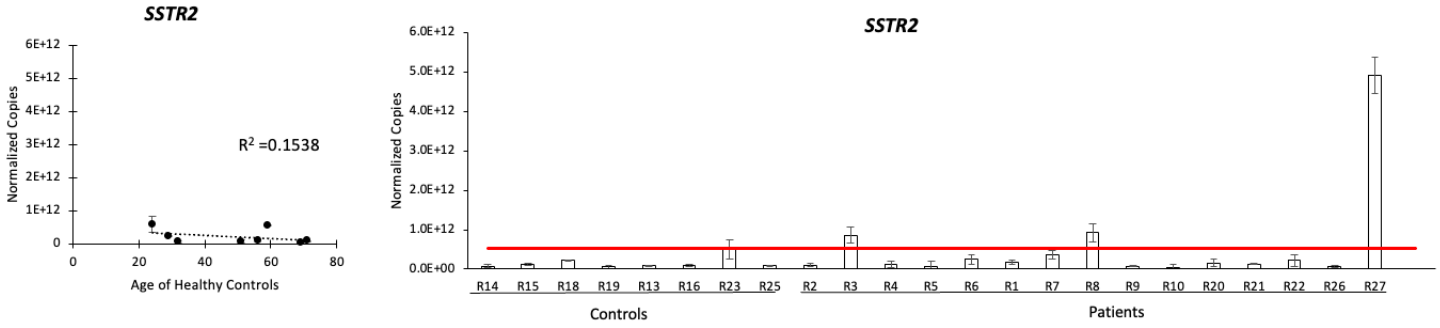

Figure 10.12: Normalized Expression of SSTR2

Bibliography

[1] LaTayia Aaron, Omar E Franco, and Simon W Hayward. Review of prostate anatomy and embryology and the etiology of benign prostatic hyperplasia. *Urologic Clinics*, 43(3):279–288, 2016.

[2] John E McNeal. The zonal anatomy of the prostate. *The prostate*, 2(1):35–49, 1981.

[3] Anil Bhavsar and Sadhna Verma. Anatomic imaging of the prostate. *BioMed research international*, 2014, 2014.

[4] Bryan D Hudson, Kristen S Kulp, and Gabriela G Loots. Prostate cancer invasion and metastasis: insights from mining genomic data. *Briefings in functional genomics*, 12(5):397–410, 2013.

[5] Charles Huggins, Clarence V Hodges, et al. Studies on prostatic cancer. *Cancer Res*, 1:297, 1941.

[6] William Tabayoyong and Robert Abouassaly. Prostate cancer screening and the associated controversy. *Surgical Clinics*, 95(5):1023–1039, 2015.

[7] Sarah K Martin, Taylor B Vaughan, Timothy Atkinson, Haining Zhu, and Natasha Kyprianou. Emerging biomarkers of prostate cancer. *Oncology reports*, 28(2):409–417, 2012.

[8] Sharanjot Saini. Psa and beyond: alternative prostate cancer biomarkers. *Cellular Oncology*, 39(2):97–106, 2016.

[9] Donald F Gleason. Histologic grading of prostate cancer: a perspective. *Human pathology*, 23(3):273–279, 1992.

[10] Hemamali Samaratunga, Brett Delahunt, John Yaxley, John R Srigley, and Lars Egevad. From gleason to international society of urological pathology (isup) grading of prostate cancer. *Scandinavian journal of urology*, 50(5):325–329, 2016.

[11] Mark S Litwin and Hung-Jui Tan. The diagnosis and treatment of prostate cancer: a review. *Jama*, 317(24):2532–2542, 2017.

[12] E David Crawford, Paul F Schellhammer, David G McLeod, Judd W Moul, Celestia S Higano, Neal Shore, Louis Denis, Peter Iversen, Mario A Eisenberger, and Fernand Labrie. Androgen receptor targeted treatments of prostate cancer: 35 years of progress with antiandrogens. *The Journal of urology*, 200(5):956–966, 2018.

[13] Vincent Faugeroux, Emma Pailler, Marianne Oulhen, Olivier Deas, Laura Brulle-Soumare, Céline Hervieu, Virginie Marty, Kamelia Alexandrova, Kiki C Andree, Nikolas H Stoecklein, et al. Genetic characterization of a unique neuroendocrine transdifferentiation prostate circulating tumor cell-derived explant model. *Nature communications*, 11(1):1–16, 2020.

[14] Himisha Beltran, Davide Prandi, Juan Miguel Mosquera, Matteo Benelli, Loredana Puca, Joanna Cyrta, Clarisse Marotz, Eugenia Giannopoulou, Balabhadrapatruni V. S. K. Chakravarthi, Sooryanarayana Varambally, Scott A. Tomlins, David M. Nanus, Scott T. Tagawa, Eliezer M. Van Allen, Olivier Elemento, Andrea Sboner, Levi A. Garraway, Mark A. Rubin, and Francesca Demichelis. Divergent clonal evolution of castration-resistant neuroendocrine prostate cancer. *Nature medicine*, 22(3):298–305, 2016.

[15] Vamsi Parimi, Rajen Goyal, Kate Poropatich, and Ximing J. Yang. Neuroendocrine differentiation of prostate cancer: a review. *American journal of clinical and experimental urology*, 2(4):273–285, 2014.

[16] D. S. Rickman, H. Beltran, F. Demichelis, and M. A. Rubin. Biology and evolution of poorly differentiated neuroendocrine tumors. *Nat Med*, 23(6):1–10, 2017.

[17] S. Koochekpour. Androgen receptor signaling and mutations in prostate cancer. *Asian J Androl*, 12(5):639–57, 2010.

[18] Thenappan Chandrasekar, Joy C. Yang, Allen C. Gao, and Christopher P. Evans. Mechanisms of resistance in castration-resistant prostate cancer (crpc). *Translational andrology and urology*, 4(3):365–380, 2015.

[19] Elisabeth A. Messner, Thomas M. Steele, Maria Malvina Tsamouri, Nazila Hejazi, Allen C. Gao, Maria Mudryj, and Paramita M. Ghosh. The androgen receptor in prostate cancer: Effect of structure, ligands and spliced variants on therapy. *Biomedicines*, 8(10):422, 2020.

[20] Daniel J. Crona and Young E. Whang. Androgen receptor-dependent and -independent mechanisms involved in prostate cancer therapy resistance. *Cancers*, 9(6):67, 2017.

[21] Scott M Dehm and Donald J Tindall. Alternatively spliced androgen receptor variants. *Endocrine-Related Cancer*, 18(5):R183–R196, 2011.

[22] Alexandra M. Blee and Haojie Huang. Lineage plasticity-mediated therapy resistance in prostate cancer. *Asian journal of andrology*, 21(3):241–248, 2019.

[23] Zhiyong Guo, Xi Yang, Feng Sun, Richeng Jiang, Douglas E. Linn, Hege Chen, Hegang Chen, Xiangtian Kong, Jonathan Melamed, Clifford G. Tepper, Hsing-Jien Kung, Angela M. H. Brodie, Joanne Edwards, and Yun Qiu. A novel androgen receptor splice variant is up-regulated during prostate cancer progression and promotes androgen depletion-resistant growth. *Cancer research*, 69(6):2305–2313, 2009.

[24] Yingming Li, Siu Chiu Chan, Lucas J. Brand, Tae Hyun Hwang, Kevin A. T. Silverstein, and Scott M. Dehm. Androgen receptor splice variants mediate enzalutamide

resistance in castration-resistant prostate cancer cell lines. *Cancer research*, 73(2):483–489, 2013.

[25] Eleni Efstathiou, Mark Titus, Sijin Wen, Anh Hoang, Maria Karlou, Robynne Ashe, Shi Ming Tu, Ana Aparicio, Patricia Troncoso, James Mohler, and Christopher J. Logothetis. Molecular characterization of enzalutamide-treated bone metastatic castration-resistant prostate cancer. *European urology*, 67(1):53–60, 2015.

[26] Xichun Liu, Elisa Ledet, Dongying Li, Ary Dotiwala, Allie Steinberger, Allison Feibus, Jianzhuo Li, Yanfeng Qi, Jonathan Silberstein, Benjamin Lee, Yan Dong, Oliver Sartor, and Haitao Zhang. A whole blood assay for ar-v7 and ar(v567es) in patients with prostate cancer. *The Journal of urology*, 196(6):1758–1763, 2016.

[27] Scott T. Tagawa, Emmanuel S. Antonarakis, Ada Gjyrezi, Giuseppe Galletti, Seaho Kim, Daniel Worroll, John Stewart, Atef Zaher, Ted P. Szatrowski, Karla V. Ballman, Katsuhiro Kita, Shinsuke Tasaki, Yang Bai, Luigi Portella, Brian J. Kirby, Fred Saad, Mario A. Eisenberger, David M. Nanus, and Paraskevi Giannakakou. Expression of ar-v7 and arv¡sup¿567es¡/sup¿ in circulating tumor cells correlates with outcomes to taxane therapy in men with metastatic prostate cancer treated in taxynergy. *Clinical Cancer Research*, 25(6):1880–1888, 2019.

[28] Yang Zhan, Guanyi Zhang, Xiaojie Wang, Yanfeng Qi, Shanshan Bai, Dongying Li, Tianfang Ma, Oliver Sartor, Erik K. Flemington, Haitao Zhang, Peng Lee, and Yan Dong. Interplay between cytoplasmic and nuclear androgen receptor splice variants mediates castration resistance. *Molecular Cancer Research*, 15(1):59–68, 2017.

[29] E. Jernberg, A. Bergh, and P. Wikström. Clinical relevance of androgen receptor alterations in prostate cancer. *Endocr Connect*, 6(8):R146–r161, 2017.

[30] Heini M. L. Kallio, Reija Hieta, Leena Latonen, Anniina Brofeldt, Matti Annala, Kati Kivinummi, Teuvo L. Tammela, Matti Nykter, William B. Isaacs, Hans G. Lilja, G. Steven Bova, and Tapio Visakorpi. Constitutively active androgen receptor splice

variants ar-v3, ar-v7 and ar-v9 are co-expressed in castration-resistant prostate cancer metastases. *British journal of cancer*, 119(3):347–356, 2018.

[31] Kathryn E. Ware, Mariano A. Garcia-Blanco, Andrew J. Armstrong, and Scott M. Dehm. Biologic and clinical significance of androgen receptor variants in castration resistant prostate cancer. *Endocrine-related cancer*, 21(4):T87–T103, 2014.

[32] Álvaro Quintanal-Villalonga, Joseph M. Chan, Helena A. Yu, Dana Pe'er, Charles L. Sawyers, Sen Triparna, and Charles M. Rudin. Lineage plasticity in cancer: a shared pathway of therapeutic resistance. *Nature Reviews Clinical Oncology*, 2020.

[33] Ferenc Sipos, Miklós Constantinovits, and Györgyi Műzes. Intratumoral functional heterogeneity and chemotherapy. *World journal of gastroenterology*, 20(10):2429–2432, 2014.

[34] Victoria R. Zellmer and Siyuan Zhang. Evolving concepts of tumour heterogeneity. *Cell and bioscience*, 4:69–69, 2014.

[35] A. Dongre and R. A. Weinberg. New insights into the mechanisms of epithelial-mesenchymal transition and implications for cancer. *Nat Rev Mol Cell Biol*, 20(2):69–84, 2019.

[36] Min Zou, Roxanne Toivanen, Antonina Mitrofanova, Nicolas Floch, Sheida Hayati, Yanping Sun, Clémentine Le Magnen, Daniel Chester, Elahe A. Mostaghel, Andrea Califano, Mark A. Rubin, Michael M. Shen, and Cory Abate-Shen. Transdifferentiation as a mechanism of treatment resistance in a mouse model of castration-resistant prostate cancer. *Cancer discovery*, 7(7):736–749, 2017.

[37] E. G. Bluemn, I. M. Coleman, J. M. Lucas, R. T. Coleman, S. Hernandez-Lopez, R. Tharakan, D. Bianchi-Frias, R. F. Dumpit, A. Kaipainen, A. N. Corella, Y. C. Yang, M. D. Nyquist, E. Mostaghel, A. C. Hsieh, X. Zhang, E. Corey, L. G. Brown, H. M. Nguyen, K. Pienta, M. Ittmann, M. Schweizer, L. D. True, D. Wise, P. S. Rennie, R. L.

Vessella, C. Morrissey, and P. S. Nelson. Androgen receptor pathway-independent prostate cancer is sustained through fgf signaling. *Cancer Cell*, 32(4):474–489.e6, 2017.

[38] Archana Sehrawat, Lina Gao, Yuliang Wang, Armand Bankhead, Shannon K. McWeeney, Carly J. King, Jacob Schwartzman, Joshua Urrutia, William H. Bisson, Daniel J. Coleman, Sunil K. Joshi, Dae-Hwan Kim, David A. Sampson, Sheila Weinmann, Bhaskar V. S. Kallakury, Deborah L. Berry, Reina Haque, Stephen K. Van Den Eeden, Sunil Sharma, Jared Bearss, Tomasz M. Beer, George V. Thomas, Laura M. Heiser, and Joshi J. Alumkal. Lsd1 activates a lethal prostate cancer gene network independently of its demethylase function. *Proceedings of the National Academy of Sciences*, 115(18):E4179–E4188, 2018.

[39] Himisha Beltran, David S. Rickman, Kyung Park, Sung Suk Chae, Andrea Sboner, Theresa Y. MacDonald, Yuwei Wang, Karen L. Sheikh, Stéphane Terry, Scott T. Tagawa, Rajiv Dhir, Joel B. Nelson, Alexandre de la Taille, Yves Allory, Mark B. Gerstein, Sven Perner, Kenneth J. Pienta, Arul M. Chinnaiyan, Yuzhuo Wang, Colin C. Collins, Martin E. Gleave, Francesca Demichelis, David M. Nanus, and Mark A. Rubin. Molecular characterization of neuroendocrine prostate cancer and identification of new drug targets. *Cancer discovery*, 1(6):487–495, 2011.

[40] J. Kim, H. Jin, J. C. Zhao, Y. A. Yang, Y. Li, X. Yang, X. Dong, and J. Yu. Foxa1 inhibits prostate cancer neuroendocrine differentiation. *Oncogene*, 36(28):4072–4080, 2017.

[41] E. J. Adams, W. R. Karthaus, E. Hoover, D. Liu, A. Gruet, Z. Zhang, H. Cho, R. DiLoreto, S. Chhangawala, Y. Liu, P. A. Watson, E. Davicioni, A. Sboner, C. E. Barbieri, R. Bose, C. S. Leslie, and C. L. Sawyers. Foxa1 mutations alter pioneering activity, differentiation and prostate cancer phenotypes. *Nature*, 571(7765):408–412, 2019.

[42] C. E. Barbieri, S. C. Baca, M. S. Lawrence, F. Demichelis, M. Blattner, J. P. Theurillat, T. A. White, P. Stojanov, E. Van Allen, N. Stransky, E. Nickerson, S. S. Chae, G. Boysen, D. Auclair, R. C. Onofrio, K. Park, N. Kitabayashi, T. Y. MacDonald, K. Sheikh, T. Vuong, C. Guiducci, K. Cibulskis, A. Sivachenko, S. L. Carter, G. Saksena, D. Voet, W. M. Hussain, A. H. Ramos, W. Winckler, M. C. Redman, K. Ardlie, A. K. Tewari, J. M. Mosquera, N. Rupp, P. J. Wild, H. Moch, C. Morrissey, P. S. Nelson, P. W. Kantoff, S. B. Gabriel, T. R. Golub, M. Meyerson, E. S. Lander, G. Getz, M. A. Rubin, and L. A. Garraway. Exome sequencing identifies recurrent spop, foxa1 and med12 mutations in prostate cancer. *Nat Genet*, 44(6):685–9, 2012.

[43] J. M. Mosquera, H. Beltran, K. Park, T. Y. MacDonald, B. D. Robinson, S. T. Tagawa, S. Perner, T. A. Bismar, A. Erbersdobler, R. Dhir, J. B. Nelson, D. M. Nanus, and M. A. Rubin. Concurrent aurka and mycn gene amplifications are harbingers of lethal treatment-related neuroendocrine prostate cancer. *Neoplasia*, 15(1):1–10, 2013.

[44] X. Gong, J. Du, S. H. Parsons, F. F. Merzoug, Y. Webster, P. W. Iversen, L. C. Chio, R. D. Van Horn, X. Lin, W. Blosser, B. Han, S. Jin, S. Yao, H. Bian, C. Ficklin, L. Fan, A. Kapoor, S. Antonysamy, A. M. Mc Nulty, K. Froning, D. Manglicmot, A. Pustilnik, K. Weichert, S. R. Wasserman, M. Dowless, C. Marugán, C. Baquero, M. J. Lallena, S. W. Eastman, Y. H. Hui, M. Z. Dieter, T. Doman, S. Chu, H. R. Qian, X. S. Ye, D. A. Barda, G. D. Plowman, C. Reinhard, R. M. Campbell, J. R. Henry, and S. G. Buchanan. Aurora a kinase inhibition is synthetic lethal with loss of the rb1 tumor suppressor gene. *Cancer Discov*, 9(2):248–263, 2019.

[45] G. H. Heppner. Tumor heterogeneity. *Cancer Res*, 44(6):2259–65, 1984.

[46] D. L. Dexter, H. M. Kowalski, B. A. Blazar, Z. Fligiel, R. Vogel, and G. H. Heppner. Heterogeneity of tumor cells from a single mouse mammary tumor. *Cancer Res*, 38(10):3174–81, 1978.

[47] Corbin E. Meacham and Sean J. Morrison. Tumour heterogeneity and cancer cell plasticity. *Nature*, 501:328, 2013.

[48] A. Kreso and J. E. Dick. Evolution of the cancer stem cell model. *Cell Stem Cell*, 14(3):275–91, 2014.

[49] J. A. Magee, E. Piskounova, and S. J. Morrison. Cancer stem cells: impact, heterogeneity, and uncertainty. *Cancer Cell*, 21(3):283–96, 2012.

[50] Roxanne Toivanen and Michael M. Shen. Prostate organogenesis: tissue induction, hormonal regulation and cell type specification. *Development*, 144(8):1382–1398, 2017.

[51] Jonathan I. Epstein, Mahul B. Amin, Himisha Beltran, Tamara L. Lotan, Juan-Miguel Mosquera, Victor E. Reuter, Brian D. Robinson, Patricia Troncoso, and Mark A. Rubin. Proposed morphologic classification of prostate cancer with neuroendocrine differentiation. *The American journal of surgical pathology*, 38(6):756–767, 2014.

[52] P. A. Abrahamsson. Neuroendocrine cells in tumour growth of the prostate. *Endocr Relat Cancer*, 6(4):503–19, 1999.

[53] P. A. Abrahamsson, L. B. Wadström, J. Alumets, S. Falkmer, and L. Grimelius. Peptide-hormone- and serotonin-immunoreactive tumour cells in carcinoma of the prostate. *Pathol Res Pract*, 182(3):298–307, 1987.

[54] S. Chevalier, I. Defoy, J. Lacoste, L. Hamel, L. Guy, L. R. Bégin, and A. G. Aprikian. Vascular endothelial growth factor and signaling in the prostate: more than angiogenesis. *Molecular and Cellular Endocrinology*, 189(1):169–179, 2002.

[55] Jaroslaw Szczyrba, Anne Niesen, Mathias Wagner, Petra M. Wandernoth, Gerhard Aumüller, and Gunther Wennemuth. Neuroendocrine cells of the prostate derive from the neural crest. *The Journal of biological chemistry*, 292(5):2021–2031, 2017.

[56] Epstein J.I. Sesterhenn I.A. Eble J. N., Sauter G. *World Health Organization Classification of Tumours. Pathology and Genetics of Tumours of the Urinary System and Male Genital Organs*. IARC Press, Lyon, France, 2004.

[57] Qi Li, Connie S. Zhang, and Yifen Zhang. Molecular aspects of prostate cancer with neuroendocrine differentiation. *Chinese journal of cancer research = Chung-kuo yen cheng yen chiu*, 28(1):122–129, 2016.

[58] Emily M. Garabedian, Peter A. Humphrey, and Jeffrey I. Gordon. A transgenic mouse model of metastatic prostate cancer originating from neuroendocrine cells. *Proceedings of the National Academy of Sciences*, 95(26):15382–15387, 1998.

[59] Alastair H. Davies, Himisha Beltran, and Amina Zoubeidi. Cellular plasticity and the neuroendocrine phenotype in prostate cancer. *Nature Reviews Urology*, 15:271, 2018.

[60] S. Y. Ku, S. Rosario, Y. Wang, P. Mu, M. Seshadri, Z. W. Goodrich, M. M. Goodrich, D. P. Labbé, E. C. Gomez, J. Wang, H. W. Long, B. Xu, M. Brown, M. Loda, C. L. Sawyers, L. Ellis, and D. W. Goodrich. Rb1 and trp53 cooperate to suppress prostate cancer lineage plasticity, metastasis, and antiandrogen resistance. *Science*, 355(6320):78–83, 2017.

[61] E. Dardenne, H. Beltran, M. Benelli, K. Gayvert, A. Berger, L. Puca, J. Cyrta, A. Sboner, Z. Noorzad, T. MacDonald, C. Cheung, K. S. Yuen, D. Gao, Y. Chen, M. Eilers, J. M. Mosquera, B. D. Robinson, O. Elemento, M. A. Rubin, F. Demichelis, and D. S. Rickman. N-myc induces an ezh2-mediated transcriptional program driving neuroendocrine prostate cancer. *Cancer Cell*, 30(4):563–577, 2016.

[62] J. K. Lee, J. W. Phillips, B. A. Smith, J. W. Park, T. Stoyanova, E. F. McCaffrey, R. Baertsch, A. Sokolov, J. G. Meyerowitz, C. Mathis, D. Cheng, J. M. Stuart, K. M. Shokat, W. C. Gustafson, J. Huang, and O. N. Witte. N-myc drives neuroendocrine

prostate cancer initiated from human prostate epithelial cells. *Cancer Cell*, 29(4):536–547, 2016.

[63] D. Lin, A. W. Wyatt, H. Xue, Y. Wang, X. Dong, A. Haegert, R. Wu, S. Brahmbhatt, F. Mo, L. Jong, R. H. Bell, S. Anderson, A. Hurtado-Coll, L. Fazli, M. Sharma, H. Beltran, M. Rubin, M. Cox, P. W. Gout, J. Morris, L. Goldenberg, S. V. Volik, M. E. Gleave, C. C. Collins, and Y. Wang. High fidelity patient-derived xenografts for accelerating prostate cancer discovery and drug development. *Cancer Res*, 74(4):1272–83, 2014.

[64] B. Helpap, J. Köllermann, and U. Oehler. Neuroendocrine differentiation in prostatic carcinomas: histogenesis, biology, clinical relevance, and future therapeutical perspectives. *Urol Int*, 62(3):133–8, 1999.

[65] W. Wang and J. I. Epstein. Small cell carcinoma of the prostate. a morphologic and immunohistochemical study of 95 cases. *Am J Surg Pathol*, 32(1):65–71, 2008.

[66] H. L. Tan, A. Sood, H. A. Rahimi, W. Wang, N. Gupta, J. Hicks, S. Mosier, C. D. Gocke, J. I. Epstein, G. J. Netto, W. Liu, W. B. Isaacs, A. M. De Marzo, and T. L. Lotan. Rb loss is characteristic of prostatic small cell neuroendocrine carcinoma. *Clin Cancer Res*, 20(4):890–903, 2014.

[67] Tamara L. Lotan, Nilesh S. Gupta, Wenle Wang, Antoun Toubaji, Michael C. Haffner, Alcides Chaux, Jessica L. Hicks, Alan K. Meeker, Charles J. Bieberich, Angelo M. De Marzo, Jonathan I. Epstein, and George J. Netto. Erg gene rearrangements are common in prostatic small cell carcinomas. *Modern pathology : an official journal of the United States and Canadian Academy of Pathology, Inc*, 24(6):820–828, 2011.

[68] J. L. Bishop, D. Thaper, S. Vahid, A. Davies, K. Ketola, H. Kuruma, R. Jama, K. M. Nip, A. Angeles, F. Johnson, A. W. Wyatt, L. Fazli, M. E. Gleave, D. Lin, M. A.

Rubin, C. C. Collins, Y. Wang, H. Beltran, and A. Zoubeidi. The master neural transcription factor brn2 is an androgen receptor-suppressed driver of neuroendocrine differentiation in prostate cancer. *Cancer Discov*, 7(1):54–71, 2017.

[69] Ping Mu, Zeda Zhang, Matteo Benelli, Wouter R. Karthaus, Elizabeth Hoover, Chi-Chao Chen, John Wongvipat, Sheng-Yu Ku, Dong Gao, Zhen Cao, Neel Shah, Elizabeth J. Adams, Wassim Abida, Philip A. Watson, Davide Prandi, Chun-Hao Huang, Elisa de Stanchina, Scott W. Lowe, Leigh Ellis, Himisha Beltran, Mark A. Rubin, David W. Goodrich, Francesca Demichelis, and Charles L. Sawyers. Sox2 promotes lineage plasticity and antiandrogen resistance in tp53- and rb1-deficient prostate cancer. *Science (New York, N.Y.)*, 355(6320):84–88, 2017.

[70] Marco Vincenzo Russo, Silvia Esposito, Maria Grazia Tupone, Lamberto Manzoli, Irma Airoldi, Paolo Pompa, Luca Cindolo, Luigi Schips, Carlo Sorrentino, and Emma Di Carlo. Sox2 boosts major tumor progression genes in prostate cancer and is a functional biomarker of lymph node metastasis. *Oncotarget*, 7(11):12372–12385, 2016.

[71] S. Akamatsu, A. W. Wyatt, D. Lin, S. Lysakowski, F. Zhang, S. Kim, C. Tse, K. Wang, F. Mo, A. Haegert, S. Brahmbhatt, R. Bell, H. Adomat, Y. Kawai, H. Xue, X. Dong, L. Fazli, H. Tsai, T. L. Lotan, M. Kossai, J. M. Mosquera, M. A. Rubin, H. Beltran, A. Zoubeidi, Y. Wang, M. E. Gleave, and C. C. Collins. The placental gene peg10 promotes progression of neuroendocrine prostate cancer. *Cell Rep*, 12(6):922–36, 2015.

[72] A. V. Lapuk, C. Wu, A. W. Wyatt, A. McPherson, B. J. McConeghy, S. Brahmbhatt, F. Mo, A. Zoubeidi, S. Anderson, R. H. Bell, A. Haegert, R. Shukin, Y. Wang, L. Fazli, A. Hurtado-Coll, E. C. Jones, F. Hach, F. Hormozdiari, I. Hajirasouliha, P. C. Boutros, R. G. Bristow, Y. Zhao, M. A. Marra, A. Fanjul, C. A. Maher, A. M. Chinnaiyan, M. A. Rubin, H. Beltran, S. C. Sahinalp, M. E. Gleave, S. V. Volik, and C. C.

Collins. From sequence to molecular pathology, and a mechanism driving the neuroendocrine phenotype in prostate cancer. *J Pathol*, 227(3):286–97, 2012.

[73] Xiaotun Zhang, Ilsa M. Coleman, Lisha G. Brown, Lawrence D. True, Lori Kollath, Jared M. Lucas, Hung-Ming Lam, Ruth Dumpit, Eva Corey, Lisly Chéry, Bryce Lakely, Celestia S. Higano, Bruce Montgomery, Martine Roudier, Paul H. Lange, Peter S. Nelson, Robert L. Vessella, and Colm Morrissey. Srrm4 expression and the loss of rest activity may promote the emergence of the neuroendocrine phenotype in castration-resistant prostate cancer. *Clinical cancer research : an official journal of the American Association for Cancer Research*, 21(20):4698–4708, 2015.

[74] P. L. Clermont, D. Lin, F. Crea, R. Wu, H. Xue, Y. Wang, K. L. Thu, W. L. Lam, C. C. Collins, Y. Wang, and C. D. Helgason. Polycomb-mediated silencing in neuroendocrine prostate cancer. *Clin Epigenetics*, 7(1):40, 2015.

[75] Eric Jay Small, Rahul Raj Aggarwal, Jiaoti Huang, Artem Sokolov, Li Zhang, Joshi J. Alumkal, Jack Youngren, Charles J. Ryan, Adam Foye, Robert Evan Reiter, Christopher P. Evans, Martin Gleave, Owen Witte, Josh Stuart, Theodore C. Goldstein, George V. Thomas, Lawrence D. True, Himisha Beltran, Mark A. Rubin, Tomasz M. Beer, and West Coast Prostate Cancer Dream Team. Clinical and genomic characterization of metastatic small cell/neuroendocrine prostate cancer (scnc) and intermediate atypical prostate cancer (iac): Results from the su2c/pcf/aacrwest coast prostate cancer dream team (wcdt). *Journal of Clinical Oncology*, 34(15):5019–5019, 2016.

[76] Vera Genitsch, Inti Zlobec, Roland Seiler, George N. Thalmann, and Achim Fleischmann. Neuroendocrine differentiation in metastatic conventional prostate cancer is significantly increased in lymph node metastases compared to the primary tumors. *International journal of molecular sciences*, 18(8):1640, 2017.

[77] S. L. Burgio, V. Conteduca, C. Menna, E. Carretta, L. Rossi, E. Bianchi, B. Kopf, F. Fabbri, D. Amadori, and U. De Giorgi. Chromogranin a predicts outcome in prostate cancer patients treated with abiraterone. *Endocr Relat Cancer*, 21(3):487–93, 2014.

[78] V. Conteduca, S. L. Burgio, C. Menna, E. Carretta, L. Rossi, E. Bianchi, C. Masini, D. Amadori, and U. De Giorgi. Chromogranin a is a potential prognostic marker in prostate cancer patients treated with enzalutamide. *Prostate*, 74(16):1691–6, 2014.

[79] A. Sciarra, F. Di Silverio, A. M. Autran, S. Salciccia, A. Gentilucci, A. Alfarone, and V. Gentile. Distribution of high chromogranin a serum levels in patients with nonmetastatic and metastatic prostate adenocarcinoma. *Urol Int*, 82(2):147–51, 2009.

[80] D. V. Matei, G. Renne, M. Pimentel, M. T. Sandri, L. Zorzino, E. Botteri, C. De Cicco, G. Musi, A. Brescia, F. Mazzoleni, V. Tringali, S. Detti, and O. de Cobelli. Neuroendocrine differentiation in castration-resistant prostate cancer: a systematic diagnostic attempt. *Clin Genitourin Cancer*, 10(3):164–73, 2012.

[81] Alfredo Berruti, Luigi Dogliotti, Alessandra Mosca, Maurizio Bellina, Mauro Mari, Mirella Torta, Roberto Tarabuzzi, Enrico Bollito, Dario Fontana, and Alberto Angeli. Circulating neuroendocrine markers in patients with prostate carcinoma. *Cancer*, 88(11):2590–2597, 2000.

[82] Alfredo Berruti, Enrico Bollito, Cecilia M. Cracco, Marco Volante, Giovannino Ciccone, Francesco Porpiglia, Mauro Papotti, Roberto Mario Scarpa, and Luigi Dogliotti. The prognostic role of immunohistochemical chromogranin a expression in prostate cancer patients is significantly modified by androgen-deprivation therapy. *The Prostate*, 70(7):718–726, 2010.

[83] B. Wiedenmann and W. W. Franke. Identification and localization of synaptophysin, an integral membrane glycoprotein of mr 38,000 characteristic of presynaptic vesicles. *Cell*, 41(3):1017–28, 1985.

[84] H. Bonkhoff. Neuroendocrine differentiation in human prostate cancer. morphogenesis, proliferation and androgen receptor status. *Ann Oncol*, 12 Suppl 2:S141–4, 2001.

[85] Burkhard Helpap. Morphology and therapeutic strategies for neuroendocrine tumors of the genitourinary tract. *Cancer*, 95(7):1415–1420, 2002.

[86] John C. Cheville, Donald Tindall, Christopher Boelter, Robert Jenkins, Christine M. Lohse, V. Shane Pankratz, Thomas J. Sebo, Brian Davis, and Michael L. Blute. Metastatic prostate carcinoma to bone. *Cancer*, 95(5):1028–1036, 2002.

[87] M. Ferrero-Poüs, A. M. Hersant, A. Pecking, M. Brésard-Leroy, and M. F. Pichon. Serum chromogranin-a in advanced prostate cancer. *BJU Int*, 88(7):790–6, 2001.

[88] N. Kamiya, K. Akakura, H. Suzuki, S. Isshiki, A. Komiya, T. Ueda, and H. Ito. Pretreatment serum level of neuron specific enolase (nse) as a prognostic factor in metastatic prostate cancer patients treated with endocrine therapy. *Eur Urol*, 44(3):309–14; discussion 314, 2003.

[89] S. Ranno, M. Motta, E. Rampello, C. Risino, E. Bennati, and M. Malaguarnera. The chromogranin-a (cga) in prostate cancer. *Arch Gerontol Geriatr*, 43(1):117–26, 2006.

[90] Barbara Muoio, Mariarosa Pascale, and Enrico Roggero. The role of serum neuron-specific enolase in patients with prostate cancer: a systematic review of the recent literature. *The International Journal of Biological Markers*, 33(1):10–21, 2018.

[91] Feng Guan, Xin Wang, and Fa He. Promotion of cell migration by neural cell adhesion molecule (ncam) is enhanced by psa in a polysialyltransferase-specific manner. *PLOS ONE*, 10(4):e0124237, 2015.

[92] Yi-Tsung Lu, Kevin Delijani, Andrew Mecum, and Amir Goldkorn. Current status of liquid biopsies for the detection and management of prostate cancer. *Cancer management and research*, 11:5271–5291, 2019.

[93] Catherine Alix-Panabières and Klaus Pantel. Clinical prospects of liquid biopsies. *Nature Biomedical Engineering*, 1(4):0065, 2017.

[94] Liancheng Fan, Yan Yang, Chenfei Chi, Xiaowei Ma, Rui Wang, Yiming Gong, Hongying Zheng, Jiahua Pan, Yinjie Zhu, Baijun Dong, and Wei Xue. Neuroendocrine differentiation markers guide treatment sequence selection in metastatic castration-resistant prostate cancer. 79(6):567–573, 2019.

[95] D. C. Danila, G. Heller, G. A. Gignac, R. Gonzalez-Espinoza, A. Anand, E. Tanaka, H. Lilja, L. Schwartz, S. Larson, M. Fleisher, and H. I. Scher. Circulating tumor cell number and prognosis in progressive castration-resistant prostate cancer. *Clin Cancer Res*, 13(23):7053–8, 2007.

[96] H. I. Scher, X. Jia, J. S. de Bono, M. Fleisher, K. J. Pienta, D. Raghavan, and G. Heller. Circulating tumour cells as prognostic markers in progressive, castration-resistant prostate cancer: a reanalysis of immc38 trial data. *Lancet Oncol*, 10(3):233–9, 2009.

[97] H. Beltran, A. Jendrisak, M. Landers, J. M. Mosquera, M. Kossai, J. Louw, R. Krupa, R. P. Graf, N. A. Schreiber, D. M. Nanus, S. T. Tagawa, D. Marrinucci, R. Dittamore, and H. I. Scher. The initial detection and partial characterization of circulating tumor cells in neuroendocrine prostate cancer. *Clin Cancer Res*, 22(6):1510–9, 2016.

[98] G. Heller, R. McCormack, T. Kheoh, A. Molina, M. R. Smith, R. Dreicer, F. Saad, R. de Wit, D. T. Aftab, M. Hirmand, A. Limon, K. Fizazi, M. Fleisher, J. S. de Bono, and H. I. Scher. Circulating tumor cell number as a response measure of prolonged survival for metastatic castration-resistant prostate cancer: A comparison with prostate-specific antigen across five randomized phase iii clinical trials. *J Clin Oncol*, 36(6):572–580, 2018.

[99] Mohid S. Khan, Theodora Tsigani, Mohammed Rashid, Jeremy S. Rabouhans, Dominic Yu, Tu Vinh Luong, Martyn Caplin, and Tim Meyer. Circulating tumor

cells and epcam expression in neuroendocrine tumors. *Clinical Cancer Research*, 17(2):337–345, 2011.

[100] M. S. Khan, A. Kirkwood, T. Tsigani, J. Garcia-Hernandez, J. A. Hartley, M. E. Caplin, and T. Meyer. Circulating tumor cells as prognostic markers in neuroendocrine tumors. *J Clin Oncol*, 31(3):365–72, 2013.

[101] M. Yu, S. Stott, M. Toner, S. Maheswaran, and D. A. Haber. Circulating tumor cells: approaches to isolation and characterization. *J Cell Biol*, 192(3):373–82, 2011.

[102] Rita Lampignano, Helen Schneck, Martin Neumann, Tanja Fehm, and Hans Neubauer. *Enrichment, Isolation and Molecular Characterization of EpCAM-Negative Circulating Tumor Cells*, pages 181–203. Springer International Publishing, Cham, 2017.

[103] M. Mego, U. De Giorgi, S. Dawood, X. Wang, V. Valero, E. Andreopoulou, B. Handy, N. T. Ueno, J. M. Reuben, and M. Cristofanilli. Characterization of metastatic breast cancer patients with nondetectable circulating tumor cells. *Int J Cancer*, 129(2):417–23, 2011.

[104] Cecilia Bozzetti, Federico Quaini, Anna Squadrilli, Marcello Tiseo, Caterina Frati, Costanza Lagrasta, Cinzia Azzoni, Lorena Bottarelli, Maricla Galetti, Angela Alama, Silvana Belletti, Rita Gatti, Antonio Passaro, Angela Gradilone, Andrea Cavazzoni, Roberta Alfieri, Pier Giorgio Petronini, Mara Bonelli, Angela Falco, Cecilia Carubbi, Giuseppe Pedrazzi, Rita Nizzoli, Nadia Naldi, Carmine Pinto, and Andrea Ardizzoni. Isolation and characterization of circulating tumor cells in squamous cell carcinoma of the lung using a non-epcam-based capture method. *PloS one*, 10(11):e0142891–e0142891, 2015.

[105] S. de Wit, G. van Dalum, A. T. Lenferink, A. G. Tibbe, T. J. Hiltermann, H. J. Groen, C. J. van Rijn, and L. W. Terstappen. The detection of epcam(+) and epcam(-) circulating tumor cells. *Sci Rep*, 5:12270, 2015.

[106] J. Chudziak, D. J. Burt, S. Mohan, D. G. Rothwell, B. Mesquita, J. Antonello, S. Dalby, M. Ayub, L. Priest, L. Carter, M. G. Krebs, F. Blackhall, C. Dive, and G. Brady. Clinical evaluation of a novel microfluidic device for epitope-independent enrichment of circulating tumour cells in patients with small cell lung cancer. *Analyst*, 141(2):669–78, 2016.

[107] J. P. Thiery. Epithelial-mesenchymal transitions in tumour progression. *Nat Rev Cancer*, 2(6):442–54, 2002.

[108] Jie-Fu Chen, Hao Ho, Jake Lichterman, Yi-Tsung Lu, Yang Zhang, Mitch A. Garcia, Shang-Fu Chen, An-Jou Liang, Elisabeth Hodara, Haiyen E. Zhau, Shuang Hou, Rafi S. Ahmed, Daniel J. Luthringer, Jiaoti Huang, Ker-Chau Li, Leland W. K. Chung, Zunfu Ke, Hsian-Rong Tseng, and Edwin M. Posadas. Subclassification of prostate cancer circulating tumor cells by nuclear size reveals very small nuclear circulating tumor cells in patients with visceral metastases. *Cancer*, 121(18):3240–3251, 2015.

[109] H. B. Hsieh, D. Marrinucci, K. Bethel, D. N. Curry, M. Humphrey, R. T. Krivacic, J. Kroener, L. Kroener, A. Ladanyi, N. Lazarus, P. Kuhn, R. H. Bruce, and J. Nieva. High speed detection of circulating tumor cells. *Biosens Bioelectron*, 21(10):1893–9, 2006.

[110] D. Marrinucci, K. Bethel, R. H. Bruce, D. N. Curry, B. Hsieh, M. Humphrey, R. T. Krivacic, J. Kroener, L. Kroener, A. Ladanyi, N. H. Lazarus, J. Nieva, and P. Kuhn. Case study of the morphologic variation of circulating tumor cells. *Hum Pathol*, 38(3):514–9, 2007.

[111] D. Marrinucci, K. Bethel, A. Kolatkar, M. S. Luttgen, M. Malchiodi, F. Baehring, K. Voigt, D. Lazar, J. Nieva, L. Bazhenova, A. H. Ko, W. M. Korn, E. Schram, M. Coward, X. Yang, T. Metzner, R. Lamy, M. Honnatti, C. Yoshioka, J. Kunken,

Y. Petrova, D. Sok, D. Nelson, and P. Kuhn. Fluid biopsy in patients with metastatic prostate, pancreatic and breast cancers. *Phys Biol*, 9(1):016003, 2012.

[112] Shannon L. Werner, Ryon P. Graf, Mark Landers, David T. Valenta, Matthew Schroeder, Stephanie B. Greene, Natalee Bales, Ryan Dittamore, and Dena Marrinucci. Analytical validation and capabilities of the epic ctc platform: Enrichment-free circulating tumour cell detection and characterization. *Journal of Circulating Biomarkers*, 4:3, 2015.

[113] Lise Tremblay, Wendy Hauck, Armen G. Aprikian, Louis R. Begin, Alcide Chapdelaine, and Simone Chevalier. Focal adhesion kinase (pp125fak) expression, activation and association with paxillin and p50csk in human metastatic prostate carcinoma. *International Journal of Cancer*, 68(2):164–171, 1996.

[114] A. G. Aprikian, K. Han, S. Chevalier, M. Bazinet, and J. Viallet. Bombesin specifically induces intracellular calcium mobilization via gastrin-releasing peptide receptors in human prostate cancer cells. *J Mol Endocrinol*, 16(3):297–306, 1996.

[115] A. G. Aprikian, L. Tremblay, K. Han, and S. Chevalier. Bombesin stimulates the motility of human prostate-carcinoma cells through tyrosine phosphorylation of focal adhesion kinase and of integrin-associated proteins. *International Journal of Cancer*, 72(3):498–504, 1997.

[116] J. Lacoste, A. G. Aprikian, and S. Chevalier. Focal adhesion kinase is required for bombesin-induced prostate cancer cell motility. *Mol Cell Endocrinol*, 235(1-2):51–61, 2005.

[117] Fei Sun, Claudia Báez-Díaz, and Francisco Miguel Sánchez-Margallo. Canine prostate models in preclinical studies of minimally invasive interventions: part i, canine prostate anatomy and prostate cancer models. *Translational Andrology and Urology*, 6(3):538–546, 2017.

[118] Hazem R. Ismail A, France Landry, Armen G. Aprikian, and Simone Chevalier. Androgen ablation promotes neuroendocrine cell differentiation in dog and human prostate. *The Prostate*, 51(2):117–125, 2002.

[119] Jacques Lapointe, Chunde Li, John P. Higgins, Matt van de Rijn, Eric Bair, Kelli Montgomery, Michelle Ferrari, Lars Egevad, Walter Rayford, Ulf Bergerheim, Peter Ekman, Angelo M. DeMarzo, Robert Tibshirani, David Botstein, Patrick O. Brown, James D. Brooks, and Jonathan R. Pollack. Gene expression profiling identifies clinically relevant subtypes of prostate cancer. *Proceedings of the National Academy of Sciences of the United States of America*, 101(3):811–816, 2004.

[120] H. Ross-Adams, A. D. Lamb, M. J. Dunning, S. Halim, J. Lindberg, C. M. Massie, L. A. Egevad, R. Russell, A. Ramos-Montoya, S. L. Vowler, N. L. Sharma, J. Kay, H. Whitaker, J. Clark, R. Hurst, V. J. Gnanapragasam, N. C. Shah, A. Y. Warren, C. S. Cooper, A. G. Lynch, R. Stark, I. G. Mills, H. Grönberg, D. E. Neal, and P. Study Group CamCa. Integration of copy number and transcriptomics provides risk stratification in prostate cancer: A discovery and validation cohort study. *EBioMedicine*, 2(9):1133–1144, 2015.

[121] B. S. Taylor, N. Schultz, H. Hieronymus, A. Gopalan, Y. Xiao, B. S. Carver, V. K. Arora, P. Kaushik, E. Cerami, B. Reva, Y. Antipin, N. Mitsiades, T. Landers, I. Dolgalev, J. E. Major, M. Wilson, N. D. Socci, A. E. Lash, A. Heguy, J. A. Eastham, H. I. Scher, V. E. Reuter, P. T. Scardino, C. Sander, C. L. Sawyers, and W. L. Gerald. Integrative genomic profiling of human prostate cancer. *Cancer Cell*, 18(1):11–22, 2010.

[122] Wassim Abida, Joanna Cyrta, Glenn Heller, Davide Prandi, Joshua Armenia, Ilsa Coleman, Marcin Cieslik, Matteo Benelli, Dan Robinson, Eliezer M. Van Allen, Andrea Sboner, Tarcisio Fedrizzi, Juan Miguel Mosquera, Brian D. Robinson, Navonil De Sarkar, Lakshmi P. Kunju, Scott Tomlins, Yi Mi Wu, Daniel Nava Rodrigues, Massimo Loda, Anuradha Gopalan, Victor E. Reuter, Colin C. Pritchard, Joaquin Mateo, Diletta Bianchini, Susana Miranda, Suzanne Carreira, Pasquale Rescigno,

Julie Filipenko, Jacob Vinson, Robert B. Montgomery, Himisha Beltran, Elisabeth I. Heath, Howard I. Scher, Philip W. Kantoff, Mary-Ellen Taplin, Nikolaus Schultz, Johann S. deBono, Francesca Demichelis, Peter S. Nelson, Mark A. Rubin, Arul M. Chinnaiyan, and Charles L. Sawyers. Genomic correlates of clinical outcome in advanced prostate cancer. *Proceedings of the National Academy of Sciences*, 116(23):11428–11436, 2019.

[123] Network Cancer Genome Atlas Research. The molecular taxonomy of primary prostate cancer. *Cell*, 163(4):1011–1025, 2015.

[124] Akash Kumar, Ilsa Coleman, Colm Morrissey, Xiaotun Zhang, Lawrence D. True, Roman Gulati, Ruth Etzioni, Hamid Bolouri, Bruce Montgomery, Thomas White, Jared M. Lucas, Lisha G. Brown, Ruth F. Dumpit, Navonil DeSarkar, Celestia Higano, Evan Y. Yu, Roger Coleman, Nikolaus Schultz, Min Fang, Paul H. Lange, Jay Shendure, Robert L. Vessella, and Peter S. Nelson. Substantial interindividual and limited intraindividual genomic diversity among tumors from men with metastatic prostate cancer. *Nature medicine*, 22(4):369–378, 2016.

[125] V. S. Sabbisetti, S. Chirugupati, S. Thomas, K. S. Vaidya, D. Reardon, M. Chiriva-Internati, K. A. Iczkowski, and G. V. Shah. Calcitonin increases invasiveness of prostate cancer cells: role for cyclic amp-dependent protein kinase a in calcitonin action. *Int J Cancer*, 117(4):551–60, 2005.

[126] Lichun Sun and David H Coy. Somatostatin and its analogs. *Current drug targets*, 16, 2014.

[127] Gabor Halmos, Andrew V. Schally, Baodong Sun, Rodney Davis, David G. Bostwick, and Artur Plonowski. High expression of somatostatin receptors and messenger ribonucleic acid for its receptor subtypes in organ-confined and locally advanced human prostate cancers1. *The Journal of Clinical Endocrinology and Metabolism*, 85, 2000.

[128] Giordano Savelli, Alfredo Muni, Roberta Falchi, Alberto Zaniboni, Roberto Barbieri, Giuseppe Valmadre, Chiara Minari, Camilla Casi, and Pierluigi Rossini. Somatostatin receptors over-expression in castration resistant prostate cancer detected by pet/ct: preliminary report of in six patients. *Annals of translational medicine*, 3(10):145–145, 2015.

[129] C. Liolios, M. Schäfer, U. Haberkorn, M. Eder, and K. Kopka. Novel bispecific psma/grpr targeting radioligands with optimized pharmacokinetics for improved pet imaging of prostate cancer. *Bioconjugate Chemistry*, 27(3):737–751, 2016.